

Iridium-Catalyzed C–H Activation Methods for Late-Stage Functionalization of Pharmaceuticals

Erik Weis



Iridium-Catalyzed C–H Activation Methods for Late-Stage Functionalization of Pharmaceuticals

Erik Weis

Academic dissertation for the Degree of Doctor of Philosophy in Organic Chemistry at Stockholm University to be publicly defended on Thursday 27 January 2022 at 09.00 in Magnélsalen, Kemiska övningslaboratoriet, Svante Arrhenius väg 16 B and online via Zoom: <https://stockholmuniversitet.zoom.us/j/63066246042>.

Abstract

C–H activations have over the recent decades risen from a mere curiosity to a viable synthetic strategy. However, challenges in terms of accessible transformations, selectivity and functional group tolerance limit the widespread applicability of this approach. The aim of the work presented in this thesis was to develop directed *ortho* C–H activation methodologies specifically designed for applications in drug discovery. The [Cp*Ir(III)] catalytic system was key for the herein described transformations.

Chapter 2 covers the development of selective monoiodination of benzoic acids. A mono/di selectivity >20:1 was observed throughout a range of diversely functionalized substrates. Mechanistic investigations revealed the key role of the Ag(I) additive in controlling selectivity.

Chapter 3 discusses C–H methylations applied to a wide range of benzoic acids, including examples of late-stage functionalization of marketed drugs. The methodology also allows for introduction of CD₃ groups. Biological studies demonstrated positive effect on biological and physical properties of pharmaceuticals as the result of methylation.

In chapter 4 the C–H amination and sulfonamidation of benzoic acids is described, with applications for the synthesis of aminated analogues of drug-like molecules. Rapid synthesis of conjugates relevant to drug discovery is also demonstrated.

Chapter 5 is dedicated to the development of a general C–H amination protocol, successfully applied to 21 distinct directing groups. The utility of the method is demonstrated by the functionalization of 11 complex drugs and natural products. Directing group informer libraries and functional group tolerance studies enabled the generation of guidelines for reaction outcome prediction.

Keywords: *amination, catalysis, C–H activation, C–H functionalization, high-throughput experimentation, iodination, iridium, isotope labelling, late-stage functionalization, methylation.*

Stockholm 2022
<http://urn.kb.se/resolve?urn=urn:nbn:se:su:diva-199212>

ISBN 978-91-7911-716-0
ISBN 978-91-7911-717-7



Stockholm
University

Department of Organic Chemistry

Stockholm University, 106 91 Stockholm

IRIDIUM-CATALYZED C–H ACTIVATION METHODS FOR LATE-STAGE FUNCTIONALIZATION OF PHARMACEUTICALS

Erik Weis

Iridium-Catalyzed C–H Activation Methods for Late- Stage Functionalization of Pharmaceuticals

Erik Weis

©Erik Weis, Stockholm University 2022

ISBN print 978-91-7911-716-0

ISBN PDF 978-91-7911-717-7

Printed in Sweden by Universitetsservice US-AB, Stockholm 2021

“Je suis de ceux qui pensent que la science est d'une grande beauté. Un scientifique dans son laboratoire n'est pas seulement un technicien: c'est aussi un enfant placé devant des phénomènes naturels qui l'impressionnent comme un conte de fées.”

I am among those who think that science is a great beauty. A scientist in his laboratory is not a mere technician: he is also a child confronting natural phenomena that impress him as though they were fairy tales.

Marie Curie

Popular Science Summary

Organic compounds are all around us; from the DNA in our bodies, the paper this thesis is printed on, all the way to the medicines used to treat our illnesses. Many of the organic compounds we encounter on a daily basis are human-made, and many have become indispensable to our everyday lives. The development of new procedures to make these compounds is crucial not only to maintain, but also to further improve the quality of our lives. Here the synthetic chemists come into the picture, as our job is to develop ways to prepare these chemicals, found everywhere, from household products, through plastics, and all the way to agrochemicals and medicines.

By definition, organic compounds contain carbon-hydrogen (C–H) bonds. Under normal conditions these bonds do not undergo chemical reactions. If they did, all the previously mentioned compounds would be constantly reacting, and life as we know it would not be possible. However, if we could make these bonds react in a controlled way, this would allow us not only to access known compounds in a more straightforward and sustainable way, but also access new materials and medicines. Catalysis offers a solution to this challenging task, by using metals for activation of otherwise unreactive C–H bonds. While most people know catalysis perhaps only from the catalytic converter of their car, this remarkable technology is of tremendous value to synthetic chemists. Although a number of metal catalyzed reactions have become a staple of medicinal chemistry, C–H bond activations are only now beginning to be implemented. The reality of applications to pharmaceuticals is complicated by the structural complexity of this compound class. This dissertation explores such reactivity and complexity.

The aim of the work described in this dissertation was to develop catalytic C–H activations for the synthesis of chemical building blocks useful in drug discovery, and ultimately for applications on pharmaceuticals themselves. Four distinct methodologies were developed, centered around the use of iridium catalysts. These were applied to the synthesis of known building blocks in a more streamlined fashion, gave access to previously unknown building blocks, and even enabled modifications of clinically used drugs and synthesis of analogues with improved properties. The results presented in this work have the potential for direct uptake in drug discovery, leading to the development of the next generation of life-saving medicines.

Populärvetenskaplig Sammanfattning

Organiska ämnen finns runt omkring oss; från DNA i våra kroppar, det papper som denna avhandling är tryckt på, hela vägen till de läkemedel som används för att behandla våra sjukdomar. Många av de organiska föreningar vi möter dagligen är gjorda av människor och många har blivit oundgängliga i vår vardag. Utveckling av nya procedurer för att tillverka organiska föreningar är avgörande inte bara för att upprätthålla, utan även för att förbättra, kvaliteten i våra liv. I denna kontext kommer syntetiska kemister in i bilden, eftersom vårt jobb är att utveckla sätt att producera dessa kemikalier.

Organiska föreningar innehåller bindningar mellan kol och väte (C–H) och under normala förhållanden genomgår dessa bindningar inte kemiska reaktioner. Om de gjorde det så skulle alla de tidigare nämnda föreningar ständigt reagera och livet se mycket annorlunda ut. Däremot, om vi kan få dessa bindningar att reagera på ett kontrollerat sätt skulle detta inte bara ge oss tillgång till kända föreningar på ett mer hållbart sätt utan även tillgång till nya material och läkemedel. Katalys erbjuder en lösning på denna utmanande uppgift genom att använda metaller för att aktivera annars oreaktiva C–H-bindningar. Medan de flesta endast känner till katalys från katalysatorn i sin bil, är denna anmärkningsvärda teknik av enormt värde för syntetiska kemister. Även om ett antal metallkatalyserade reaktioner har blivit en stapelvara i läkemedelskemi så börjar aktivering av C–H-bindningar först nu att implementeras. I verkligheten så kompliceras tillämpningar för läkemedel av den strukturella komplexiteten hos denna föreningsklass. Denna avhandling utforskar sådan reaktivitet och komplexitet.

Syftet med det arbete som beskrivs i denna avhandling var att utveckla katalytiska C–H-aktiveringar för syntes av kemiska byggstenar som är användbara vid upptäckt och tillämpning av läkemedel. Fyra distinkta metoder, centrerade kring användningen av iridiumkatalysatorer, utvecklades. Dessa metoder applicerades på syntesen av kända byggstenar på ett mer strömlinjeformat sätt, vilket gav tillgång till tidigare okända byggstenar, möjliggjorde modifieringar av kliniskt använda läkemedel och syntes av förbättrade analoger. Resultaten som presenteras i detta arbete har potentialen att användas i kommande läkemedelsupptäckter, vilket kan leda till utvecklingen av framtidens livsavgörande läkemedel.

Abstract

C–H activations have over the recent decades risen from a mere curiosity to a viable synthetic strategy. However, challenges in terms of accessible transformations, selectivity and functional group tolerance limit the widespread applicability of this approach. The aim of the work presented in this thesis was to develop directed *ortho* C–H activation methodologies specifically designed for applications in drug discovery. The [Cp*Ir(III)] catalytic system was key for the herein described transformations.

Chapter 2 covers the development of selective monoiodination of benzoic acids. A mono/di selectivity >20:1 was observed throughout a range of diversely functionalized substrates. Mechanistic investigations revealed the key role of the Ag(I) additive in controlling selectivity.

Chapter 3 discusses C–H methylations applied to a wide range of benzoic acids, including examples of late-stage functionalizations of marketed drugs. The methodology also allows for introduction of CD₃ groups. Biological studies demonstrated positive effect on biological and physical properties of pharmaceuticals as the result of methylation.

In chapter 4 the C–H amination and sulfonamidation of benzoic acids is described, with applications for the synthesis of aminated analogues of drug-like molecules. Rapid synthesis of conjugates relevant to drug discovery is also demonstrated.

Chapter 5 is dedicated to the development of a general C–H amination protocol, successfully applied to 21 distinct directing groups. The utility of the method is demonstrated by the functionalization of 11 complex drugs and natural products. Directing group informer libraries and functional group tolerance studies enabled the generation of guidelines for reaction outcome prediction.

List of Publications

This dissertation is based on the following publications, referred to in the text by their roman numerals **I-IV**. The author's contributions are clarified in *Appendix A*. Copyright information related to reprints are specified in *Appendix B*.

- I. Ir^{III}-Catalyzed Selective *ortho*-Monoiodination of Benzoic Acids with Unbiased C–H Bonds**
Weis, E.; Johansson, M. J.; Martín-Matute, B.
Chem. Eur. J. **2020**, *26*, 10185.
- II. Iridium-catalyzed C–H methylation and *d*₃-methylation of benzoic acids with application to late-stage functionalizations**
Weis, E.; Hayes, M. A.; Johansson, M. J.; Martín-Matute, B.
iScience **2021**, *24*, 102467
- III. Late-stage amination of drug-like benzoic acids: Access to anilines and drug conjugates via directed iridium-catalyzed C–H activation**
Weis, E.; Johansson, M. J.; Martín-Matute, B.
Chem. Eur. J. **2021**, *Accepted*
<https://doi.org/10.1002/chem.202103510> (Preprint)
- IV. Merging directed C–H activations with high-throughput experimentation: Development of predictable Iridium-catalyzed C–H aminations applicable to late-stage functionalization**
Weis, E.; Johansson, M.; Korsgren, P.; Martín-Matute, B.; Johansson, M. J. *ChemRxiv* **2021**, Cambridge: Cambridge Open Engage; This content is a preprint and has not been peer-reviewed.
DOI: 10.26434/chemrxiv-2021-vp0kl

Abbreviations

Abbreviations are used in accordance with the standards of the subject area.[§]
Non-standard and unconventional abbreviations are listed below.

CMD	Concerted metalation-deprotonation
DCE	1,2-Dichloroethane
DG	Directing group
DoM	Directed <i>ortho</i> -metalation
HFIP	1,1,1,3,3,3-Hexafluoroisopropanol
L	L-type ligand, non-charged ligand donating two electrons
LCMS	Liquid chromatography-mass spectrometry
MeCN	Acetonitrile
Moz	p-Methoxybenzyl carbonyl
MS	Mass spectrometry
N.B.	Nota bene
NHS	N-Hydroxy succinimide
NIS	<i>N</i> -Iodosuccinimide
NMP	<i>N</i> -Methyl-2-pyrrolidone
Ns	Nosyl
NR	No reaction
PROTACs	Proteolysis targeting chimeras
RT	Room temperature
SFC	Supercritical fluid chromatography
TBME	<i>tert</i> -Butyl methyl ether
TFE	2,2,2-Trifluoroethanol
TON	Turnover number

[§] Petronella, K. M. Abbreviations List, *The ACS Guide to Scholarly Communication*. **2020** (DOI:10.1021/acsguide.50308)

Previous Documents Based on This Work

This dissertation is partly based on the author's half-time report presented on the 27th of March 2020.

Chapter 1 (Introduction): This chapter was included in the half-time report. For this dissertation it has been reviewed and updated, and around 70% of the text is new. References were added.

Chapter 2 (Paper I): This chapter was included in the half-time report. For this thesis it has been reviewed, updated and shortened. The manuscript in preparation from the half-time report was updated to the published paper.

Chapter 3 (Paper II): This chapter was included in the half-time report. For this dissertation it has been reviewed and updated with new results and references. The paper itself is new.

Chapter 4 (Paper III): This chapter is new.

Chapter 5 (Paper IV): This chapter is new.

Contents

Popular Science Summary	i
Populärvetenskaplig Sammanfattning	ii
Abstract	iii
List of Publications	iv
Abbreviations	v
Previous Documents Based on This Work	vi
1. Introduction	1
1.1 C–H Bonds in Organic Compounds	1
1.2 C–H Functionalization	1
1.3 C–H Activation vs C–H Functionalization	3
1.4 C–H Functionalization: Reaction and Mechanistic Considerations	3
1.4.1 C–H Activations: Mechanistic Considerations	5
1.4.2 Transition Metal-Catalyzed C–H Activation Catalytic Cycle: Case Study ..	7
1.5 Challenges and Opportunities in Aromatic C–H Bond Activation	9
1.6 High-Throughput Experimentation, Automation and Miniaturization	12
1.7 Objectives of This Dissertation	15
2. Ir(III)-Catalyzed Selective <i>ortho</i>-Monoiodination of Benzoic Acids with Unbiased C–H Bonds (Paper I).....	16
2.1 Background	16
2.2 Results and Discussion	17
2.2.1 Optimization	17
2.2.2 Scope	19
2.2.3 Mechanistic Studies	22
2.3 Conclusions	29
3. Iridium-Catalyzed C–H Methylation and <i>d</i>₃-Methylation of Benzoic Acids with Application to Late-Stage Functionalization (Paper II)	30
3.1 Background	30
3.2 Results and Discussion	32
3.2.1 Optimization	32
3.2.2 Scope	37
3.2.3 Biological Studies	41
3.2.4 Solvent Recovery and Recycling	43
3.3 Conclusions	43

4. Late-Stage Amination of Drug-like Benzoic Acids: Access to Anilines and Drug Conjugates <i>via</i> Directed Iridium-Catalyzed C–H Activation (Paper III)	45
4.1 Background	45
4.2 Results and Discussion	46
4.2.1 Optimization	46
4.2.2 Functional Group Tolerance Studies	49
4.2.3 Substrate Scope: Sulfonamidation	51
4.2.4 Substrate Scope: Amination	55
4.2.5 Synthesis of Conjugates	56
4.2.6 Mechanistic Studies	59
4.3 Conclusion	60
5. Merging Directed C–H Activations with High-Throughput Experimentation: Development of Predictable Iridium-Catalyzed C–H Aminations Applicable to Late-Stage Functionalizations (Paper IV)	62
5.1 Background	62
5.2 Results and Discussion	64
5.2.1 Optimization	64
5.2.2 Reaction Scope	68
5.2.3 Functional Group Tolerance Studies	70
5.2.4 Reaction Scope: Late-stage Functionalization	72
5.2.5 Deprotection Studies	76
5.2.6 Miniaturization Studies	77
5.2.7 Application Guidelines	79
5.3 Conclusions	80
6. Concluding remarks	81
Appendix A: Author’s Contributions	82
Appendix B: Reprint Permissions	83
Acknowledgements	84
References	86

1. Introduction

1.1 C–H Bonds in Organic Compounds

Carbon-hydrogen (C–H) bonds can be found in a large number compounds with a wide range of applications (Figure 1). Such is the abundance of C–H bonds in organic chemistry, that by consensus these are not even depicted in chemical structures. For the purpose of this introduction only C(sp²)–H bonds, specifically in aromatic organic compounds will be discussed.

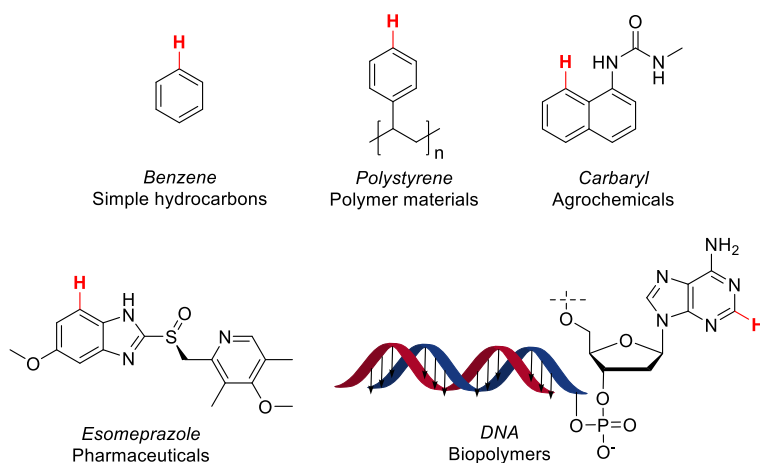


Figure 1. Selected examples of C–H bonds in different compound classes.

1.2 C–H Functionalization

Given the great abundance of aromatic C–H bonds in organic compounds, their functionalization has long captured the imagination of chemists. The field has undergone rich development since the seminal work of Mitscherlich on the nitration of benzene in 1834,¹ all the way to the functionalization of highly complex substrates such as drugs and natural products accessible with modern methodologies.^{2–4} Many C–H functionalization reactions became a staple in organic synthesis, enabling the production of commodity chemicals on ton scale, as well as small scale synthesis of compounds of interest in research laboratories. However, only recently has this approach become feasible for the functionalization of complex drug-like molecules, facilitated by the

development of chemoselective methods with broad functional group tolerance.²⁻⁴ Given the symbiotic relationship between organic synthesis and drug discovery, further developments in the field have the potential to greatly aid the development of new therapeutic agents, and are thus highly desirable. Taking small molecule pharmaceuticals as an example, as of 2020, 88% of the top 200 small molecule drugs by retail sales contained at least one aromatic C(sp²)-H group.⁵ The utility of functionalizing this abundant functional group is further strengthened by its potential impact, as the exchange of a single C-H can significantly improve the properties of drug candidates (Figure 2).⁶

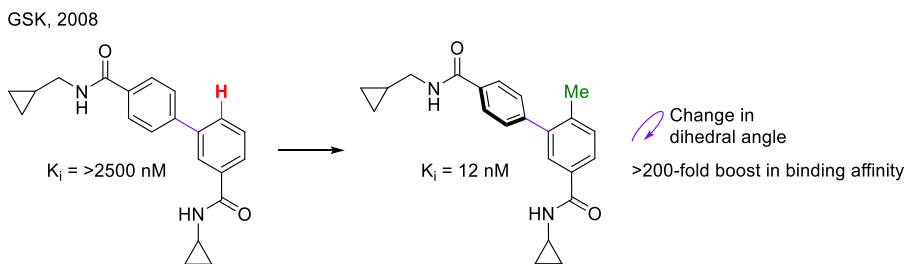


Figure 2. Impact of the functionalization of a single C-H bond in a drug candidate.⁶

Compared to more well established synthetic tactics applied in medicinal chemistry, such as functional group (FG) interconversions and transition metal-catalyzed cross-coupling reactions, C-H functionalizations do not rely on the presence of reactive synthetic handles and pre-functionalized substrates. From a medicinal chemistry point of view, this allows for direct use of available hit or lead compounds for obtaining desired analogues, rather than reverting to time intensive *de novo* synthesis (Figure 3).

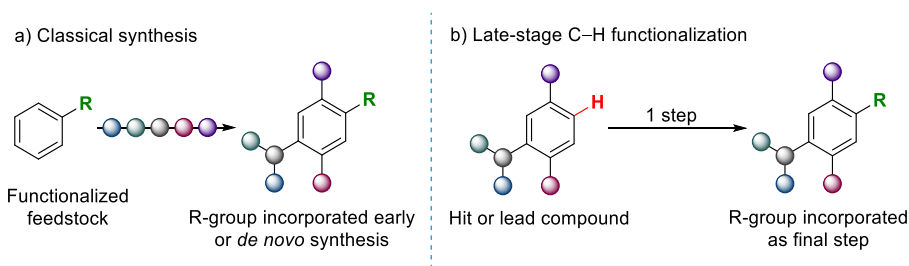


Figure 3. General representation of approaches towards the synthesis of analogues of complex compounds.⁷

This has a myriad of benefits, perhaps best expressed with a quote from Paul A. Wender: “while the best solution [to a synthetic problem] might be defined in various ways, most practitioners would agree that it will be the one that comes closest to the ‘ideal synthesis’... defined as one in which the target molecule is prepared from readily available starting materials in one simple,

safe, environmentally acceptable, and resource-effective operation that proceeds quickly and in quantitative yield.”⁸ While most C–H functionalizations are far from the ultimate ideal reaction, they most certainly represent a step towards it.

1.3 C–H Activation vs C–H Functionalization

Before getting deeper into the discussion of C–H activation chemistry, it is important to define the terms C–H activation and C–H functionalization. C–H functionalization is a term referring to a chemical transformation resulting in the conversion of a C–H bond into a C–R bond (R referring to a functional group, typically a halide, oxygen-, nitrogen- or carbon- linked), regardless of the mechanism. Typical examples of such reactions are electrophilic aromatic substitutions (S_EAr), radical additions, deprotonations or transition metal-catalyzed C–H functionalizations.

C–H activation is defined as a process where a previously unreactive C–H bond is “activated” by a transition metal catalyst, resulting in a species with a C-bound metal.⁹ This intermediate species can then undergo subsequent functionalization. Thus C–H activation reactions can be viewed as a mechanistically distinct subset of a broader class of C–H functionalization reactions.

1.4 C–H Functionalization: Reaction and Mechanistic Considerations

The non-polar character of non-acidic C–H bonds and the high kinetic barrier of the C–H bond cleavage renders these stable towards many reaction conditions.¹⁰ Despite this, a number of distinct approaches towards C–H functionalization have been developed over the years.^{11–16} It is important to note that the applicability of the following approaches and their regioselectivity is highly dependent on the structural motifs present in the substrate, as well as electronic properties of the system. As shown in the example of benzoic acid as substrate, the “classical” and perhaps most widely utilized C–H functionalization reaction class is electrophilic aromatic substitution (S_EAr). In this reaction, an electrophilic species (E^+ , Figure 4, a) reacts with an arene nucleophile, resulting in the formation of a carbocation intermediate. After deprotonation, the aromaticity is restored, yielding a functionalized arene. The regioselectivity of this reaction is governed by the steric and electronic properties

of the substrate and the electrophilic reagent. In case of benzoic acid, the functionalization occurs predominantly at the less electropositive *meta* position.^{17,18} The applicability towards the functionalization of complex molecules is limited by the aforementioned regioselectivity, but also by functional group tolerance, as the reaction often relies on the use of reactive electrophilic reagents.

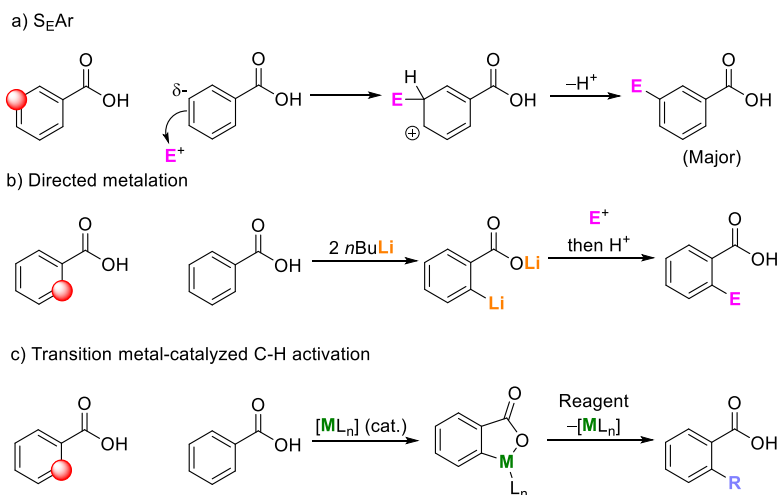


Figure 4. General representation of selected C–H functionalization approaches.

Directed *ortho*-metalation (*DoM*) (Figure 4, b) offers complementary regioselectivity to S_EAr and excellent control for selective *ortho* functionalization.¹⁵ In this case, the carboxylate moiety serves as a Lewis-basic directing group for an organometallic reagent (typically organolithium), resulting in directed *ortho*-lithiation.^{15,19} The *ortho*-lithiated product is subsequently quenched with an electrophile to yield the *ortho*-functionalized product. While highly regioselective, this approach presents its own set of limitations due to the use of strongly basic and nucleophilic organolithium reagents.

The third approach presented herein is the transition metal-catalyzed C–H activation/functionalization (Figure 4, c). In this particular scenario, the selectivity is once again governed by the Lewis-basic moiety. A metallacycle is formed in the C–H bond activation step, which can subsequently undergo transformation to the desired product. After this, the catalyst is regenerated, and the cycle repeated. Compared to the first two scenarios, this approach allows for the expansion of suitable reaction partners outside of electrophilic reagents. While the varying functional group tolerance of the catalytic systems, when challenged with complex molecules, poses a major hurdle for the

widespread application of this approach, there are many recent examples of methodologies capable of late-stage functionalization (LSF).^{2,11-13,20,21}

1.4.1 C–H Activations: Mechanistic Considerations

The progress made in the development of modern C–H activation methods has been enabled, to a large extent, by the increased mechanistic understanding of the underlying processes. The main approaches to C–H activation can be divided into 2 categories: directed and undirected (Figure 5). Each approach comes with its own set of benefits and limitations, and the accessibility of each is largely dependent on catalyst and substrate selection. With directed C–H activations, the regioselectivity of the reaction is guided by the interaction of the catalyst with a Lewis-basic directing group (Figure 5, a). While this approach has the potential to offer excellent regiocontrol when applied to complex substrates bearing multiple C–H bonds, its application is limited to substrates with suitable directing groups. Activations of C–H bonds *ortho* to the directing group are by far the most common, and a wealth of methodologies utilizing directing groups commonly present in pharmaceuticals have been reported over the years.¹³ Although less common, *meta*- and *para*-directed activations are also possible, however, this usually requires the installation of purpose-made directing groups.²²⁻²⁴ Another, alternative, approach to directed C–H activation is the templated strategy, where distal positions can be accessed by utilizing suitable ligands in combination with directing groups.²⁵

Undirected C–H activations offer applicability to a wide variety of substrates, as this approach can be applied to substrates that do not contain appropriate directing groups (Figure 5, b). Electronic and steric factors are decisive, and the most acidic and/or least sterically hindered C–H bond is typically cleaved.^{26,27} This, however, also comes with the drawback of the formation of regioisomers with compounds where more than one suitable C–H bond is present.

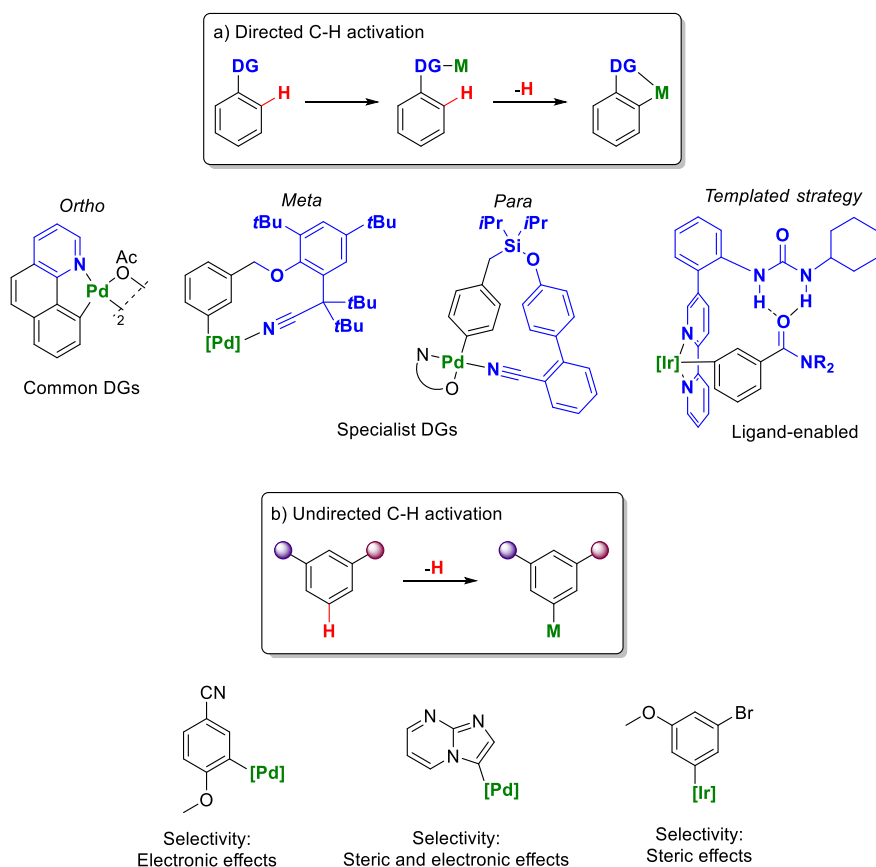


Figure 5. General representation of transition metal-catalyzed C–H activation approaches in terms of regioselectivity. a) Directed C–H activation, metallacycle formation. Regioselectivity: Ortho,²⁸ meta,²⁹ para,²³ templated.²⁵ b) Undirected C–H activations. Regioselectivity: Electronic effects,²⁷ steric and electronic effects,³⁰ steric effects.³¹

The C–H activation itself can occur *via* several distinct mechanisms.^{10,32} Once again, the mode of action is largely dependent on catalyst and substrate selected. Electron-rich metal catalysts can undergo oxidative addition to a C–H bond, resulting in a change of oxidation state on the metal center (Figure 6, a).³³ Some electron-poor catalysts can undergo a S_EAr reaction with electron-rich aromatics, followed by deprotonation (Figure 6, b).¹² Sigma-bond metathesis yields the metallated aryl without change in the oxidation state of the metal catalyst *via* a 4-membered cyclic transition state (Figure 6, c).^{34,35} With concerted metalation-deprotonation (CMD), the cleavage of the C–H bond is mediated by a ligand, typically a carboxylate, and occurs simultaneously with the formation of the C–M bond. The oxidation state of the catalyst remains unchanged (Figure 6, d).³⁶ A stepwise version of this mechanism is represented by base-assisted intramolecular electrophilic substitution (BIES), where the metalation and C–H cleavage occur in 2 distinct steps (Figure 6, e).³⁷ This

mechanism is a variant of the S_EAr mechanism as presented (Figure 6, b), with the important difference that the base is in the catalyst's coordination sphere.

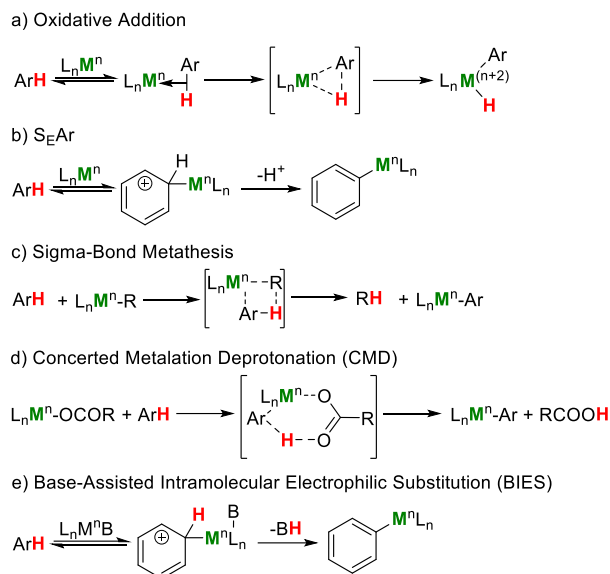


Figure 6. General representation of mechanistically distinct C–H activation modes.

As a result of their distinct mechanisms, many C–H activation methodologies allow for functionalization of C–H bonds in the presence of functional groups such as halides, which would normally undergo oxidative addition with transition metals.³⁸

1.4.2 Transition Metal-Catalyzed C–H Activation Catalytic Cycle: Case Study

Given the large number of reported C–H activation methodologies with a wide range of transformations, reaction modes and variations in catalytic cycles, it is beyond the scope of this thesis to discuss all potential reaction modes associated with transition metal-catalyzed C–H activations. To simplify the discussion of the catalytic cycles, while allowing the reader to appreciate their intricacies, the iridium-catalyzed C–H iodination of benzoic acids from 2018 is herein discussed as a model system (Figure 7).³⁹ *Ortho*-iodination was achieved with complete suppression of the electrophilic iodination in the *meta*-position by careful choice of *N*-iodosuccinimide (NIS) as iodinating agent, in combination with the catalyst $[Cp^*Ir(H_2O)_3]SO_4$ and 1,1,1,3,3,3-hexafluoroisopropanol (HFIP) as solvent. Under these conditions a series of benzoic acids were functionalized under mild conditions and in absence of base and further additives. The following catalytic cycle was proposed based on experimental and computational mechanistic studies (Figure 7).

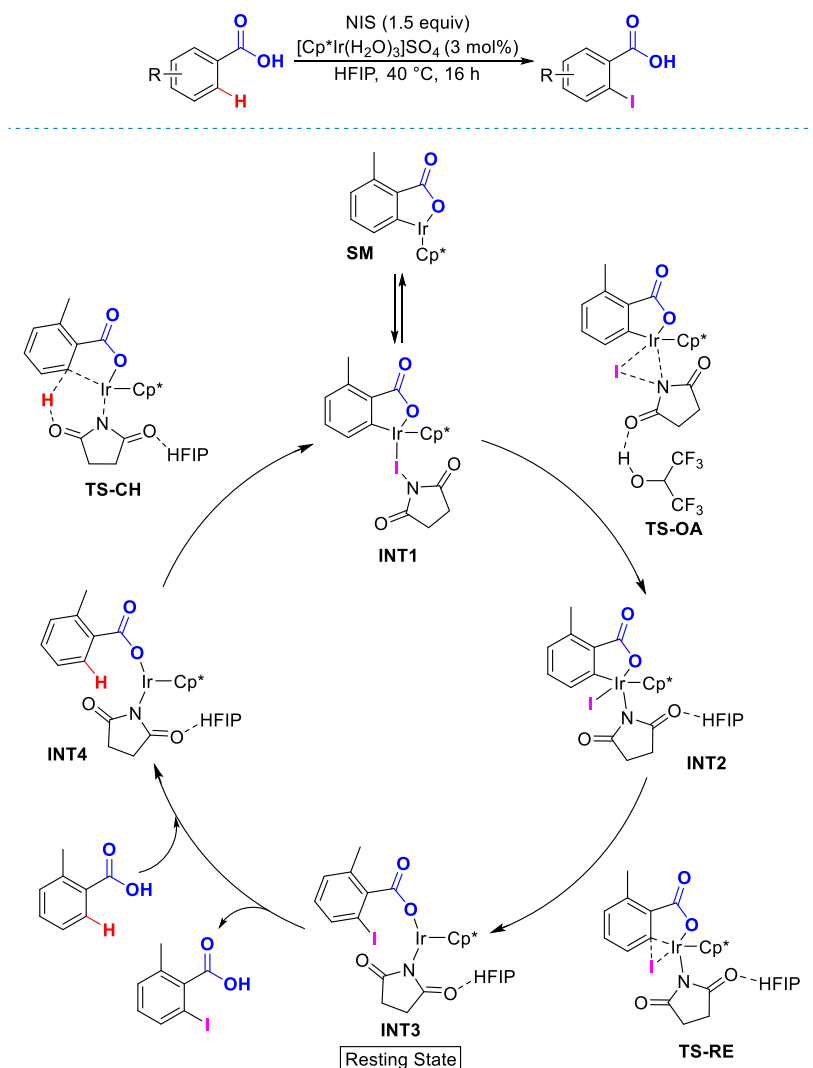


Figure 7. Representative transition metal-catalyzed C–H activation catalytic cycle.³⁹

The proposed mechanism is initiated from a 16-electron catalytically active iridacycle (**SM**) which, after coordination of NIS, leads to formation of **INT1**. It was demonstrated experimentally that this iridacycle was easily formed when mixing stoichiometric amounts of benzoic acid and iridium complex, in the absence of NIS. Oxidative addition of NIS leads to the formation of Ir(V) species **INT2**. An explanation of the superior performance of HFIP compared to other solvents is provided with the reductive elimination step, as a molecule of HFIP is proposed to undertake hydrogen bonding with the complex, further decreasing the electron density on the metal, and thus resulting in lowering of

the energy barrier associated with the reductive elimination. The product-coordinated complex **INT3** is suggested as the resting state of the catalytic cycle, which after ligand exchange with a molecule of substrate forms **INT4**. The C–H activation step is then facilitated by the succinate ligand *via* a CMD mechanism, and the catalytically active species is reformed. This is in agreement with experimental mechanistic studies, including KIE studies.

1.5 Challenges and Opportunities in Aromatic C–H Bond Activation

The diversity of catalytic systems and elementary steps, as discussed in the previous chapter, in combination with the abundance of C–H bonds in pharmaceuticals shows great promise for controlled C–H activation and functionalization in specific positions. Demonstrated in the example of Pritelivir (Figure 8, a), the differences of stereoelectronic properties associated to specific C–H functional groups can, in theory, allow for accessing a number of analogues from one common substrate by utilizing different reaction manifolds. The streamlined access to analogues would have direct positive impact on the timelines, material consumption and cost associated with drug discovery.

However, in order to realize the full potential of C–H functionalization, specifically when employed in LSF, several limitations need to be addressed. As the vast majority of target substrates contain several C–H bonds, regioselectivity is essential. Lack of selectivity would result in lower yield of the desired product, as well as significant complications in the purification due to the similar properties encountered with regioisomers. While selectivity can be tuned by the choice of reaction manifold for C–H bonds with different stereoelectronic properties, the situation is further complicated by differentiation of C–H bonds with similar properties (Figure 8, b). Taking the 2-phenylpyridine core as an example, the formation of regioisomers has been observed with Ir-catalyzed C–H borylation,⁴⁰ as well as formation of mixtures of mono/di-functionalized products with directed C–H activations.^{28,41,42}

Functional group tolerance presents another significant challenge for the development of C–H functionalization methodologies. Pharmaceuticals and natural products contain a plethora of functional motifs potentially problematic for transition metal-catalysis (Figure 8, c), including groups with nucleophilic and electrophilic character, Lewis-basic groups, acidic protons and stereocenters. From the perspective of C–H activation methodologies, the presence of polar and Lewis-basic groups gives opportunities for selectivity control *via* directed C–H activations, but at the same time can be challenging due to potential catalyst poisoning.

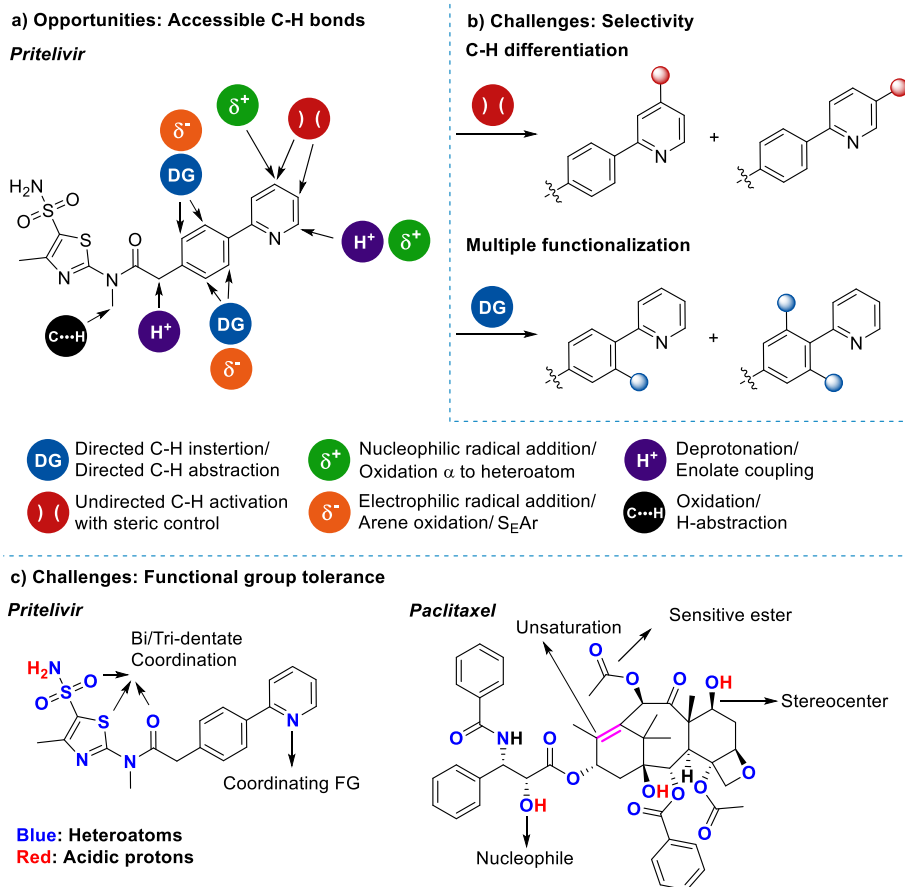


Figure 8. Challenges and opportunities within directed C–H functionalizations of pharmaceuticals. *a)* Hypothetical LSF strategies for Pritelivir. Reactivity descriptors based on published review.⁴ *b)* Potential selectivity challenges of late-stage C–H functionalizations. *c)* Representative functional group tolerance challenges in late-stage C–H functionalizations.

While the challenges presented are significant, so is the pay-off from successful reactions. The key areas where C–H functionalizations are anticipated to transform drug discovery are depicted in Figure 9. The overarching benefits for all three applications are decreased time and material cost for synthesis and access to analogues previously discarded due to synthetic intractability. Firstly, the introduction of synthetic handles enables late-stage diversification (Figure 9, a). In fragment-based drug discovery, this would enable rapid elaboration of desired growth vectors, expansion to previously inaccessible growth vectors, as well as increasing the speed of the fragment-to-ligand design cycle.⁴³ The same principle could also be applied to late-stage diversification of hit and lead compounds, where the controlled introduction of a syn-

thetic handle followed by subsequent transformation, ideally in a library format, could lead to analogue series important for structure-activity relationship (SAR) investigations. Secondly, the late-stage installation of small functional groups would allow rapid synthesis of molecular matched pairs (Figure 9, b).⁴⁴ Applications include, but are not limited to, fine-tuning physicochemical properties of drug candidates, aiding SAR investigations, and even addressing metabolic stability and target selectivity issues in later stages of the drug discovery process. Finally, the introduction of linkers suitable for the synthesis of small molecule drug conjugates can enable rapid investigation of different modes of action of drug candidates, such as targeted drug delivery, targeted protein degradation, as well as synthesis of fluorescent-labelled and other tool compounds for chemical biology (Figure 9, c).⁴⁵

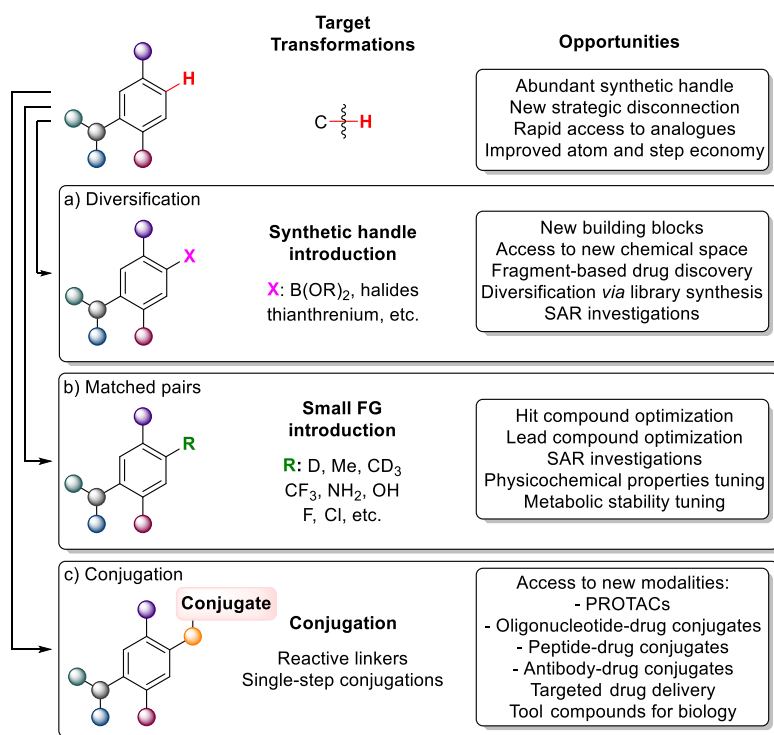
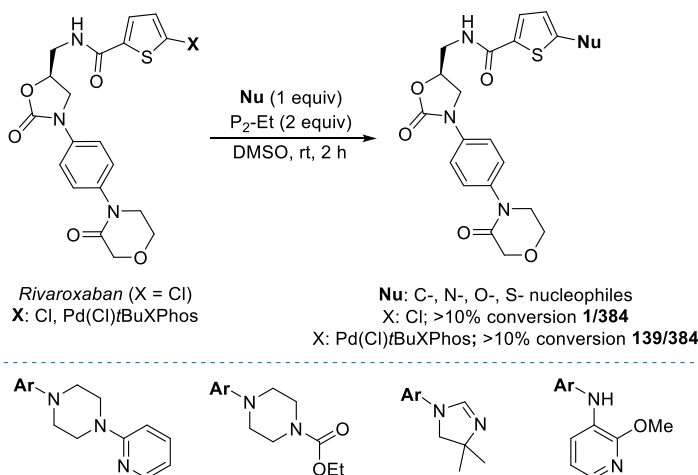


Figure 9. Opportunities within C–H functionalizations with respect to applications in medicinal chemistry.

1.6 High-Throughput Experimentation, Automation and Miniaturization

High-throughput experimentation (HTE) is an approach in organic synthesis that allows for the execution of large sets of hypothesis-driven experiments in parallel.⁴⁶ HTE is closely tied with automation and miniaturization. As a whole, this allows for rapid testing of hypotheses, while minimizing reagent, catalyst and solvent consumption, increasing time efficiency, and generating high quality data sets with good reproducibility. Not surprisingly, the last decade has seen significant uptake and innovations in the HTE field within the pharmaceutical industry.^{47,48} On the medicinal chemistry side, HTE has enabled rapid synthesis and screening of compound libraries against therapeutic targets. In the presented example (Scheme 1), scientist from Merck in collaboration with Buchwald and co-workers reported the application of palladium oxidative addition complexes for the generation of cross-coupling libraries.⁴⁹



Scheme 1. Example of HTE application for synthesis of Rivaroxaban analogues.⁴⁹

In this work, the groups demonstrated successful screening of 384 distinct reactions in a single plate with a variety of nucleophiles. The hits obtained from the screening could then be scaled up and used for SAR investigations. The results of this study serve as an excellent example for the discussion of HTE applications with informer libraries containing complex compounds. The group demonstrated a significant increase in reaction success rate using the palladium oxidative addition complex, with 206 out of 384 reactions resulting in hits (139 instances with >10% conversion), compared to 39 out of 384 hits (1 instance with >10% conversion) with the corresponding aryl chloride and 5 mol% *t*BuXPhos Pd G3 catalyst. The massively improved success rate with the protocol using stoichiometric palladium illustrates one possible approach

of addressing the challenges of generating libraries of complex, densely functionalized substrates. Despite requiring stoichiometric amounts of palladium, relatively low amounts of the precious metal were used given the nanomolar scale of the reaction, demonstrating the potential benefits of miniaturization in terms of material consumption.

Another powerful application of HTE is presented by rapid reaction discovery and optimization. Beyond the speed and scale advantages, an added benefit compared to standard one-factor-at-a-time optimizations is covering a broader chemical space.^{47,48,50} In yet another example from the Merck laboratories, the discovery of room temperature photoredox radical methylation of 4-methylquinoline was described (Table 1). The presented results not only allow the potential user to choose highest yielding conditions, but also give information about conditions where the reaction fails, and complementary reaction conditions. For example, substitution of the precious metal catalyst for an organocatalyst (Fluorescein), or opportunities for solvent selection to match substrate solubility (polar MeCN, non-polar DCE, aqueous conditions).

Table 1. Example of HTE application for multiparameter reaction optimization.⁵⁰

	[Ru(bpy) ₃]Cl ₂	[Ru(bpy) ₃](PF ₆) ₂	[Ru(phen) ₃]Cl ₂	[Ru(dip) ₃]Cl ₂	[Ir(ppy) ₂ (dtbpy)]PF ₆	[Ir(dF-CF ₃ -ppy) ₂ (dtbpy)]PF ₆	Ir(dF-ppy) ₃	Ir(-ppy) ₃	Ir(btpy) ₃	Ir(piq) ₃	Fluorescein	None
MeCN	0	0	0	0	26	72	0	0	0	0	0	0
DMF	0	0	0	0	0	0	0	0	0	0	0	0
DMSO	0	0	0	0	0	37	0	0	0	0	0	0
DCE	0	0	0	59	13	71	0	9	0	0	19	0
Acetoene	0	0	0	27	21	42	0	0	0	0	0	0
AcOH	0	0	0	34	32	75	0	0	0	0	0	0
AcOH/H ₂ O	0	0	0	0	12	74	0	0	0	0	0	0
MeCN/H ₂ O	0	0	0	13	20	0	0	0	0	0	0	0

Photoredox methylation of 4-methylquinoline. 12 photocatalysts screened against 8 solvent sets. Color coding based on conversion (red to green gradient, red lowest, green highest).

HTE has also been utilized to investigate the functional group tolerance and applicability of reactions for the functionalization of complex substrates.⁵¹⁻⁵³ Importantly, implementation of HTE approaches facilitates the generation of large, high quality datasets within all of the aforementioned applications, crucial for applications within machine learning and artificial intelligence (AI),

which in turn have the potential to further increase efficiency and predictability in synthesis, both within and outside drug discovery. Despite all the potential benefits, according to a 2019 report,⁴⁷ C–H activations accounted for only 2% of the most common reaction types studied by HTE in pharma on average. However, this number is expected to grow in the future. The lack of applications might be linked to practical challenges within C–H activation methodologies such as high reaction temperature, incompatibility with plastic reaction plates, high metal loading, use of insoluble reagents and related issues with mixing, and/or limited substrate scope.

1.7 Objectives of This Dissertation

The aim of this dissertation is to expand the synthetic chemistry toolbox with directed C–H activation methodologies complementary to reported chemistry in terms of regioselectivity, functional group tolerance and accessible transformations. The overarching characteristics of the four manuscripts this dissertation is built around is the development of directed *ortho* C–H activation methodologies utilizing directing groups innately present in building blocks relevant to drug discovery and in pharmaceuticals.

The first thematic part is focused on the *ortho*-functionalization of benzoic acids, a substrate class of high importance for medicinal chemistry. The aim was to develop methodologies to further expand the utility of reaction products by introducing synthetic handles by means of iodination, by introducing small substituents with methylation and amination, and finally by introducing linkers for conjugation chemistry in form of bifunctional sulfonamide linkers.

The second thematic part is centered around the development of directed C–H activations for a wide range of substrates. Here the goal was to develop a single amination methodology allowing for the utilization of a broad array of Lewis-basic directing groups.

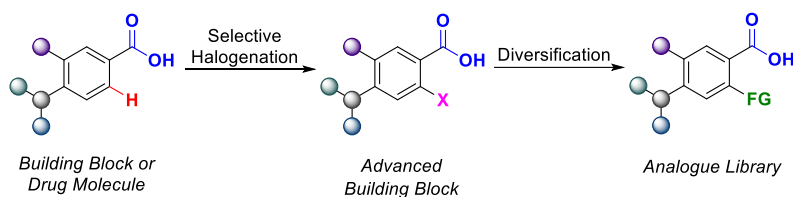
With all methodologies we sought to demonstrate their applicability and limitations by reaction scope investigation, and in later stages also by functional group tolerance studies. In parallel with methodology development, an important goal of this dissertation is to enhance the understanding of the underlying processes in the reactions by means of experimental mechanistic studies. Alongside these efforts, we sought to increase the utility of the methodologies for modern drug discovery by developing methods applicable to HTE, while highlighting key challenges and opportunities for further development of transition metal-catalyzed C–H activations in this direction.

Last but not least, this dissertation aims to give a more detailed picture of the motivations and investigations behind the four publications and tie these together as one coherent, continuous story of the work carried out over the last four years.

2. Ir(III)-Catalyzed Selective *ortho*-Monoiodination of Benzoic Acids with Unbiased C–H Bonds (Paper I)

2.1 Background

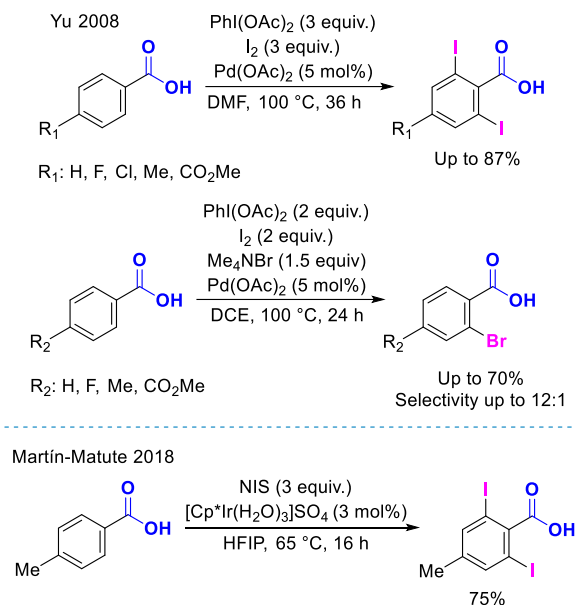
Benzoic acids present an important substrate class frequently used as a starting point in synthesis given the utility of the carboxylic acid functional group for further functionalization. A routine example of this is amide bond formation. The synthetic utility of benzoic acids as building blocks can be further increased by the presence of other synthetic handles, such as halides (Scheme 2).



Scheme 2. General representation of the diversification synthetic approach enabled by selective C–H halogenation.

However, substrates with certain substitution patterns can be more difficult to obtain than others. The innate reactivity of benzoic acids in electrophilic aromatic substitutions, leading to the formation of *meta*-functionalized products, can be greatly supplemented by methods allowing *ortho*-functionalization. While DoM offers a solution to this, lithiation of benzoic acids is generally limited by yields and substrate scope.^{54,55} Transition metal-catalyzed C–H activations allow for *ortho*-iodination of a significantly wider range of benzoic acids and improved yields, as demonstrated by published examples (Scheme 3).^{39,56} However, the useful scope of these transformations is limited to *ortho*- and *meta*-substituted benzoic acids, due to formation of disubstituted derivatives following activation of two C–H bonds in *para*-substituted substrates. Catalyst-controlled monoselective bromination of symmetrical benzoic acids was successfully achieved by Yu and co-workers,⁵⁶ with four substrates displaying a respectable mono/di selectivity ranging from 8:1 to

12:1. Based on the knowledge of applicability of the $[\text{Cp}^*\text{Ir(III)}]$ catalytic system to C–H iodination of benzoic acids,³⁹ the herein presented C–H monoiodination of symmetrical benzoic acids was developed.⁵⁷



Scheme 3. Selected work on C–H iodination of benzoic acid by Yu and co-workers⁵⁶ and by Martín-Matute and co-workers.³⁹

2.2 Results and Discussion

2.2.1 Optimization

Following previous work,³⁹ $[\text{Cp}^*\text{Ir(H}_2\text{O)}_3]\text{SO}_4$ was chosen as the precatalyst. Iodination of benzoic acid at room temperature resulted in a 8:1 mixture of mono/diiodinated products **2a**:**2a'** (Table 2, Entry 1) in moderate yield. In entry 2, a large improvement in selectivity was observed, with a >20:1 ratio of **2a**:**2a'** with the use of potassium benzoate as starting material, albeit at a lower yield (Entry 2). Under these conditions, rapid decomposition of NIS was observed. Thus, we decided to test a different iodine source. Iodine monoacetate (AcOI) has been previously reported to be generated from I_2 and AgOAc .⁵⁸ To our delight, the use of this reagent (Entry 3) brought a large improvement in conversion, and maintained good selectivity. Further investigations revealed that using HFIP as solvent, with an excess of AgOAc over I_2 led to improved selectivity (Entry 4). In the absence of a silver salt, no conversion was observed (Entry 5). The next logical step was to test the commercially available complex $[\text{Cp}^*\text{IrCl}_2]_2$. Gratifyingly, excellent yield (92%) and good

selectivity (>20:1) was obtained (Entry 6). The yield was further improved with increased AgOAc and I₂ loading (Entry 7). Under these conditions no diiodinated species **2a'** was detected, and full conversion of the starting material to **2a** was achieved. Finally, the direct use of benzoic acid as the starting material was successful, although a decrease in yield was observed (Entry 8). The excellent conversion was restored with the use of stoichiometric base (Et₃N, Entry 9). This modification enabled the direct use of widely commercially available benzoic acids as starting materials and was used in the investigation of the scope and limitations.

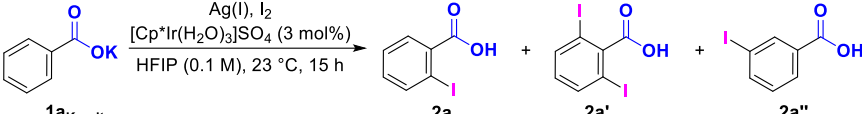
Table 2. Selected entries from the optimization of the C–H iodination reaction.^a

Entry	Substrate	Ag(I) (equiv)	I source (equiv)	[Ir]	Yield (%)	2a/2a'
1	BzOH	-	NIS (1.5)	I	45	8:1
2	BzOK	-	NIS (1.5)	I	25	>20:1
3	BzOK	AgOAc (1.3)	I ₂ (1.2)	I	91	13:1
4	BzOK	AgOAc (2.2)	I ₂ (1.2)	I	89	>20:1
5	BzOK	-	I ₂ (1.2)	I	0	-
6	BzOK	AgOAc (2.2)	I ₂ (1.1)	II	92	>20:1
7	BzOK	AgOAc (3.7)	I ₂ (2.2)	II	>99	>20:1
8	BzOH	AgOAc (3.7)	I ₂ (2.2)	II	68	>20:1
9 ^a	BzOH	AgOAc (3.7)	I ₂ (2.2)	II	>99	>20:1

Product distribution and yield determined by ¹H NMR spectroscopy. ^a Et₃N (1 equiv).

The optimization described in Table 2 presents a simplified view of the key findings from a total of 121 conditions investigated.⁵⁷ To reinforce the discussion of reagent effects on selectivity, two further optimization tables are presented. The nature of the silver salt used was shown to be crucial for regioselectivity (Table 3). Silver salts such as AgOAc, Ag₂CO₃ and Ag₂O provided good selectivity for *ortho*-functionalization, while silver salts having weakly coordinating counterions, such as in AgSbF₆ and AgNTf₂, gave, in addition to **2a**, 3-iodobenzoic acid (**2a''**), formed through a non-catalyzed S_EAr pathway.

Table 3. Effect of the silver additive on regioselectivity and yield.

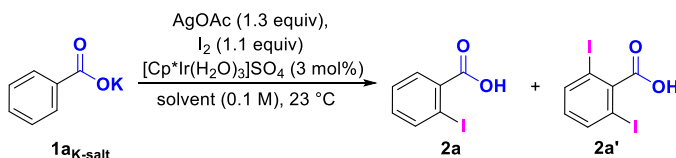


Reaction scheme: 1a_{K-salt} (benzoic acid potassium salt) reacts with Ag(I), I₂, [Cp*Ir(H₂O)₃]SO₄ (3 mol%), and HFIP (0.1 M) at 23 °C for 15 h to produce 2a (2-iodobenzoic acid), 2a' (2,6-diiodobenzoic acid), and 2a'' (4-iodobenzoic acid).

Entry	Ag(I) (equiv)	I ₂ (equiv)	2a:2a':2a''	Yield (%)
1	AgOAc (2.3)	1.2	>20:1:0	91
2	Ag ₂ CO ₃ (1.2)	1.2	>20:1:0	85
3	Ag ₂ O (1.2)	1.2	>20:1:0	85
4	AgSbF ₆ (2.3)	1.2	1:0:2	71
5	AgNTf ₂ (2.3)	1.2	2:0:1	74

Product distribution and yield determined by ¹H NMR spectroscopy.

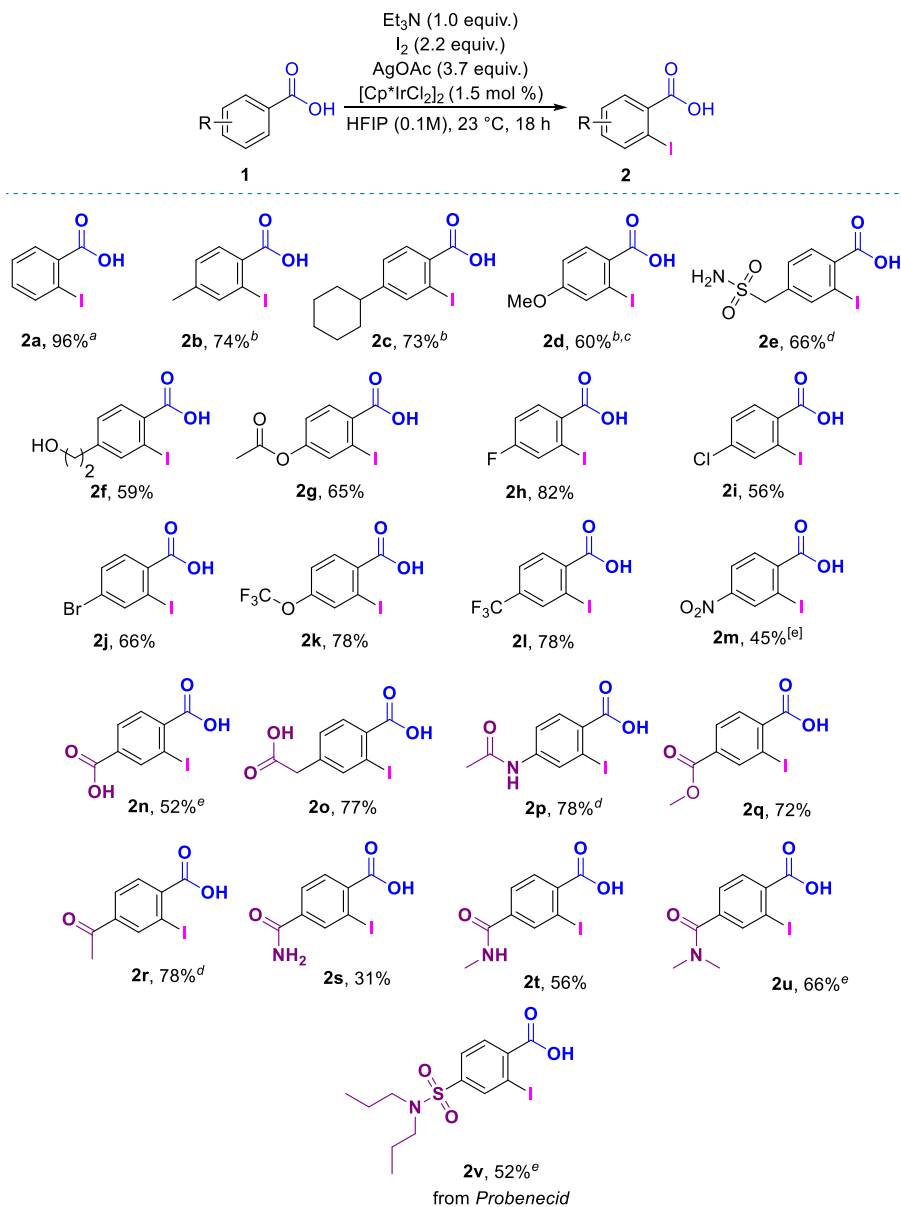
Another key component to the developed method was the use of 1,1,1,3,3,3-hexafluoroisopropanol as the solvent. Most tested solvents provided no conversion at all (Scheme 4). 2,2,2-Trifluoroethanol (TFE, Entry 5) was the only other solvent in which conversion was observed, albeit with lower yield and selectivity than when using HFIP.



Scheme 4. Solvent effect on the C–H iodination reaction. No conversion with CH₂Cl₂, CHCl₃, THF and AcOH. In TFE 51% yield (2:1 selectivity). In HFIP 89% yield (13:1 selectivity).

2.2.2 Scope

With the optimized reaction conditions in hand (Scheme 5, top), the reaction scope and limitations were investigated. A broad array of *para*-substituted benzoic acids were monoiodinated with near perfect monoselectivity and exclusive functionalization of the *ortho* C–H bond (Scheme 5). In all cases, with the exception of **2d** (4-OMe, 14:1) the mono:di ratio was of >20:1, with unreacted starting material accounting for most of the remaining mass balance. The importance of this high selectivity was underlined by the parent compound **2a**, which was obtained as an inseparable mixture with 2,6-diiodobenzoic acid **2a'** in a ratio of >20:1.



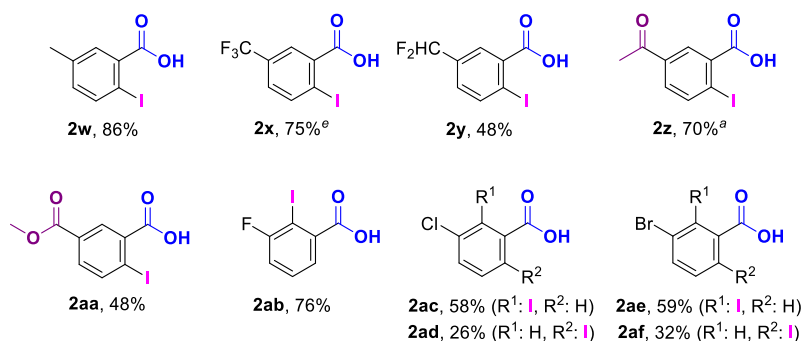
Scheme 5. Scope: Monoiodination of para substituted benzoic acids. Isolated yields shown.

^a Isolated as mono/disubstituted mixture, >20:1 mono/di ratio. ^b Reaction time 2 h. ^c Mono/di ratio 14:1. ^d $[\text{Cp}^*\text{IrCl}_2]_2$ (2.5 mol%), AgOAc (3.8 equiv.). ^e $[\text{Cp}^*\text{IrCl}_2]_2$ (3.0 mol %), AgOAc (3.8 equiv.). Potential competing DGs highlighted in purple.

Substrates bearing electron-donating substituents were readily iodinated to provide the desired products **2b-2d**. The carboxylic acid functionality in **2e**, as well as the Lewis-basic primary sulfonamide in **2f**, did not affect the reac-

tion outcome. Neither did the presence of the free hydroxyl group on **2g**. Halides were compatible with the reaction conditions, giving rise to synthetically attractive dihalogenated compounds **2h-2j**. Electron withdrawing groups such as the trifluoromethoxy **2k**, trifluoromethyl **2l**, and nitro **2m** were tolerated. Interestingly, terephthalic acid afforded the monoiodinated product **2n** rather than the expected 2,5-diiodoterephthalic acid. Importantly, high regioselectivity was also observed in the presence of other coordinating groups commonly used as directing groups in C–H functionalizations (Scheme 5).¹³ The acetamide directing group was well tolerated, providing **2o** with no observed iodination *ortho* to the acetanilide. Similarly, the ester functional groups in **2p** and **2q**, as well as the ketone in **2r**, did not serve as competing directing groups under these mild reaction conditions. Even strongly coordinating functional groups like primary, secondary and tertiary amides (**2s-2u**) were tolerated. The method was also successfully applied to the late-stage functionalization (LSF) of Probenecid, a therapeutic agent used for the treatment of gout,⁵⁹ providing the iodo-analogue **2v** in a synthetically useful yield.

While this methodology was developed for the selective monoiodination of *para* substituted benzoic acids, a series of *meta* substituted benzoic acids were shown to be equally competent substrates (Scheme 6). Iodination of 3-toluic acid provided the expected product **2w** in high yield. Electron poor fluorinated products **2x** and **2y** were readily obtained. The potential competing directing groups in **2z** and **2aa** did not interfere with the expected regioselectivity.



Scheme 6. Scope: *Meta* substituted benzoic acids. Isolated yields shown. ^a [Cp*IrCl₂]₂ (3.0 mol %), AgOAc (3.8 equiv.). Potential competing DGs highlighted in purple.

3-fluorobenzoic acid was iodinated in the 2-position in agreement with previously published results,³⁹ providing **2ab**. Interestingly, the iodination of 3-chloro- and 3-bromobenzoic acids provided mixtures of 2- and 6-iodinated products **2ac-2af**, both with high monoselectivity, with the more sterically congested 2-iodo derivative being the major product in both cases. The observed regioselectivity is potentially the result of an interaction between the

catalyst and the electron pairs of the Lewis-basic substituents in the *meta* position. When the Lewis-basic moiety is one carbon further away from the aromatic system, the expected less sterically congested regioisomer can be obtained as a single product (**2x–2aa**).

An increase of catalyst loading resulted in improvements of conversions for some substrates (Schemes 5 and 6). However, further increase of the catalyst loading did not lead to full conversion, and in some cases, this even led to a diminished selectivity.

2.2.3 Mechanistic Studies

Considering the unprecedented levels of selectivity displayed by the catalytic system, we turned our attention to rationalizing its origin. Figure 10 shows the kinetic profile of the catalytic transformation. We observed no significant formation of diiodinated product **2a'** irrespective of reaction times. Only trace amounts of **2a'** were detected even after 72 h (not shown), which further demonstrates the robustness of this methodology with respect to selectivity.

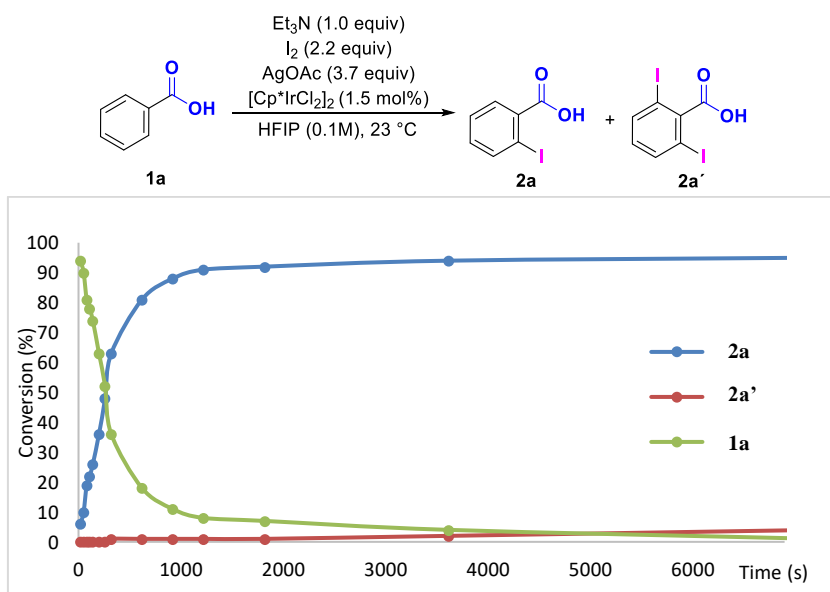
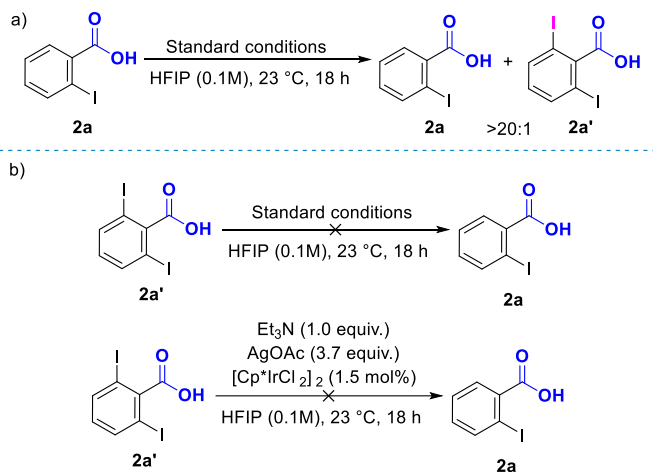


Figure 10. Kinetic profile of the C–H monoiodination of **1a**. Note that even after prolonged time no major formation of the diiodinated **2a'** is observed.

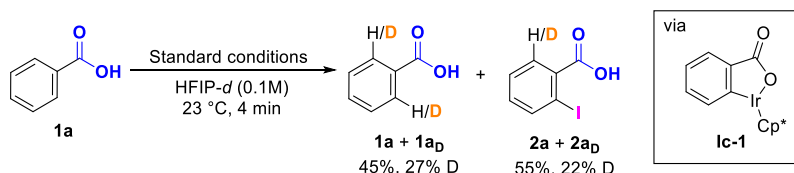
Even when the product, 2-iodobenzoic acid (**2a**), was subjected to the standard reaction conditions, only a trace amount of **2a'** was formed (Scheme 7, a). To rule out a carbon-iodine bond cleavage as a contributing factor to the selectivity,

ity, 2,6-diiodobenzoic acid (**2a'**) was subjected to the standard reaction conditions, both in the presence and in the absence of iodine (Scheme 7, b). After 18 h, 2-iodobenzoic acid (**2a**) was not detected in the reaction mixtures, indicating that the C–I bond is not cleaved under the reaction conditions.



Scheme 7. a) Diiodination study. b) C–I cleavage study. Standard conditions: Et₃N (1.0 equiv.), I₂ (2.2 equiv.), AgOAc (3.7 equiv.), [Cp*IrCl₂]₂ (1.5 mol%).

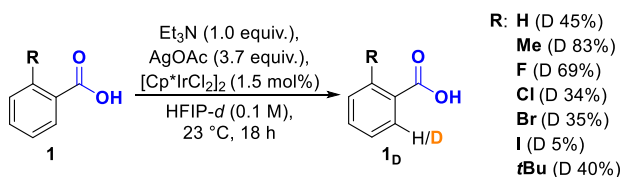
We next hypothesized that reversibility of the C–H activation step could play a role in the observed selectivity. An acetate-assisted concerted metalation-deprotonation (CMD) pathway for a similar iridium-catalyzed C–H activation has previously been proposed by Ison when using methanol as the solvent, and in this case no protodemetalation of the iridacycle was described.⁶⁰ Stirring **1a** in deuterated HFIP under otherwise standard reaction conditions for 4 min resulted in a significant amount of deuterium incorporation in both the starting material **1a** and product **2a** (Scheme 8). This is strong evidence that the iridacycle (**Ic-1**) formed via C–H activation does undergo protodemetalation under the reaction conditions and its formation is reversible.



Scheme 8. Deuterium incorporation study. Standard conditions: Et₃N (1.0 equiv.), I₂ (2.2 equiv.), AgOAc (3.7 equiv.), [Cp*IrCl₂]₂ (1.5 mol%).

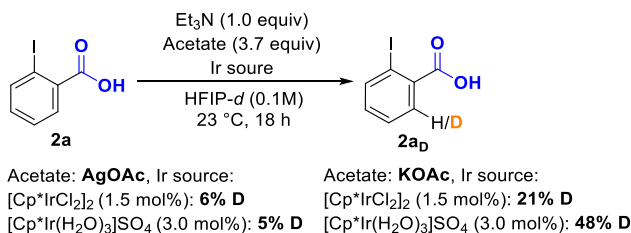
This key observation was further utilized in studying how the C–H activation is affected by several different *ortho* and *para* substituents. Subjecting **1a** to the standard reaction conditions, albeit in absence of iodine, and using

HFIP-*d*, led to 45% deuterium incorporation at the *ortho* positions (Scheme 9). Deuterium incorporation occurs with complete regioselectivity in the positions *ortho* to the carboxylate functionality.⁵⁷ Applying the same experimental set-up to a series of *ortho*-substituted analogues gave a varied deuterium incorporation, depending on the nature of the substituent (Scheme 9). While relatively high incorporation was observed with the methylated material, incorporation was lower with the fluorinated substrate (Scheme 9), and a further decrease was observed for the chloro- and bromo-substituted substrates. The lowest incorporation was observed for the 2-iodo compound (Scheme 9). From the observed 40% deuterium incorporation with the *t*Bu-substituted benzoic acid, it was clear that the lower incorporation of D in the reaction of **2a** is not caused solely by steric effects.



Scheme 9. Deuterium incorporation study: *ortho*-substituent effect.

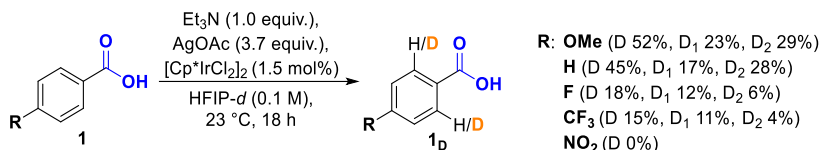
We speculated that the observed decrease in deuterium incorporation in the halide series might be a result of an unprecedented Ag(I) effect. To probe this, a comparison study was conducted using AgOAc and KOAc in separate experiments (Scheme 10). Both precatalysts from the initial studies were tested. In this study a clear suppression of deuterium incorporation was shown when AgOAc was used, while deuterium was incorporated to a larger extent when KOAc was used as a control.



Scheme 10. Ag(I) effect study. Comparison of AgOAc (left) and KOAc (right) as additives. Deuterium incorporation established by ¹H NMR.

The extent of deuterium incorporation was also studied with a number of *para* substituted substrates. Deuterium incorporation to a far larger extent was observed with *p*-MeO- (**1d**) and unsubstituted (**1a**) benzoic acids (Scheme 11), than with substrates bearing electron-withdrawing groups. Interestingly, while the fluoro- and trifluoromethyl-substituted derivatives showed only modest

deuterium incorporation, they afforded the corresponding iodinated compounds in good yields when the reactions are run in the presence of I₂ (*vide supra*, Scheme 5, **2h** and **2l**). Even the nitro-substituted material, which showed no deuterium incorporation, was iodinated in synthetically useful yields (Scheme 11). This shows that substrate electronics can influence the reversibility of the C–H activation step in the C–H iodination reaction.



Scheme 11. Deuterium incorporation study: *para* substituent effect. D incorporation established by ¹H NMR. D₁ and D₂ compound ratio quantified by HRMS, adjusted to ¹³C content.

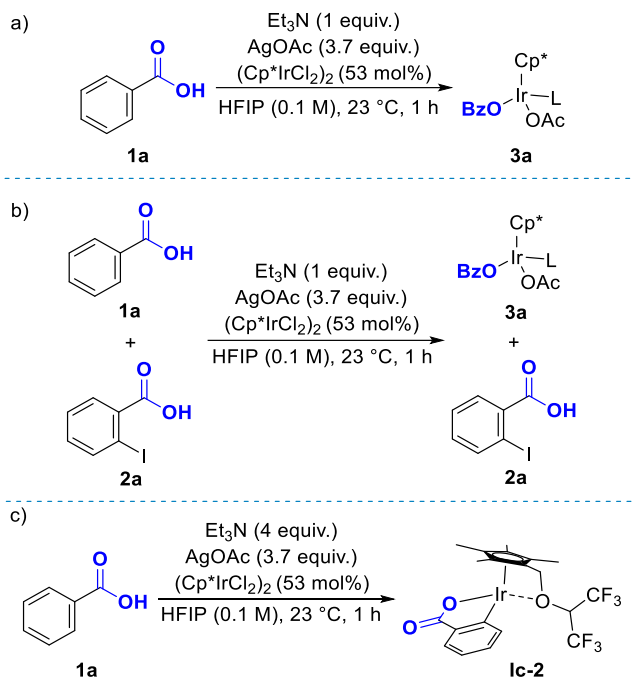
We next turned our attention towards identifying the resting state of the catalytic cycle. Previous work by our group on iridium catalyzed C–H iodination with NIS had indicated that a 2-iodobenzoic acid bound to the iridium center was the resting state.³⁹ We hypothesized this was an unlikely resting state in the current work, as the selectivity would not have been high towards the moniodination product **2a**. We performed a selection of control experiments (Scheme 12). When benzoic acid (**1a**) was treated with a stoichiometric amount of the iridium catalyst in absence of iodine (Scheme 12, a), the chemical shift of the carbonyl signal did not match the standards (Table 4, Entries 1 and 2), and complete disappearance of the signal was observed by ¹³C NMR spectroscopy (Entry 3). Signal reappearance was observed when a HMBC experiment, conducted at 50 °C, was executed, with a chemical shift different from the standards (Entry 4, for standards see Entries 1 and 2).

Table 4. Resting state study.

Entry	Composition	¹³ C shift carboxylate	Note
1	BzOH, HFIP	170.4	
2	BzOH, HFIP, Et ₃ N	176.5	
3	Reaction mixture (Scheme 12, a)	Missing (broad)	Not detected by HMBC
4	Reaction mixture (Scheme 12, a)	173.9	HMBC, 50 °C

Comparison of standards (Entries 1 and 2) to reaction conditions (entry 3 and 4, according to Scheme 12, a).

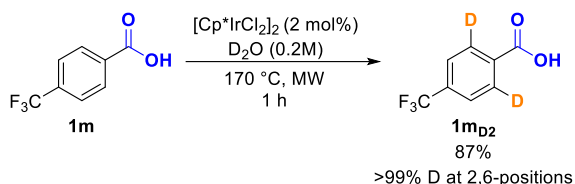
This observation indicates coordination of the substrate molecule to iridium and formation of a complex undergoing dynamic structural changes, possibly changes in coordination mode of ligands. A general representation of such a complex is presented with **3a**.



Scheme 12. Catalyst resting state investigation. a) Formation of proposed resting state with structure **3a**. Change in ^{13}C carbonyl shift of the substrate observed. b) Competitive reaction of **1a** with **2a**. Complete incorporation of **1a** observed, while **2a** remained unchanged. c) Experiment with excess base resulting in the formation of catalytically inactive iridacycle **Ic-2**.

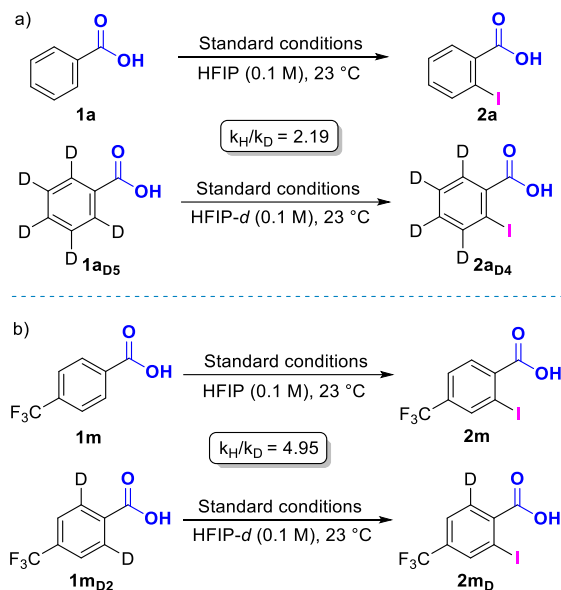
Next, benzoic acid (**1a**) and 2-iodobenzoic acid (**2a**) were applied in a competition experiment, again with a stoichiometric amount of iridium catalyst and in absence of iodine (Scheme 12, b). Complete disappearance of the carbonyl signal from benzoic acid (**1a**) was observed by ^{13}C NMR, consistent with the previously obtained results (Scheme 12, a), while the 2-iodobenzoic acid (**2a**) carbonyl signal remained unchanged. In combination, the experiments shown in Scheme 12, together with the observed selectivity, indicate that the resting state of the catalytic cycle is a benzoic acid bound to the iridium center, such as **3a** (Scheme 12), where L may be an oxygen from a μ_2 bound acetate, as reported by Ison.⁶⁰ In the process of identifying the catalyst resting state, an excess of Et_3N was added to a reaction mixture containing a stoichiometric amount of iridium catalyst (Scheme 12, c). This resulted in the formation of iridacycle **Ic-2** as the major species, which was isolated and characterized by NMR spectroscopy. However, when using complex **Ic-2** instead of $[\text{Cp}^*\text{IrCl}_2]_2$ as the catalyst, under otherwise identical reaction conditions, conversion was not observed. Thus, **Ic-2** is not an active catalytic intermediate, but rather a potential catalyst deactivation pathway.

Next, we turned our attention towards identifying and studying the nature of the turnover-limiting step of the catalytic cycle. For this, a kinetic isotope effect (KIE) study using parallel experiments was conducted.⁶¹ As differences in the extent of deuterium incorporation, and thus the reversibility of the potentially turnover-limiting C–H activation step were observed (Scheme 11), two distinct substrates were chosen for the study. While benzoic acid **1a** and its deuterated analogue **1a_{D5}** were commercially available, the deuterated analogue of **1m** (**1m_{D2}**) was not. For this reason, we developed an *ortho*-deuteration methodology utilizing the commercially available [Cp*IrCl₂]₂ precatalyst and D₂O as the deuterium source (Scheme 13).



Scheme 13. C–H deuteration methodology developed for the synthesis of the isotope-labelled compound **1m_{D2}** required for the KIE study.

After one hour in a microwave reactor at 170 °C, the desired compound was obtained with deuterium incorporation selectively *ortho* to the carboxylate.



Scheme 14. KIE investigations. Parallel experiments.⁶¹ a) Benzoic acid b) 4-(trifluoromethyl)benzoic acid. Standard conditions: Et₃N (1.0 equiv.), I₂ (2.2 equiv.), AgOAc (3.7 equiv.), [Cp*IrCl₂]₂ (1.5 mol%).

With **1a** and **1a_{D5}** as substrates a k_H/k_D value of 2.19 was obtained (Scheme 14, a). This relatively low value indicates that the C–H activation is partially rate determining for **1a**. With the C–H activation step for this substrate being reversible to a large extent, as previously shown (Scheme 8), we hypothesize that the turnover-limiting step for this substrate is a combination of the C–H activation and the subsequent oxidative addition (Figure 11). On the other hand, for **1m** and **1m_{D2}**, a k_H/k_D value of 4.95 was obtained (Scheme 14, b), indicating that the C–H bond is broken in the turnover-limiting step. Thus, the turnover-limiting step in the catalytic cycle is proposed to be dependent on the electronic properties of the substrate.

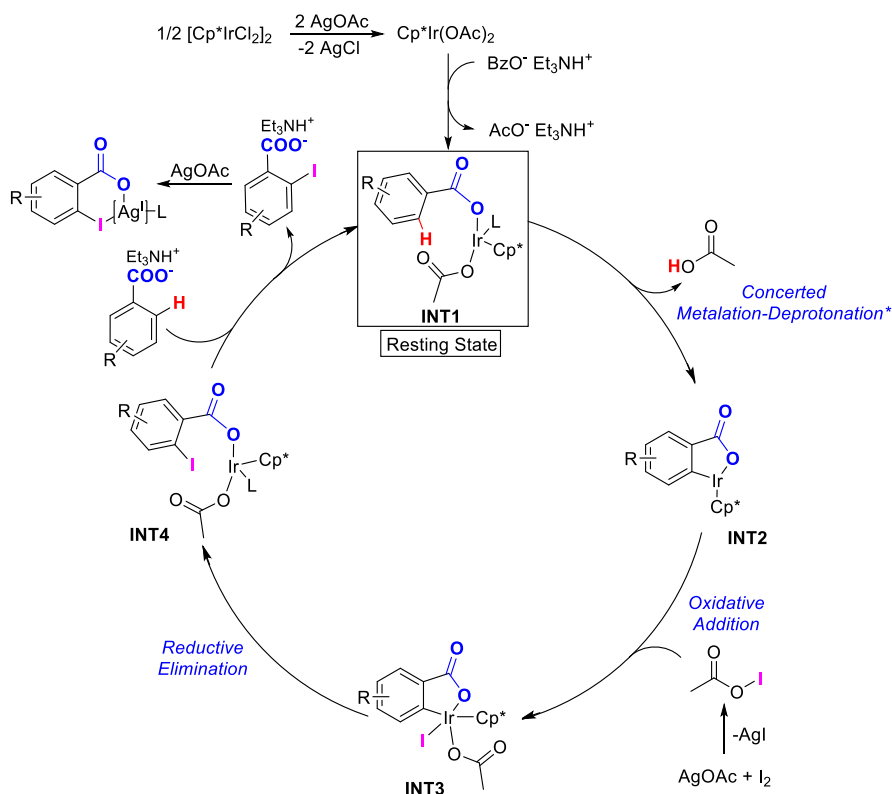


Figure 11. Proposed catalytic cycle for the Ir-catalyzed monoselective iodination. *C–H activation step substrate-dependent reversibility via protodemetalation.

With the insights from the mechanistic studies we propose the following catalytic cycle (Figure 11). The complex $[\text{Cp}^*\text{IrCl}_2]_2$ is activated by AgOAc to form the $[\text{Cp}^*\text{Ir}(\text{OAc})_2]$.⁶² After ligand exchange, **INT1** is formed, which is also proposed to be the resting state of the catalytic cycle as indicated by ^{13}C studies. The C–H activation step likely occurs *via* an acetate-mediated CMD,

providing the iridacycle **INT2**. This step is essentially irreversible for electron-poor substrates such as 4-trifluoromethylbenzoic acid **11**, and it is also the turnover limiting step as indicated by the large KIE ($k_{\text{H}}/k_{\text{D}} = 4.95$). For more electron-rich substrates, such as **1a**, the CMD is reversible to a greater extent *via* protodemetalation, and the lower KIE ($k_{\text{H}}/k_{\text{D}} = 2.19$) is observed. AgOAc and I₂ form AcOI, as previously described,⁵⁸ which then undergoes an oxidative addition to **INT2** resulting in the formation of an Ir(V) iridacycle, **INT3**. Reductive elimination from this complex yields the metal-bound product in **INT4**, which after ligand exchange closes the cycle regenerating **INT1**. After the product release, the interaction of the product with Ag(I) is proposed, forming a coordination complex inhibiting the activation of the *ortho*-C–H bond.

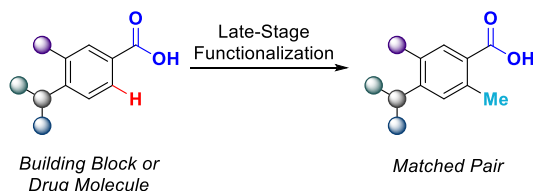
2.3 Conclusions

The presented C–H iodination methodology offers access to *ortho*-monoiodinated benzoic acids, with an emphasis on *para*-substituted, sterically unbiased substrates. For the substrates studied, their intrinsic reactivity through S_EAr iodination was completely suppressed. The clean reaction profile allows for straightforward purification of the products. The mechanistic studies conducted showed a substrate-dependent turnover-limiting step, a potential resting state of the catalytic cycle, and a profound effect of the silver additive on selectivity. A catalytic cycle was proposed based on these results. While a relatively broad substrate scope for this transformation was demonstrated, the methodology is limited to the use of substrates not undergoing S_EAr reactions with AcOI. This was observed with LSF attempts on Telmisartan and Tamibarotene, where the desired *ortho*-iodination was accompanied by iodination of other aryl systems.

3. Iridium-Catalyzed C–H Methylation and d_3 -Methylation of Benzoic Acids with Application to Late-Stage Functionalization (Paper II)

3.1 Background

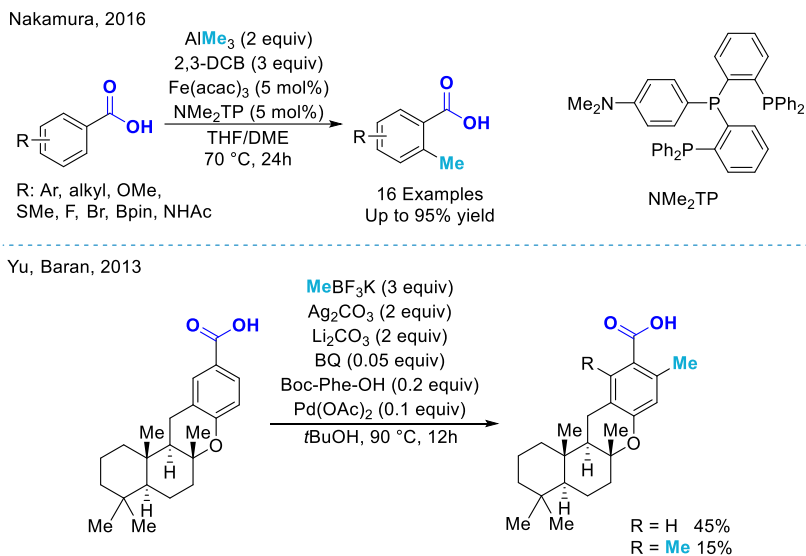
As late-stage functionalization was one of our ultimate goals for this work (Scheme 15), we decided to circumvent the limitations observed with the iodination methodology by excluding the use of electrophilic reagents altogether. Instead, we focused our attention to methodologies involving transmetallation and presence of oxidants.



Scheme 15. General representation of molecular matched pair synthesis via late-stage methylation.

C–H methylation was chosen as the targeted reaction, as this transformation is highly desirable within medicinal chemistry.^{63–65} Substitution of a single C–H to C–Me can have a profound positive effect on pharmaceutical properties of drug candidates,⁶³ by modulating, among others, metabolic stability,⁶⁶ solubility,⁶⁷ off-target selectivity,⁶⁸ effects on binding mode,⁶⁹ and target affinity.⁶ Prompted by the potential impact of this transformation, a number of approaches for late-stage C–H methylations have been developed over the recent years.^{7,51,65,70} While methodologies for directed C–H methylations of benzoic acids have been reported, these for the most part lacked applicability to complex drug-like molecules.^{71,72} Nonetheless, some exceptional reported applications demonstrate the opportunities behind this transformation. In 2016, Nakamura and co-workers reported the iron-catalyzed C–H methylation of aromatics bearing carbonyl groups, including benzoic acids (Scheme 16).⁷³

While the utilization of a non-precious metal catalyst in combination with the substrate scope containing a range of directing groups make this work highly important, the report lacks applications to pharmaceuticals, and does not discuss the scenario where multiple directing groups would be present in the same molecule. An impressive application of late-stage C–H methylation for synthesis of the natural product Hongoquercin A and its analogues was reported in 2013 by Baran, Yu and coworkers (Scheme 16).



Scheme 16. Selected work on C–H iodination of benzoic acid by Nakamura,⁷³ Yu and Baran.⁷⁴

Based on the good functional group tolerance in our iodination work, we hypothesized that a suitable method utilizing a catalytic system based on $[\text{Cp}^*\text{Ir}(\text{III})]$ could greatly complement available methodologies. We were inspired by work from Chang and co-workers,^{75,76} who showed that C–H arylation and alkylation of aromatics can be facilitated by Rh and Ir catalysts, *via* a (III)→(IV) and (III)→(IV)→(IV) stepwise oxidation facilitated by Ag(I) oxidants. In order to achieve high functional group tolerance and applicability for LSF, a benign methyl source would be required.

3.2 Results and Discussion

3.2.1 Optimization

The optimization was carried out in 3 cycles, each with a different substrate. As these studies were extensive (131 experiments)⁷⁷ and complex in their outcome, only selected key parts are discussed here. In the first round of optimization, benzoic acid was selected as the model substrate with the goal of achieving selective monofunctionalization. [Cp*IrCl₂]₂ was chosen as catalyst and HFIP as solvent based on our previous iodination studies (Chapter 2).⁵⁷ MeBF₃K, a commercially available, bench stable reagent, was chosen as methyl source.

Table 5. Oxidant screening for the C–H methylation.

Reaction scheme: Benzoic acid (3a(K-salt)) reacts with MeBF₃K (2.0 equiv), Oxidant (2.0 equiv), [Cp*IrCl₂]₂ (4 mol%), HFIP (0.15 M) at 80 °C for 16 h to yield 4a and 4a'.

Entry	Oxidant	Conversion (%) ^a	4a:4a'
1	AgF	NR	-
2 ^a	Ag ₂ O	26	2.5:1
3	AgOAc	30	3.5:1
4 ^a	Ag ₂ CO ₃	62	8.0:1
5	PhI(OAc) ₂	NR	-
6	AgNTf ₂	5	-
7	MnF ₃	NR	-
8	MnOAc ₃	NR	-
9	NFSI	NR	-
10	Cu(OAc) ₂	NR	-
11	K ₂ S ₂ O ₈	38	6.3:1
12	Selectfluor	NR	-

Conversions determined by SFC-MS (UV trace). ^a1.0 equiv. oxidant used.

An important point to note was the change of analytical method from NMR to supercritical fluid chromatography - mass spectrometry (SFC-MS). This allowed for expedient reaction analysis, without the need of work-up prior to sample preparation, and decreased analysis and interpretation time. The oxidant screening revealed superior performance of Ag₂CO₃ (Table 5, entry 4) compared to the other oxidants. The utility of silver oxidants for C–C bond formation *via* the anticipated oxidatively induced reductive elimination was consistent with the results reported by the Chang group,⁷⁵ and the exceptional performance of Ag₂CO₃ for directed C–H methylations consistent with the

results published by Johansson, Ackermann and coworkers.⁵¹ Similar to the iodination methodology, the solvent screening conducted for the methylation revealed superior results for HFIP (62% conversion, Table 6, Entry 8), with the second-best result observed in TFE (Table 6, entry 3). Out of the other 13 tested solvents only MeOH showed trace product formation (Entry 13).

Table 6. C–H methylation solvent screening.

$\text{3a}_{(\text{K-salt})} \xrightarrow[\text{solvent (0.15 M), 80 } ^\circ\text{C, 16 h}]{\text{MeBF}_3\text{K (2.0 equiv), Ag}_2\text{CO}_3 \text{ (1.0 equiv), [Cp}^*\text{IrCl}_2\text{]}_2 \text{ (4 mol\%)}}$
 $\text{4a} + \text{4a'}$

Entry	Solvent	Entry	Solvent	Entry	Solvent
1	2-MeTHF (NR)	6	MeCN (NR)	11	DMSO (NR)
2	DCE (NR)	7	H ₂ O (NR)	12	DMF (NR)
3	TFE (20%)	8	HFIP (62%)	13	MeOH (7%)
4	PhCF ₃ (NR)	9	Acetone (NR)	14	PhH (NR)
5	Dioxane (NR)	10	IPA (NR)	15	NMP (NR)

Conversions determined by SFC-MS (UV trace). Conversions in parentheses.

Gas formation was observed with successful and many unsuccessful reactions. We were able to confirm the presence of methane by ¹H NMR spectroscopy, by analyzing the overhead atmosphere of the reaction. This led to the hypothesis that the conversion is limited by the decomposition of MeBF₃K. To test this, a series of seven experiments were set up under identical conditions, and after 90 min different combinations of reaction components were added (Table 7). Indeed, increased conversion was consistently observed in entries where MeBF₃K was added (Table 7, Entries 3,5 and 7). Highest increases of conversion were observed in experiments where additional catalyst was also introduced (Entries 4 and 7). By this point of the study we observed a lack of reproducibility in reactions performed under identical reaction conditions (e. g. Table 7, Entries 1-7 after 1.5 h), as well as in the obtained **4a**:**4a'** ratios. Thus, we abandoned the efforts for monomethylation of sterically unbiased substrates.

In the second round, *ortho*-toluic acid was used as a model system. This round of optimization ultimately led to a method utilizing the corresponding benzoic acids as the starting material instead of the potassium salt. The introduction of a base additive (K₂HPO₄ identified as best performing) significantly decreased the amount of gas generated in the reaction and improved reproducibility in terms of conversion. A prestirring period of 1 h in absence of MeBF₃K was also found to have a positive effect on conversion.⁷⁷

Table 7. Reagent addition study.

MeBF_3K (2.0 equiv)
 Ag_2CO_3 (2.0 equiv)
 $[\text{Cp}^*\text{IrCl}_2]_2$ (4 mol%)
 HFIP (0.2 M)
 80 °C, 1.5 h
 then + reagents
 80 °C, 2.5 h

$3a_{(\text{K-salt})}$ → $4a$ + $4a'$

Entry	Conv. ^a 1.5 h (%)	+ Reagent	Conv. +2.5 h (%)	Δ%	4a:4a'
1	40	$[\text{Cp}^*\text{IrCl}_2]_2$	44	4	13:1
2	41	MeBF_3K	68	27	3:1
3	38	Ag_2CO_3	41	3	15:1
4	43	$[\text{Cp}^*\text{IrCl}_2]_2, \text{MeBF}_3\text{K}$	95	52	1:1
5	14	$[\text{Cp}^*\text{IrCl}_2]_2, \text{Ag}_2\text{CO}_3$	16	2	-
6	51	$\text{MeBF}_3\text{K}, \text{Ag}_2\text{CO}_3$	63	12	2:1
7	24	$[\text{Cp}^*\text{IrCl}_2]_2, \text{MeBF}_3\text{K}, \text{Ag}_2\text{CO}_3$	85	61	3:1

Conversions determined by SFC-MS (UV trace). Entries with highest conversion increase highlighted.

While a series of one-parameter-at-a-time optimizations failed to deliver reaction conditions with full conversion, a single multiparameter optimization of MeBF_3K loading against Ag_2CO_3 loading was the key to finding high yielding conditions (Table 8).

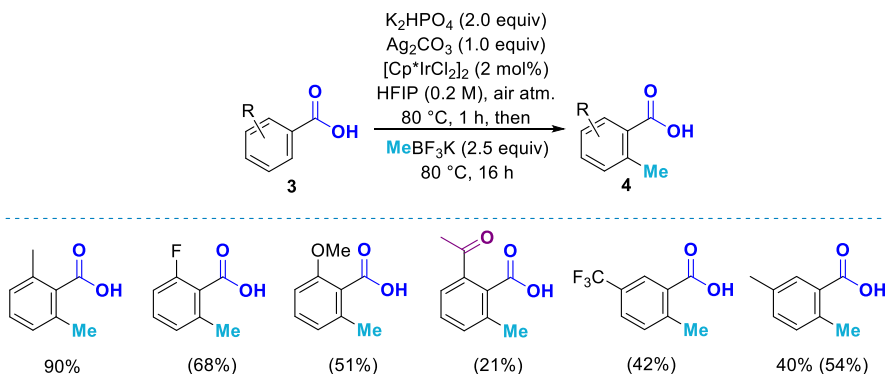
Table 8. Reoptimization for *ortho*-toluic acid.

		Conversion (%)		
MeBF_3K (equiv)	1.0	68	67	54
	2.0	63	84	69
	3.0	>99	84	71
		1.0	2.0	3.0
		Ag_2CO_3 (equiv)		

K_2HPO_4 (2.0 equiv)
 Ag_2CO_3 (x equiv)
 $[\text{Cp}^*\text{IrCl}_2]_2$ (2 mol%)
 HFIP (0.2 M)
 80 °C, 1 h, then
 MeBF_3K (y equiv)
 80 °C, 16 h

$4a$ → $4a'$

Unfortunately, the optimized reaction conditions for *ortho*-toluic acid showed poor conversions with other substrates (Scheme 17).



Scheme 17. Reoptimized conditions. Isolated yields shown. NMR yields in parentheses.

In the third round of optimization, *meta*-toluic acid was chosen as the substrate, and the reaction conditions once again revised after a single multiparameter optimization, this time with increased catalyst loading at 3 mol% (Table 9).

Table 9. Reoptimization for *ortho*-toluic acid.

MeBF ₃ K (equiv)	Conversion (%)		
	2.0	84	94 >99
	2.5	90	>99 >99
	3.0	96	>99 >99
Ag ₂ CO ₃ (equiv)			
	1.0	1.25	1.5

3f **4f**

Finally, we were able to simplify the reaction set-up by eliminating the 1 h prestirring, as under the modified conditions this had no effect on reaction outcome. The final, broadly applicable set of conditions is described in Table 10. To give the reader a better understanding of the reaction characteristics and limitations, a deviation from optimized conditions table is presented. Under the optimized conditions (Table 10, Entry 1) full conversion to product was observed by analytical SFC-MS. When an identical reaction was set up under N₂ atmosphere instead, no conversion was observed. This indicates a crucial role of O₂ in either precatalyst activation or the catalytic cycle itself. Using TFE as the reaction solvent, the second-best solvent from our initial screening (Table 6), a 41% conversion was observed. The iridium precatalyst [Cp*IrCl₂]₂ was found to be crucial, as no conversion was observed with the analogous rhodium complex (Entry 4), nor with a related ruthenium complex (Entry 5). The reaction successfully progressed at decreased temperatures, albeit with significantly lower conversions (Entries 6 and 7). Similarly, lowering the catalyst loading led to decreased conversions (Entries 8 and 9). In the

absence of base, only trace amounts of product were formed (Entry 10), while pressure generation due to the formation of a large amount of gas was observed. One of the major components of the overhead gas was identified as methane by ^1H NMR spectroscopy. During the optimization we found that an excess of the methyl source was needed in order to achieve full conversion. When the MeBF_3K loading was lowered to 1.0 equiv., only 21% conversion was observed (Entry 11). Alternative methyl sources (Entries 12 and 13) showed little or no conversion. K_2CO_3 was used as an alternative base instead of K_2HPO_4 with only slightly lower conversion (Entry 14). Use of alternative Ag(I) oxidants led to lower conversions (Entries 15 and 16).

Table 10. Optimization of the methylation of meta-toluic acids.

Reaction scheme: 3-methylbenzoic acid (**3f**) reacts with K_2HPO_4 (2.0 equiv), Ag_2CO_3 (1.25 equiv), MeBF_3K (2.5 equiv), $[\text{Cp}^*\text{IrCl}_2]_2$ (3 mol%), HFIP (0.1 M), air atm., 60°C , 18 h to produce 3-methyl-4-methylbenzoic acid (**4f**) in 90% yield.

Entry	Deviation from optimized conditions	Conversion (%) (SFC-MS, UV-trace)
1	No change	100
2	Inert atmosphere (N_2)	NR
3	TFE as solvent	41
4	$[\text{Cp}^*\text{RhCl}_2]_2$	NR
5	$[(p\text{-cymene})\text{RuCl}_2]_2$	NR
6	40°C	60
7	23°C	13
8	2 mol% cat.	61
9	1 mol% cat.	11
10	No K_2HPO_4	2
11	MeBF_3K (1 equiv)	21
12	$\text{MeB}(\text{OH})_2$	4
13	Methylboronic acid MIDA ester	NR
14	K_2CO_3 as base (2 equiv)	97
15	AgF (2.5 equiv) as oxidant	6
16	AgOAc (2.5 equiv) as oxidant	25
17	Other RBF_3K (R: Et, nBu, cyclopropyl, vinyl, Ph)	NR

Conversions determined by SFC-MS (UV trace).

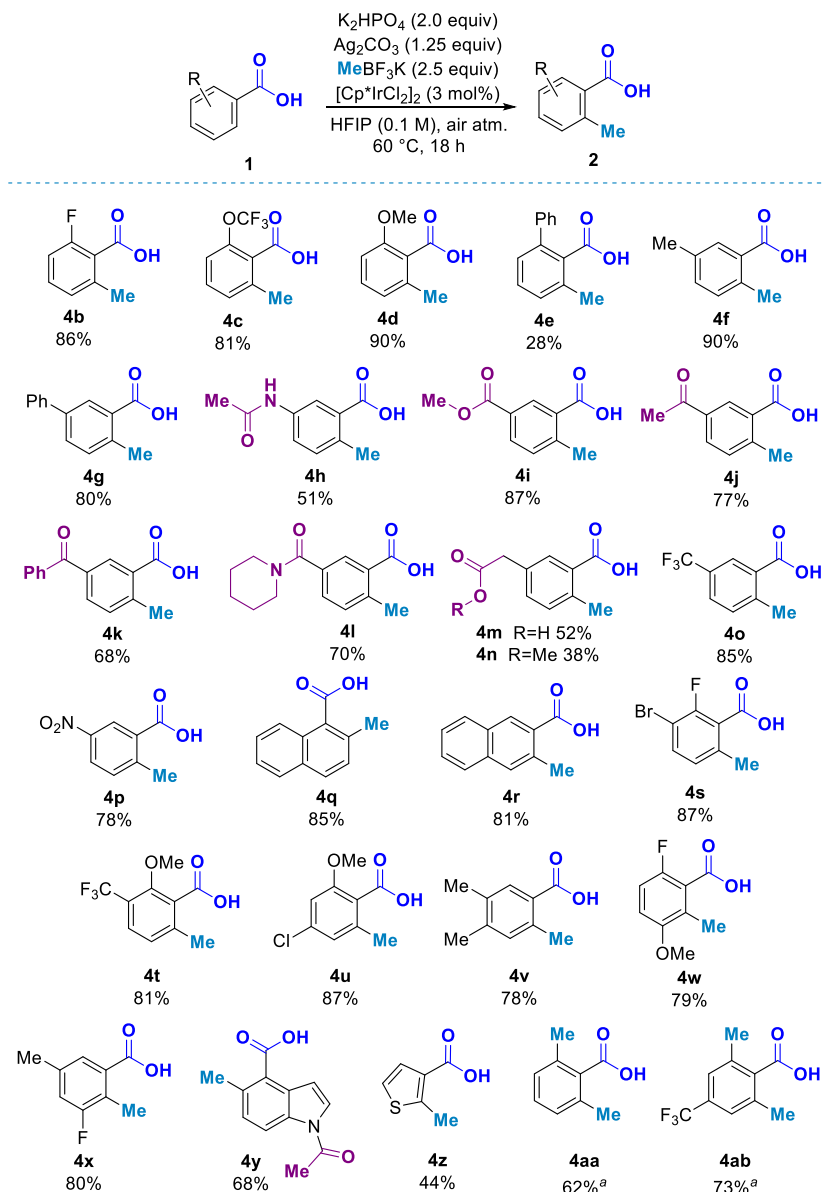
Finally, only methylation could be achieved, and other alkylations, vinylations and arylations were unsuccessful (Entry 17). An important point to be made

at the end of the optimization discussion is the use of automation and miniaturization throughout these studies. The reaction scale in the optimization was decreased from the 0.25 mmol scale in the iodination work to 0.1 mmol without any complications. Further decrease in scale was principle possible, however, we found the 0.1 mmol scale ideal for the use of automation, specifically solid dispensing systems, as the current state-of-the-art dispensing systems perform with excellent accuracy and speed when dispensing in the milligram range. During this project we started using the Quantos powder dispensing system from Mettler Toledo for repeated weighing of solids. The same automation approach was used for weighing out the reactions of the substrate scope, with only the substrates weighed in manually. This allowed the single lab-based chemist in this project to significantly decrease the time spent on weighing reagents, ultimately allowing for higher productivity and reduction of time spent on non-intellectual tasks.

3.2.2 Scope

A series of benzoic acid derivatives bearing electron donating, as well as electron withdrawing groups were successfully methylated (Scheme 18) under the conditions shown in Table 10, Entry 1. Methylated products **4b**, **4c** and **4d** containing *ortho* substituents were obtained in very good yields. Regarding the character of the *ortho* substituent, while the substituent electronics had little effect on the reaction outcome, the apparent limitation was the size of the substituent. The presence of the phenyl substituent in **3e** resulted in a significant decrease in yield, although complete regioselectivity for the methylation at the 6 position was observed. The scope of *meta*-substituted compounds is significantly broader in this respect, as substituent sterics played no significant role in the reaction outcome. Compounds **3f** and **3g** bearing electron donating substituents gave the expected methylation product with the activation of the less sterically hindered C–H bond. A series of compounds bearing two coordinating Lewis-basic groups (plausible directing groups), specifically acetamide **4h**, ester **4i**, ketones **4j** and **4k**, amide **4l**, and carboxylic acid **4m/4n** were methylated with complete regioselectivity for the carboxylate-directed functionalization. All the aforementioned coordinating groups are known to facilitate directed C–H activations.¹³ Interestingly, the methylation of **3m** resulted not only in the formation of the anticipated product **4m**, but also the corresponding methyl ester **4n**. The esterification occurred with complete selectivity for the aryl-carboxylate over the benzylic carboxylate. This reactivity appears to be specific to the substrate, as our studies on the methylation of phenacetic acid under a series of similar conditions yielded no esterification.⁷⁷ The reaction outcome was also unaffected by the presence of electron-withdrawing groups (**3o** and **3p**), and the desired products were obtained in very good yields. The naphthalene **4q** was obtained with complete regioselectivity

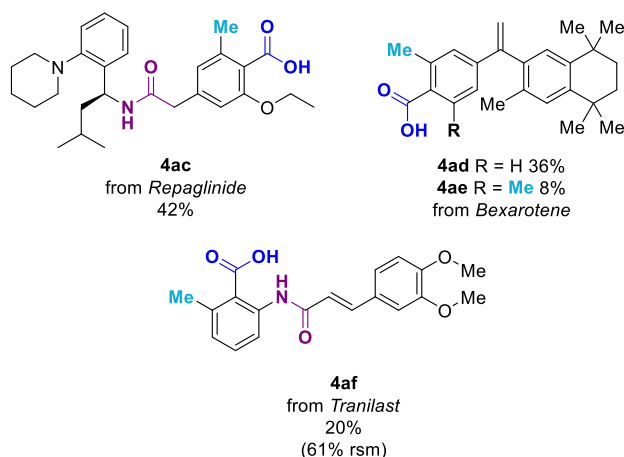
for methylation at the 2 position, suggesting the preferential formation of a 5-membered iridacycle over a 6-membered one in the C–H activation step.



Scheme 18. C–H methylation scope: Building blocks. Isolated yields shown. ^a Ag₂CO₃ (2.5 equiv), MeBF₃K (4.0 equiv). Potential competing DGs highlighted in purple.

Naphthalene **3r** was also successfully methylated at the more sterically accessible 3-position with complete selectivity. Compounds **4s** and **4t** with a 1,2,3,4-substitution pattern were successfully prepared, as well as the 1,2,4,6-

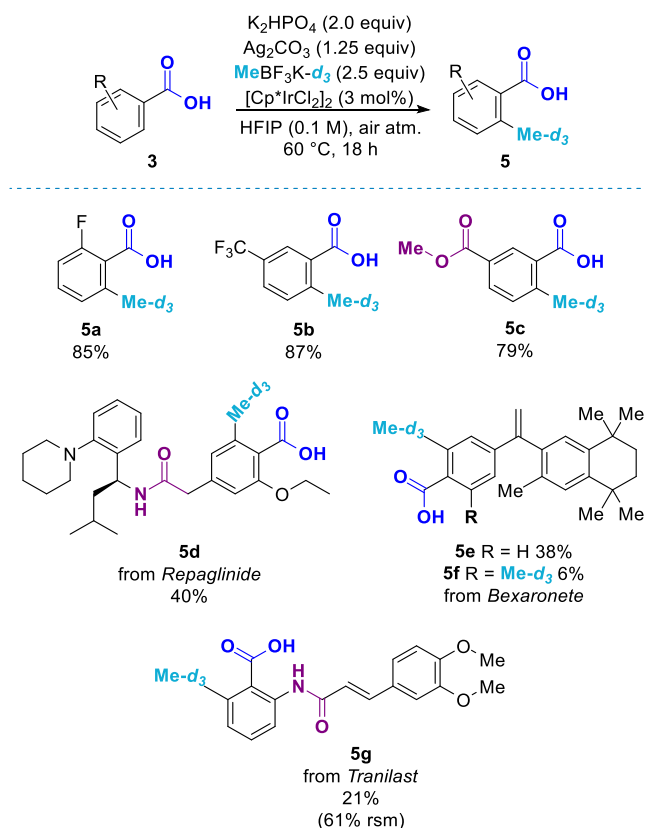
substituted **4u** and the 1,2,4,5-substituted **4v**. Compatibility with the halide series was also demonstrated with these compounds. So far, all the presented examples underwent methylation at a sterically accessible *ortho* position in the absence of a neighboring *meta* substituent. Methylation of the 2-position of substrates bearing 1,3-substitution patterns was possible in two specific cases. With **4w**, when one of the *ortho* positions was blocked, the methyl group was installed in the vicinity the methoxy group. In case of **3x**, both *ortho* positions remained unsubstituted, while the *meta*-positions contained substituents. The methylation product **4x** was obtained with complete regioselectivity in the vicinity of the smaller fluoride substituent. The common feature of these substrates and the requirement for successful 1,2,3-methylation was the presence of non-bonding electron pairs on the 3-position substituents (in this case -F and -OMe). Two applications to the functionalization of heterocycles have also been demonstrated. Indole **3y** was methylated with complete regioselectivity at the 5-position over the 3-position, as well as over the potential acyl- directed product at the 2-position. Thiophene **4z** was methylated at the 2-position with the anticipated C–H activation of the more acidic C–H bond. Finally, the reaction was also applied to the functionalization of benzoic acids with sterically unbiased *ortho*-C–H bonds **3aa** and **3ab**. While we were not able to optimize the reaction towards monomethylation, and enrichment and isolation of the monomethylated product was technically not possible due to poor separation of the mixture, we were able to push the reaction towards dimethylation with synthetically useful yields by increasing the Ag₂CO₃ and MeBF₃K loadings.



Scheme 19. C–H methylation scope: LSF. Isolated yields shown. Potential competing DGs highlighted in purple.

As applications to LSF were our ultimate goal for this methodology, a series of compounds currently used in the clinic were subjected to the standard reaction conditions. Repaglinide, a drug used for blood glucose reduction in type

2 diabetes mellitus,^{78,79} was selectively methylated in the *ortho* position in respect to the carboxylate directing group (Scheme 19, **4ac**), with the integrity of the rest of the molecule retained. Bexarotene, an antineoplastic agent used for the treatment of cutaneous T-cell lymphoma (CTCL),^{80,81} afforded after subjecting to standard reaction conditions the monomethylation product as the major (**4ad**), as well as the dimethylation product (**4ae**) as the minor. The terminal alkene functionality was unaffected by the reaction. Finally, Tranilast, an anti-allergic drug,⁸² also used in treatments of a variety of other diseases,⁸³ was successfully methylated *ortho* to the carboxylate functionality (**4af**). No functionalization directed by the amide moiety was observed. Due to the relatively low yield for this transformation the unreacted starting material was also isolated (61%). The integrity of the functional groups in both starting material and product were maintained after the reaction.



Scheme 20. d_3 -methylation. No D-H exchange was observed in the newly d_3 -methylated positions. Isolated yields shown. Potential competing DGs highlighted in purple.

Building on the success of the methylation reaction, we saw the opportunity to further expand the utility of the methodology by the introduction of an isotope-labelled methyl group, in this case CD_3 . Similar to standard methylation,

d_3 -methylation can vastly improve key properties of a drug candidate.⁸⁴ The difference with the isotope-labelled analogue is typically increased metabolic stability of the newly-acquired methyl group as a result of primary kinetic isotope effect (KIE). The potential benefits have been demonstrated in several studies,⁸⁵⁻⁸⁷ and in 2017 the first deuterated drug, Austedo, was approved by the Food and Drug Administration (FDA).⁸⁸ However, only a limited number of publications concerning C–H to C–CD₃-methylations have been published,^{84,89-91} and to the best of our knowledge, no such method was in the context of benzoic acid functionalization was reported at the time our study was published. To access this transformation, the deuterated methyl source CD₃BF₃K was prepared according to a previously published procedure.⁹² We were pleased to see that when this reagent was used under otherwise standard conditions, d_3 -methylation was observed with essentially identical yields as with the non-isotope labelled methyl trifluoroborate. Thus, compounds **5a**, **5b** and **5c** were obtained (Scheme 20). Furthermore, no D–H exchange was observed under the reaction conditions, providing products with high deuterium content on the methyl group. The d_3 -methylation was also successfully applied to the LSF of Repaglinide, Bexarotene and Tranilast, yielding the corresponding d_3 -methylated products with same regioselectivities and similar yields as their non-deuterated counterparts.

3.2.3 Biological Studies

A series of biological studies with the focus on metabolic stability and clearance was conducted with the parent compounds, methylated and d_3 -methylated analogues of Repaglinide, Bexarotene and Tranilast respectively. The results obtained for Bexarotene and its analogues did not significantly differ (not depicted). This is most likely due to the lipophilic character of the parent compound, to which further methylation did not afford any significant improvement of properties. However, major differences between the analogues and the parent compounds and general improvements in key metabolic studies were observed for the other two drugs (Table 11). First, a decrease in the logD value, and thus decreased lipophilicity was observed for all methylated analogues. This is somewhat surprising, as with the introduction of a non-polar methyl group one would expect the analogue to have a more lipophilic character and increased logD value. This observation is in accordance with a recent C–H methylation report, albeit applied to different directing groups.⁵¹ We speculate that the observed trend is a result of a change in geometry, with the carboxylate twisted out of plane with the methylated analogues. For Repaglinide, reduced clearance, and thus increased metabolic stability of analogues **4ac** and **5d** was observed in both rat hepatocyte and human microsome models (Entries 2 and 3). Furthermore, a significant improvement in metabolic stability was also observed in a human hepatocytes model.

Table 11. Selected results of the of biological studies of parent and modified compounds.

Entry	Structure	Name	logD	Rat Heps CL _{int} (μL/min/ 10 ⁶ cells)	Human Micros CL _{int} (μL/min/mg)	Human Heps CL _{int} (μL/min/10 ⁶ cells)
1		Repaglinide	2.25	26.1	47.3	35.1
2		4ac	1.65	14.4	18.8	10.1
3		5d	1.70	15.2	21.3	-
4		Tranilast	0.15	14.6	<3.0	5.17
5		4af	-0.85	<1.0	<3.0	2.37
6		5g	-0.70	<1.0	<3.0	-

CL_{int} = intrinsic clearance, Rat Heps = rat hepatocytes, Human Micros = human microsomes, Human Heps = human hepatocytes.

For Tranilast, significant increase in metabolic stability was observed in rat hepatocytes, while no change was observed in a human microsome model (Entries 5 and 6). Increased metabolic stability was observed for **4af** and **5g** in human hepatocytes.

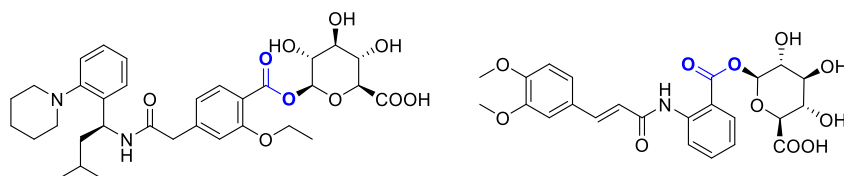


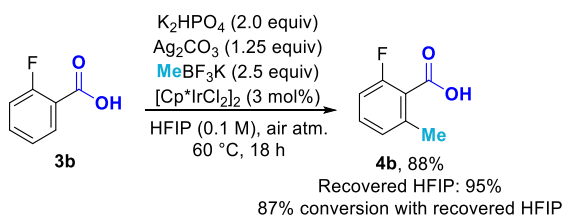
Figure 12. Left: Repaglinide glucuronidation product, significant metabolic degradation pathway.⁹³ Right: Tranilast glucuronidation product – major metabolite.⁹⁴

Both drugs are known to undergo glucuronidation as a metabolic pathway (Figure 12). While minor, yet significant for Repaglinide,⁹³ this pathway constitutes the major deactivation pathway for Tranilast.⁹⁴ A metabolite identi-

cation (MetID) study revealed complete inhibition of glucuronidation for analogue **2ae**, while control experiment confirmed the glucuronidation product of Tranilast as expected.⁷⁷ Identification of secondary metabolites of the Repaglinide analogue **2ab** was repeatedly unsuccessful due to low ionization of the obtained metabolites. We hypothesize that the decreased clearance for the analogues is at least partially due to inhibition of UDP-glucuronosyltransferase binding by the introduction of steric bulk in form of the methyl substituent. No significant differences between the CH₃- and CD₃-analogues have been observed for these particular examples (Entries 2 vs 3, Entries 5 vs 6). This is perhaps not surprising, as differences would only be observed for the methyl functionalities being metabolic hotspots, which was not expected to be the case for these analogues. However, a scenario where the introduction of these groups would result in the formation of metabolic hotspots is not unlikely.⁹⁵

3.2.4 Solvent Recovery and Recycling

Aware of the challenges of sustainability and environmental concerns over the use of solvents in chemistry,⁹⁶ the possibility of solvent recovery and recycling was investigated. The fact that only non-volatile reagents were present in the reaction mixture made this an excellent candidate for solvent recovery *via* distillation. On a 1.0 mmol scale, 95% of the solvent was successfully recovered after distillation with satisfactory purity (determined by ¹H NMR), with the reaction yielding 88% of product in accordance to previous results (Scheme 21). The recovered solvent was reused directly for the same reaction, with maintained performance and isolated yield of 87% of the desired product.



Scheme 21. Successful solvent recovery and recycling study.

3.3 Conclusions

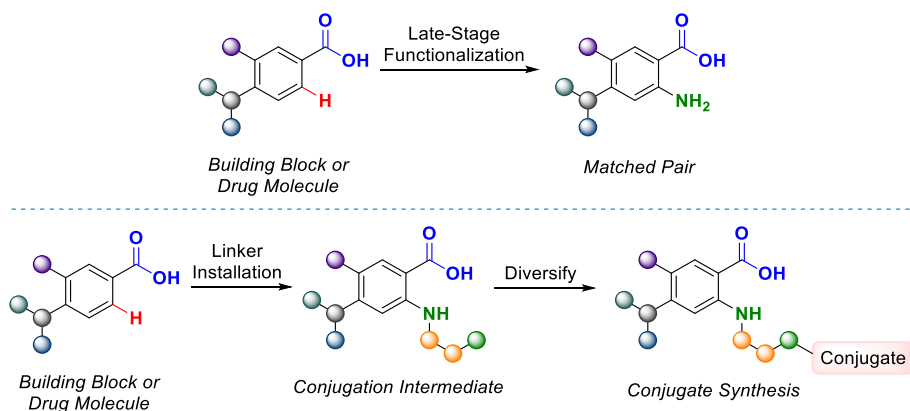
A C–H methylation method has been developed and successfully applied for the transformation of a diverse series of substrates, including marketed drugs. For the substrates studied, complete selectivity for *ortho*-functionalization in respect to the carboxylate directing group was achieved, even in presence of other directing groups. Similar to the previously described iodination protocol,

the clean reaction profile allowed for straightforward purification of the reaction products, and recovery of unreacted starting material with low conversion reactions. The utility of the methodology is further expanded by accessing the d_3 isotope-labelled analogues/matched pairs. In terms of LSF applications, a total of four methylated and four d_3 -methylated matched pairs of three drugs were prepared in a single step, saving time, materials and over 60 synthetic steps leading to the analogues *via de novo* synthesis. In the biological studies, the case for LSF was further strengthened by demonstrating improved metabolic stability and decreased logD values for a number of matched pairs. The utility of the presented method is limited by the presence of certain polar functional groups (heterocycles, primary and secondary amides, anilines, nitriles, for full list see supporting information) and large *ortho* substituents, where low or no conversion was observed.⁷⁷

4. Late-Stage Amination of Drug-like Benzoic Acids: Access to Anilines and Drug Conjugates *via* Directed Iridium-Catalyzed C–H Activation (Paper III)

4.1 Background

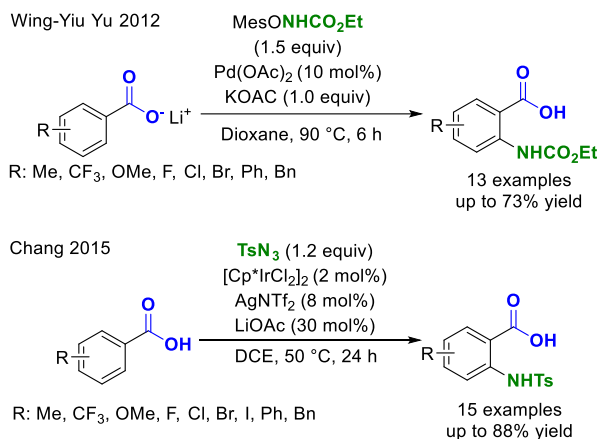
Continuing our work on the introduction of small functional groups in a late-stage fashion, and expanding to introduction of bifunctional linkers⁹⁷ for conjugation chemistry (Scheme 22), we embarked on the development of the herein presented C–N bond forming methodology.



Scheme 22. Top: General representation of molecular matched pair synthesis via late-stage amination. Bottom: General representation of conjugate synthesis via late-stage introduction of linkers.

In a recent survey of X-ray structural data, N–H hydrogen bond donors of amines were recognized as the most common polar functional groups partaking in fragment-protein binding.⁴³ Not surprisingly, C–N bond forming reactions account for more than half of the reported transformations in medicinal chemistry.⁹⁸ In combination with the abundance of C–H bonds in drug-like molecules, the development of methods for regioselective C–H amination is highly desirable.⁹⁹ In terms of directed *ortho*-aminations of benzoic acids, while a number of reports have been published in recent years, we identified several limitations and opportunities in terms of LSF applications. A major

limitation in the published methodologies was the lack of substrates containing polar functional groups (i.e. amides, heterocycles) commonly present in drug-like molecules. In an early example, a series of protected anthranilic acids was prepared by *ortho*-amination of lithium benzoates (Scheme 23, top).¹⁰⁰ In 2015 the Chang group published the Ir-catalyzed sulfonamidation of benzoic acids. This report was crucial for the development of the herein described C–H amination methodology, as it demonstrated the use of the [Cp*Ir(III)] catalytic system in combination with sulfonyl azides as preoxidized nitrogen sources. Based on our previous work on *ortho*-functionalization of complex benzoic acids under mild conditions, we hypothesized that the [Cp*Ir(III)] catalytic system with HFIP as solvent could vastly extend the C–H amination scope. By design and selection of suitable sulfonyl azides, we sought to further expand the utility of the developed method to a) the synthesis of free anilines by installing easily cleavable sulfonamides, and b) to conjugation chemistry by installing bifunctional sulfonamides for further diversification.



Scheme 23. Selected examples of C–H aminations of benzoic acids.^{100,101}

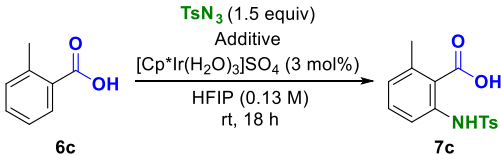
4.2 Results and Discussion

4.2.1 Optimization

The optimization of reaction conditions was carried out utilizing an HTE approach. From previous experience with the C–H methylation methodology, we identified the use of reagents with low solubility as a key limiting factor for applications miniaturization and automation. The Chang report¹⁰¹ was important for this effort, as it demonstrated the use of sulfonyl azides as a preoxidized nitrogen source, thus bypassing the requirement for stoichiometric ox-

idants such as Ag(I) salts.¹⁰² The elimination of solid reagents was further facilitated by catalyst selection. [Cp*Ir(H₂O)₃]SO₄ was chosen as catalyst, as compared to [Cp*IrCl₂]₂ it requires no Ag(I) activator. The [Cp*Ir(H₂O)₃]SO₄ catalyst is prepared in one step from the commercially available [Cp*IrCl₂]₂,¹⁰³ and is air and moisture stable, to the extent where we observed no detrimental effect on catalyst activity in a batch stored under air for 2 years. The first screening of 4 experiments confirmed the initial hypotheses and conversion to the desired product was observed at room temperature (Table 12).

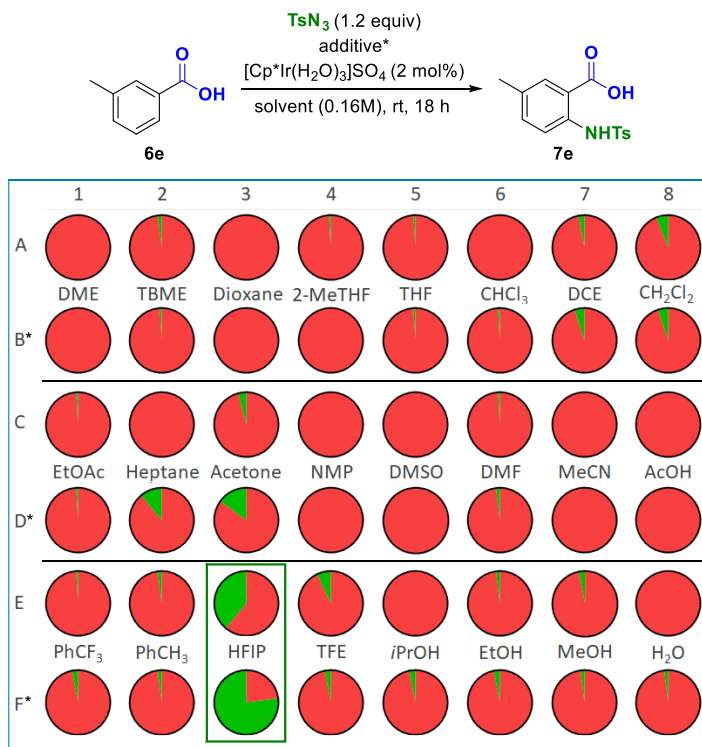
Table 12. Initial optimization

<div style="text-align: center;">  </div>			
Entry	Additive	Conversion 1h (%)	Conversion 18h (%)
1	None	29	56
2	KOAc (1.0 equiv)	51	95
3	Et ₃ N (1.0 equiv)	60	95
4	KOAc (1.0 equiv) Et ₃ N (1.0 equiv)	63	96

Conversions determined by SFC-MS (UV trace).

Albeit only moderate conversion was observed in absence of additives after 18 h (Entry 1), a significant increase in conversion was observed in presence of basic additives (Entries 2-4). As there was essentially no difference in conversion between the entries, the conditions of entry 3 were chosen for further investigation, as this utilized a liquid base Et₃N, again facilitating the HTE/miniaturization approach.

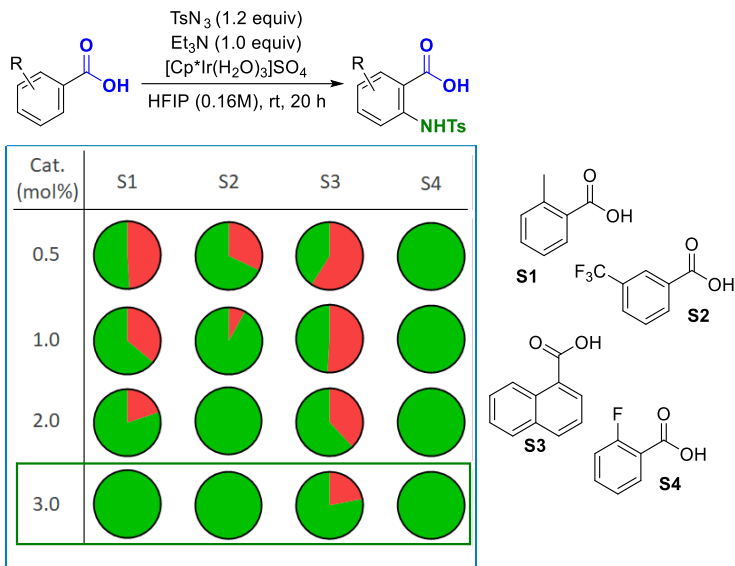
Table 13. Solvent screening



In total 24 solvents tested. * indicates reactions with Et₃N (1 equiv) additive. Conversions determined by LCMS (UV trace). Red: % unreacted starting material. Green: % product.

The applicability to HTE and miniaturization was immediately tested in the next round of optimization, carried out on a 25 μ mol scale (decreased from 0.1 mmol in the methylation optimization). Given that this was a solvent screening, the preparation of stock solutions in all the different solvents would not have been practical. Nonetheless, we were able to successfully apply liquid dispensing by first adding the substrate and catalyst as stock solutions, followed by evaporation and solvent switch. The Et₃N additive and TsN₃ (both liquids) were then added directly. As anticipated, bypassing weighing in of solids in individual wells significantly improved accuracy and increased the speed of setting up the reaction plate. The results obtained were consistent with our iodination and methylation work, with highest conversions obtained in HFIP. Best results obtained with HFIP as solvent and Et₃N additive (77%, Table 13, Entry F3)

Table 14. Catalyst loading optimization.



Conversions determined by LCMS (UV trace). Red: % unreacted starting material. Green: % product.

Next we turned our attention to establishing the optimal catalyst loading. A screening of 16 reactions, four substrates against four catalyst loadings, was conducted. Fair to excellent conversions were obtained already at 0.5 mol% catalyst loading (Table 14). However, we chose to progress with the catalyst loading of 3 mol%, as these conditions gave the highest conversion throughout the panel, and would provide general, high yielding conditions for the investigation of the substrate scope. Nonetheless, we noted the opportunity for substrate-dependent lowering of catalyst loading for reaction scale-up.

4.2.2 Functional Group Tolerance Studies

With the optimized reaction conditions in hand, the robustness of the reaction was probed by studying the effect of 53 additives on the reaction outcome (Table 15). The aim of this study was to identify functional groups limiting the applicability of the reaction, aiding our decision making process for the reaction scope investigation, and ultimately providing future users of the methodology with a predictive tool for reaction outcome when applied to complex substrates.

Table 15. Functional group tolerance

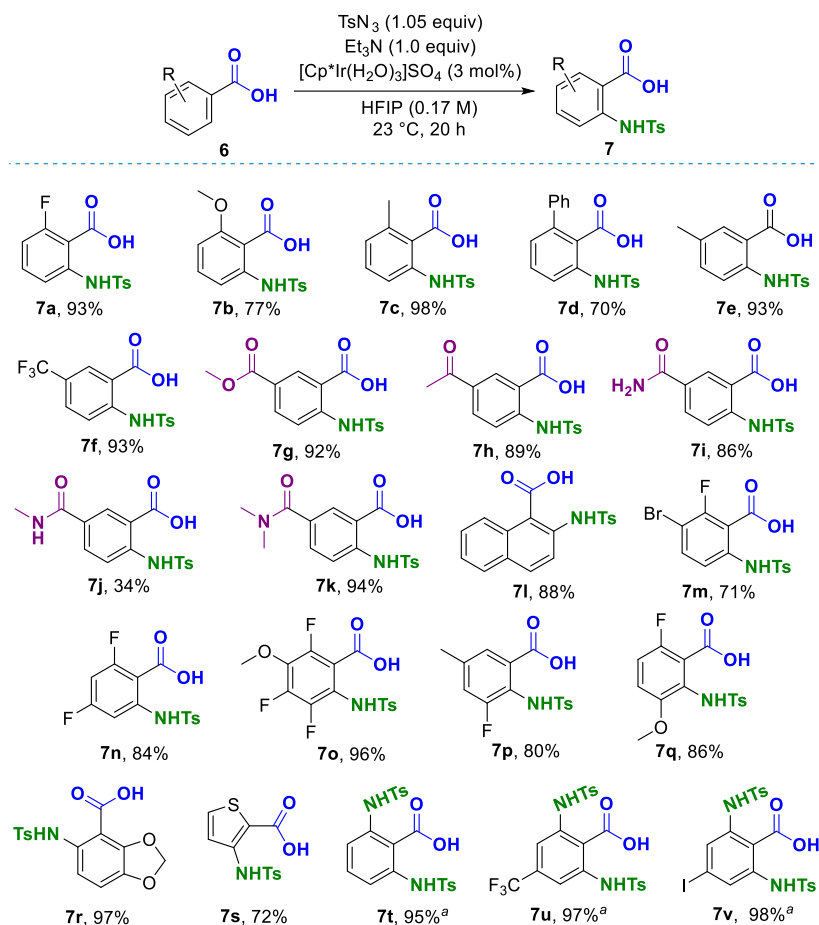
<p>TsN₃ (1.05 equiv) Et₃N (1.0 equiv) Additive (1.0 equiv) [Cp*Ir(H₂O)₃]SO₄ (3 mol%) HFIP (0.17M), rt, 20 h</p>				<p>Reaction plate format</p> <p>↓</p> <p>Automated liquid dispensing</p> <p>↓</p> <p>Plate LCMS analysis</p>		<p>Concept to results in <48 hours</p>
<p>6f → 7f NHTs</p>						
	1	2	3	4	5	6
A	None	H ₂ O (1 equiv) (10 equiv)	Me-S(=O)-Me			
B						
C						
D						
E						
F						
G						
H						
I						

The additive compatibility was quantified based on the conversion to the desired product, depicted by the colored bars (green >50%; orange 25-50%, red <25%). Conversions determined by LCMS (UV trace).

From the 54 additives tested in total (N.B. H₂O at two different loadings), >50% conversion was observed with 31 additives, 25-50% conversion with 7 additives, and <25% with 16. Polar groups commonly present in drug-like molecules, such as amides, aldehydes, ketones, esters, ureas, alcohols and carboxylic acids were well tolerated. Functional groups used in common transition metal-catalyzed cross coupling reactions as synthetic handles, i.e. boron- and halide-functionalized compounds, were also well tolerated. The following limitations were observed: (1) DMSO and MeCN were not compatible with the reaction, possibly due to inhibition of the catalyst; (2) primary amines were not tolerated; (3) nitrogen-containing heterocycles such as pyridine retard the reaction, however, introduction of steric bulk around the heteroatom and/or decreasing its electron density restores reactivity; (4) unhindered alkenes and alkynes are not tolerated.

4.2.3 Substrate Scope: Sulfonamidation

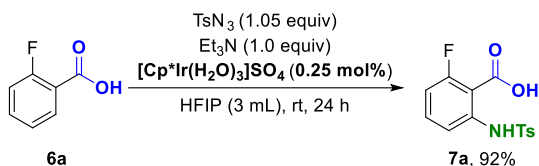
Benzoic acid derivatives with a number of diverse functional groups and substitution patterns were successfully functionalized under standard conditions (Scheme 24). *Ortho* substituents were in general well tolerated as demonstrated by the **7a** – **7d** series, even with the more sterically demanding phenyl substituent in **7d**, which posed one of the limitations in our methylation work (*vide supra*, Paper II).⁷⁷ Electronically diverse substituents in the *meta* position were also well tolerated, as demonstrated with compounds **7e** and **7f**. Importantly, the scope of substrates bearing Lewis-basic directing group was further expanded compared to the iodination and methylation methodologies, with ester, ketone, primary, secondary and tertiary amides tolerated, with complete selectivity for the functionalization of the C–H bond *ortho* to the carboxylate on the less sterically hindered site (**7g** – **7k**). The utility of the methodology was also demonstrated with a number of more heavily decorated benzoic acids. Functionalization of 1-naphthoic acid occurred selectively in the 2-position, in accordance with the selectivity observed with the methylation methodology. The 1,2,3,4-substituted product **7m** was successfully prepared, as well as 1,2,3,5-substituted **7n**. For the first time we were able to prepare a fully substituted benzoic acid derivative **7o** in excellent yield. The trends for substitution in the 2-position in substrates bearing a 1,3-substitution pattern were identical with the observations in the methylation methodology: functionalization is possible in the vicinity of small substituents with non-bonding electron pairs. In terms of functionalization of heterocycles, this remains a major limitation, with only two successful examples **7r** and **7s** demonstrated. Finally, no useful monoselectivity was achieved for *para*-substituted substrates, however, the reaction could be pushed to difunctionalization with excellent yields by simply increasing the azide loading (**7t** – **7v**).



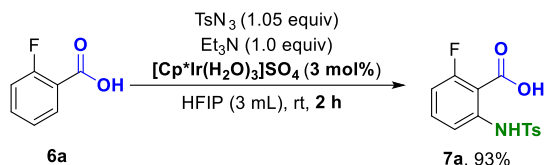
Scheme 24. C–H sulfonamidation building blocks scope. Isolated yields shown. ^aTsN₃ (2.1 equiv) was used. Potential competing DGs highlighted in purple.

Although our goal for the methodology was to develop a set of general conditions applicable to wide range of substrates, single substrate optimization was also carried out to demonstrate the full potential of the system. Using 2-fluorobenzoic acid **6a** as a model system, full conversion could be achieved with catalyst loading as low as 0.25 mol% (Scheme 25, a). In contrast, with increased catalyst loading to 3 mol% the reaction time could be decreased to 2 h (Scheme 25, b). The applicability of commercially available [Cp*IrCl₂]₂ for the transformation was also demonstrated, with addition of Ag₂SO₄ for *in situ* precatalyst activation (Scheme 25, c). With the last modification stirring was essential for reproducibility.

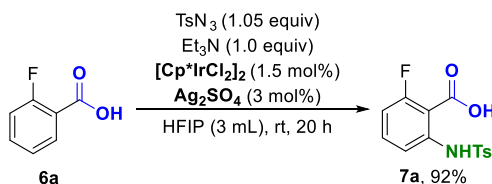
a) **Decreased Catalyst Loading**



b) **Decreased Reaction Time**



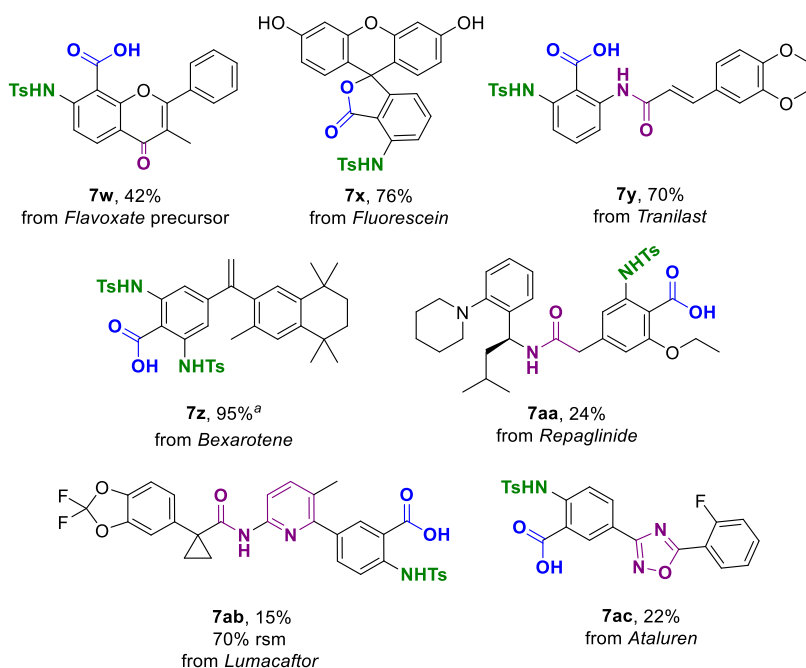
c) **Commercially Available Precatalyst**



Scheme 25. Single substrate reoptimization on 2-fluorobenzoic acid **1a**.

Returning to the reaction scope, we investigated the applicability of the developed methodology to late-stage functionalization of complex molecules (Scheme 26). The Flavoxate precursor **6w** was functionalized with complete selectivity in the expected position yielding compound **7w**. Flavoxate, a muscle relaxant used for the treatment of overactive bladder,¹⁰⁴ is prepared in 1 step from **6w**. Fluorescein, a widely used fluorescent tracer,¹⁰⁵ was also successfully functionalized with complete selectivity, yielding compound **7x**. Regarding the structure of **7x**, while the depicted ring-closed form was observed by ¹NMR spectroscopy, the corresponding starting material **6x** would under the reaction conditions be in equilibrium with the ring-opened, carboxylate form. From a functional group tolerance perspective, the phenolic hydroxy groups, as well as the quinone moiety of the ring-opened form were tolerated. The antiallergic drug Tranilast, also used for the treatment of a variety of other indications,⁸³ was successfully functionalized, with significantly improved yield compared to the previously discussed methylation methodology (Paper II). The Michael acceptor vinylic system, as well as the acylanilide directing group did not interfere with the reaction outcome (**7y**). Similar to the *para*-substituted substrates **7t** – **7v** in the building blocks scope (Scheme 24), monofunctionalization of Bexarotene, an antineoplastic agent used for the treatment of cutaneous T cell lymphoma (CTCL),^{80,81} was complicated by problematic separation of the mono and difunctionalization product mixture. The reaction was pushed to complete difunctionalization, and compound **7z** was obtained in excellent yield. Repaglinide, used for blood glucose reduction in

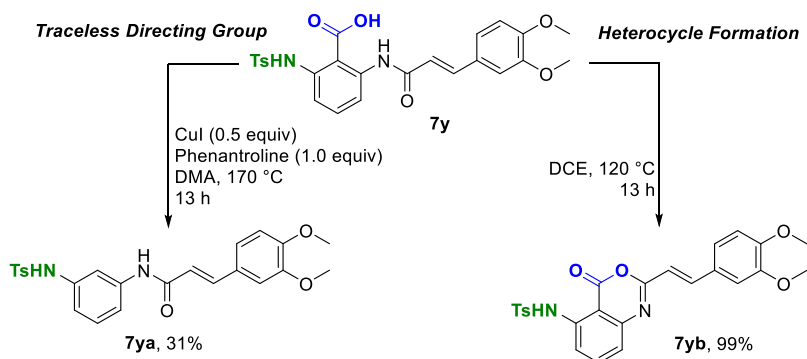
type 2 diabetes mellitus,⁷⁸ was also functionalized with complete selectivity in the anticipated position, yielding compound **7aa**, with both the secondary amide and tertiary amine tolerated. We were especially pleased to see that for the first time we were able to functionalized drugs containing heterocyclic motifs. Thus compound **7ab** was obtained from Lumacaftor, a therapeutic agent used in the treatment of cystic fibrosis,¹⁰⁶ with 70% unreacted starting material also isolated. The pyridine moiety, as well as the secondary amide were tolerated. Finally Ataluren, a therapeutic agent developed for the treatment of Duchenne muscular dystrophy,¹⁰⁷ was successfully functionalized to yield compound **7ac**. At this point it is important to note that despite the presence of Lewis-basic directing groups in several of the presented compounds, the products were obtained with complete regioselectivity as a single regioisomer. While in some cases products were obtained in modest yields, in general the majority of the remaining mass balance could be accounted for by unreacted starting material.



Scheme 26. C–H sulfonamidation LSF scope. Isolated yields shown. ^a TsN₃ (2.1 equiv), KOAc (1.0 equiv), [Cp*Ir(H₂O)₃]SO₄ (6 mol%). Potential competing DGs highlighted in purple.

The utility of the carboxylate moiety as a traceless directing group in context of C–N bond formation has been previously described by the Chang group.¹⁰¹ Intrigued by this, we sought to investigate the applicability of this approach to complex drug-like molecules, further increasing the range of accessible analogues by LSF. The envisioned decarboxylated product **7ay** was obtained under copper-catalyzed conditions based on the published procedure (Scheme

27).¹⁰¹ Interestingly, we could also obtain compound **7yb** bearing a 1,3-benzoxazin-4-one core by dehydration in DCE in quantitative yield. These two examples further expand the utility of the present late-stage sulfonamidation by accessing additional analogues. This in turn has potential to greatly aid structure-activity relationship (SAR) studies by modification and/or removal of structural motifs partaking in target binding.

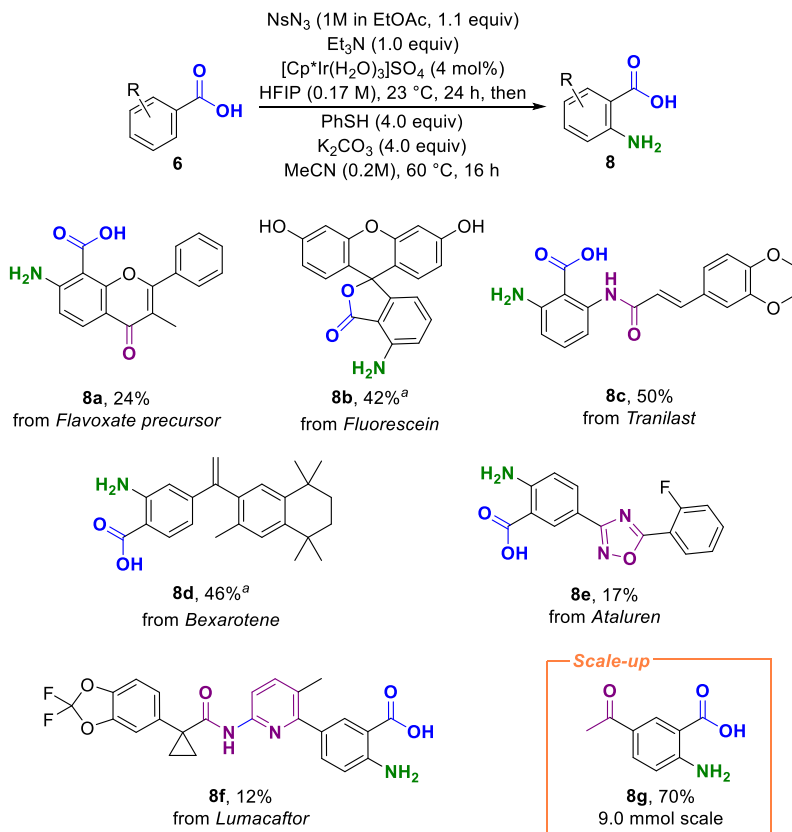


Scheme 27. Further opportunities in late-stage diversification for SAR investigations demonstrated on Tranilast analogue **7y**.

4.2.4 Substrate Scope: Amination

With an understanding of reactivity trends, opportunities and limitations from the synthesis of tosylamides, we embarked on the development of a protocol for accessing free amine analogues. For this to be successful, especially in an LSF context, a mild deprotection protocol would be necessary. For this reason we decided to prepare a series of nosylamide analogues, allowing for deprotection with PhSH and a weak base. However, during our initial risk assessment, nosylazide was identified as a high energy compound.¹⁰⁸ In order to mitigate the risks associated with handling this compound, a protocol utilizing NsN_3 as a solution in EtOAc was developed, avoiding the isolation of the material as a solid. The amination protocol itself consists of the C–H sulfonamidation step, followed by solvent swap and nosyl deprotection (Scheme 28). In general, lower conversions to the corresponding nosylamides were observed, comparing the tosyl- and nosyl-protected azides. However, we were pleased to see that with all compounds depicted in Scheme 28 deprotection of the nosyl group was possible without decomposition of the products. The regioselectivity was identical to previous observations with tosylamide formation. The only outlier in terms of selectivity was the Bexarotene analogue **8d**, where selective monofunctionalization was observed, as opposed to formation of mono/di mixtures with tosylamide formation. This behavior seems to be specific to this substrate, as we were not able to reproduce the result with other *para*-substituted benzoic acids. Additionally, the feasibility of scaling

up the reaction was demonstrated, with the previously unreported building block **8g** prepared on gram scale.



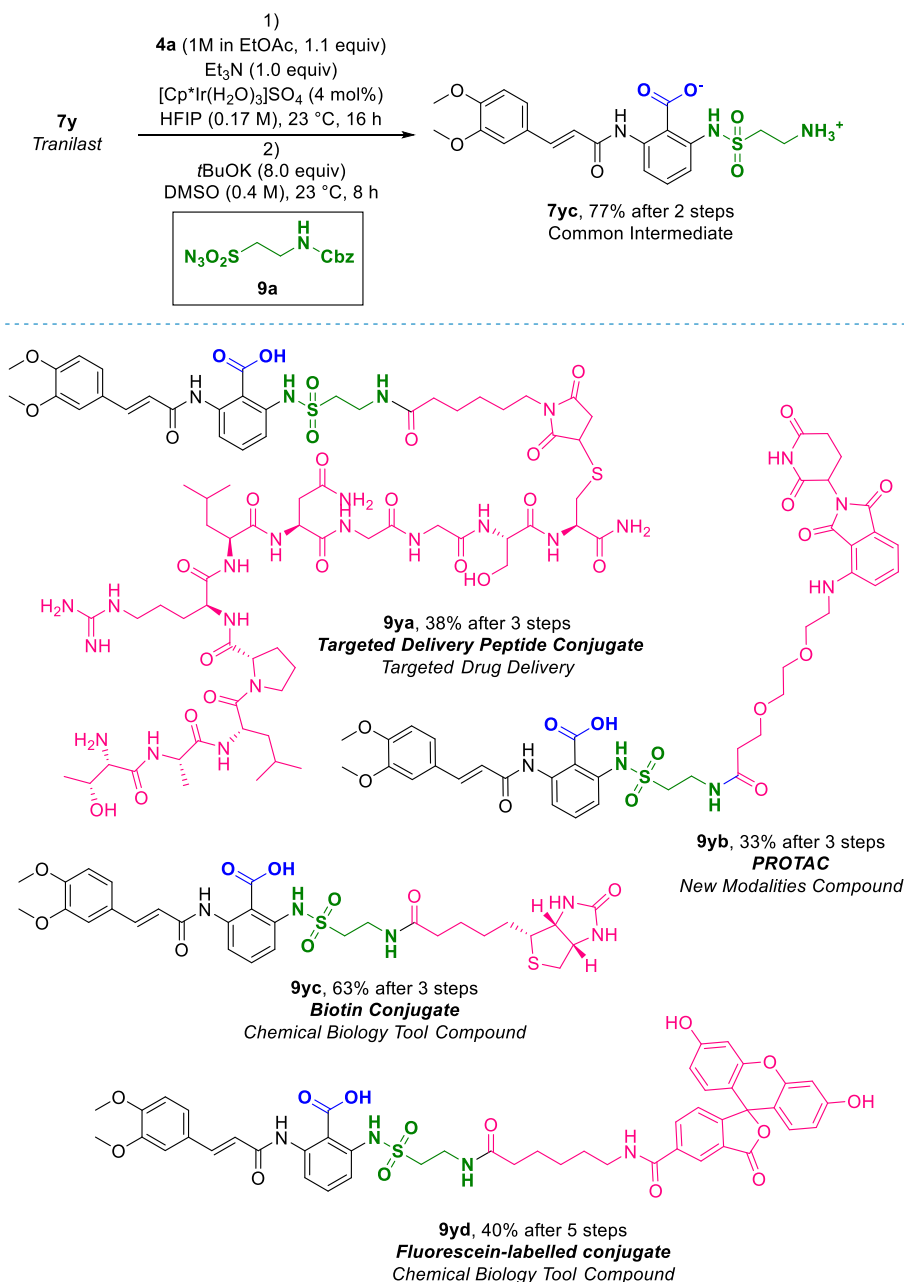
Scheme 28. C–H amination scope. Isolated yields shown. ^a Reaction time in first step 44 h. Potential competing DGs highlighted in purple.

4.2.5 Synthesis of Conjugates

In terms of applications, our final goal was to develop a protocol for installing synthetic handles for conjugation chemistry in a late-stage fashion. This would further increase the utility of C–H aminations in drug discovery by allowing rapid access to so-called new modalities compounds. New modalities have recently become a viable and relevant class of therapeutics, complementing small molecule drugs and biologicals.^{45,109,110} Compounds containing small molecule drug fragments, including but not limited to peptide- and antibody-drug conjugates (PDCs and ADCs), small molecule oligonucleotide conjugates, and Proteolysis-Targeting Chimeras (PROTACs) have attracted considerable interest from both industry and academia, and yielded therapeutics already in clinical use.⁴⁵ Targeted delivery of therapeutics to specific cell types

or tissues, widening the therapeutic window of compounds with otherwise unacceptable safety profile, changing the mechanism of action of drug candidates, or even unlocking therapeutic targets deemed undruggable by traditional approaches present some of the potential benefits of accessing these compounds. In a recent review, Valeur *et al.* called for new, creative approaches to expand the chemical space within new modalities.⁴⁵ Chemoselective C–H activations, while largely unexplored, present an attractive approach in this context, allowing controlled functionalization on predetermined positions with minimum impact on binding affinity, while maintaining the integrity of polar functional groups required for binding interactions. Furthermore, the late-stage formation of new modalities compounds for rapid preparation and evaluation of the feasibility of this approach is highly desirable.⁴⁵

For applications in conjugation chemistry we devised the bifunctional sulfonyl azide **9a** (Scheme 29). For the diversification handle an aliphatic primary amine was chosen, as this would allow for a number of well-established derivatizations, such as urea, thiourea and amide formations, reductive eliminations and transition metal-catalyzed cross coupling reactions. The Cbz protecting group would allow for deprotection under a number of conditions, with the possibility to choose suitable conditions based on the character of the substrate. Thus **9a** was prepared from the corresponding commercially available sulfonyl chloride, following the same protocol as for the synthesis of NsN₃. Tranilast was chosen as the model system, and the key intermediate **7yc** was obtained in two steps (Scheme 29). From this a series of conjugates were prepared, utilizing well established procedures and without optimization. The peptide conjugate **9ya** was obtained from **7yc** by a one pot sequential procedure. The maleimide-functionalized linker was first installed by amide bond formation with the corresponding NHS ester. This was followed by Michael addition of the cysteine thiol from the fully deprotected peptide. The peptide chosen for this conjugation has been previously reported for use in targeted delivery of liposomes applied in myocardial infarction.¹¹¹ The peptide conjugate **9ya** was obtained in 3 steps with 38% overall yield, starting from Tranilast. Engaging the proteasome for controlled degradation of therapeutic targets by Proteolysis Targeting Chimeras (PROTACs) has attracted considerable attention within drug discovery over the past years.^{112,113} From a structural perspective, PROTACs consist of two small molecules, one engaging the proteasome and one the therapeutic target, connected together with a linker. Intermediate **7yc** was successfully functionalized with linker-expanded Lenalidomide, yielding the PROTAC **9yb** in 33% isolated yield (overall yield after 3 steps starting from Tranilast). The two applications presented exemplify the



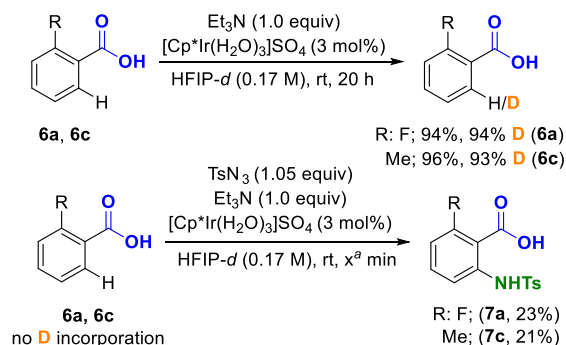
Scheme 29. Synthesis of drug conjugates. Isolated yields shown, calculated from commercially available Tranilast. Conjugated moieties highlighted in pink.

opportunities for expeditious access to conjugates with different modes of action, expanding the utility of late-stage C–H activations in drug discovery beyond the introduction of small functional groups. Another application of high importance to drug discovery and development is the elucidation of the mode

of action of therapeutics. A method commonly utilized in target validation is affinity chromatography, facilitated by the attachment of a small molecule probe to biotin.¹¹⁴ The biotinylated Tranilast analogue **9yc** was prepared in 3 steps from Tranilast with 63% overall yield. Finally, access to molecular imaging tool compounds was demonstrated with the synthesis of the Fluorescein-tagged compound **9yd**. This particular example further showcases the utility of the diversification approach by modulating the linker length with two consecutive extensions.

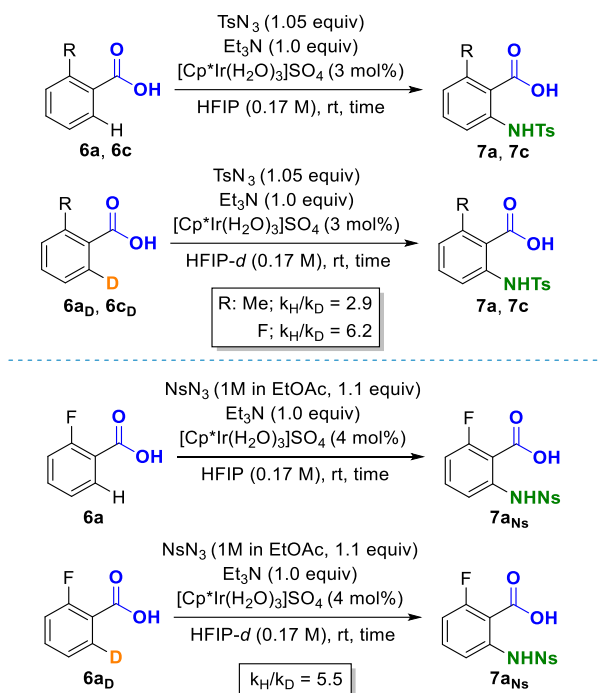
4.2.6 Mechanistic Studies

Mechanistic studies were conducted in order to explain some of the underlying processes in the reaction. First, the reversibility of the C–H activation step was studied with two electronically and sterically distinct substrates, by exchanging the solvent for deuterated HFIP. In absence of the nitrogen source, high levels of deuterium incorporation were observed with both substrates tested (Scheme 30). However, when the azide source was included, no deuterium incorporation in the remainder starting materials was observed when the reactions were run for short times. This means no protodemetalation and thus no reversibility of the C–H activation step occurs under standard reaction conditions. The fact that reversible C–H activation was demonstrated with our iodination methodology illustrates the complexity and variability in reaction mechanisms, even with systems utilizing the same substrate class, catalyst and solvent.



Scheme 30. C–H activation reversibility. ^a R = Me, 15 min reaction time. R = F, 8 min reaction time. Conversion and D incorporation determined by ¹H NMR.

As the next step a KIE investigation was conducted in a parallel reaction format,⁶¹ both with tosylamide and nosylamide formation (Scheme 31).



Scheme 31. KIE studies. Parallel experiments with H and D compounds.⁶¹

Top: TsN_3 as azide source. $\text{R} = \text{Me}$, $k_{\text{H}}/k_{\text{D}}$ of 2.9. $\text{R} = \text{F}$, $k_{\text{H}}/k_{\text{D}}$ of 6.2.

Bottom: NsN_3 as azide source. $k_{\text{H}}/k_{\text{D}}$ of 5.5.

With the first transformation, a $k_{\text{H}}/k_{\text{D}}$ value of 2.9 was observed with 2-methylbenzoic acid **6a**, suggesting the C–H activation as the turnover limiting step. With 2-fluorobenzoic acid a significantly larger KIE was observed, with a $k_{\text{H}}/k_{\text{D}}$ value of 6.2, also suggesting C–H activation as turnover limiting. The same observation was made with the nosylamide formation, with a $k_{\text{H}}/k_{\text{D}}$ value of 5.5 with 2-fluorobenzoic acid as substrate.

4.3 Conclusion

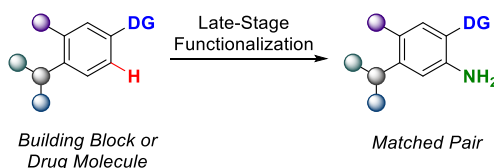
The C–H amination methodology presented in this chapter was successfully applied to sulfonamidation of a wide range of benzoic acids. Electron donating and electron withdrawing substituents, and even a large number of polar and protic functional groups were well tolerated. Out of the three methodologies presented so far, this method demonstrated the highest utility for LSF applications. The combination of the demonstrated substrate scope and functional group tolerance studies gives the potential user a good understanding of the limitations and opportunities of the method. In terms of accessible compounds with relevance to drug discovery, the method allows for the introduction of sulfonamides and the small free amine functional group in a late stage, as well

as for the installation of linkers for the synthesis of drug conjugates. The utility of the latter approach was further demonstrated by the synthesis of a number of conjugates relevant to drug discovery and chemical biology. The utility of the sulfonamidation protocol was expanded with late-stage diversifications, allowing for decarboxylation and heterocycle formation in a late-stage, further increasing the scope of analogues accessible for SAR investigations. In terms of HTE applications, the use of all soluble reagents allowed us for the first time to set up complete screening plates with liquid handling systems, further decreasing the reaction scale and material consumption, while increasing the time efficiency of the campaigns. Another important aspect of the reaction is the tolerance of air and moisture, which not only increased operational simplicity for reaction set up with larger scales, but also allowed us to use automation equipment not located in a glovebox. The utility of the method is mostly limited by the presence of certain heterocycles and unhindered alkenes and alkynes, as demonstrated by the functional group tolerance studies.

5. Merging Directed C–H Activations with High-Throughput Experimentation: Development of Predictable Iridium-Catalyzed C–H Aminations Applicable to Late-Stage Functionalizations (Paper IV)

5.1 Background

Building on the results and learnings from the projects previously described in this dissertation, we decided to depart from functionalizations of benzoic acids and focus our attention to the development directed of C–H activations applicable to a broad range of directing groups (Scheme 32). Expanding the directing group scope outside of carboxylic acids would significantly increase the utility of the reaction in terms of functionalization of drug-like molecules, as polar functional groups suitable for acting as directing groups are present in many pharmaceuticals.²

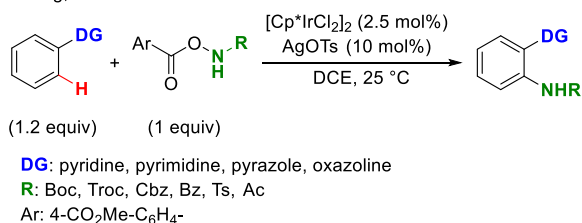


Scheme 32. General representation of molecular matched pair synthesis via late-stage amination.

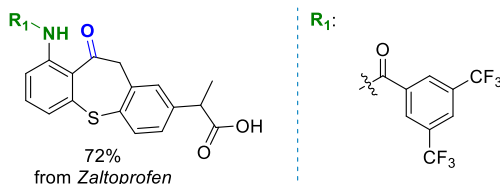
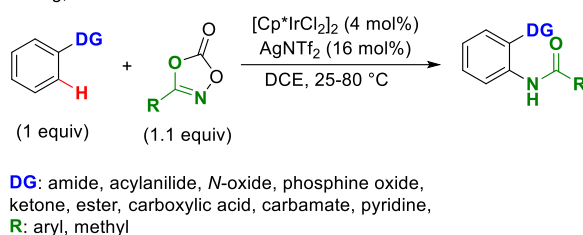
As the target transformation, C–H aminations were chosen for the importance of nitrogen-containing compounds in pharmaceuticals.^{43,98,115,116} Furthermore, the applicability of a range of directing groups frequently present in drugs and natural products for C–N bond formations has been previously demonstrated.^{99,117–121} Selected key examples are herein discussed. In 2014, the Chang group reported a methodology for the synthesis of protected anilines *via* directed C–H activation, facilitated by a number of heterocyclic directing groups (Scheme 33, top).¹²² Access to amines bearing a variety of protecting

groups allows the potential user to match deprotection conditions with the requirements of the substrate, making this protocol especially useful for applications to complex molecules. A drawback of this method is the use of excess substrate compared to the nitrogen source, and the fact that the nitrogen sources used are not commercially available. The second presented methodology, also from the Chang group, allows for amidation of a number of substrates, using dioxazolones as the nitrogen source (Scheme 33, bottom).¹²³ Under these conditions a much wider directing group scope could be reached, expanding beyond nitrogen-containing heterocycles. Importantly, applications to LSF of complex pharmaceuticals were demonstrated in this report.

Chang, 2014



Chang, 2017



Scheme 33. Selected examples of C–H aminations with broad directing group applicability.^{122,123}

To complement the published literature, we envisioned the development of a methodology utilizing directing groups present in pharmaceuticals for the introduction of a protected amine, with access to a number of deprotection protocols leading to the free amine analogue. Importantly, we wanted to create a protocol allowing the potential users to predict the applicability of the reaction to their substrates by reporting the full scope of successful and unsuccessful reactions along with functional group tolerance studies. Finally, we sought to

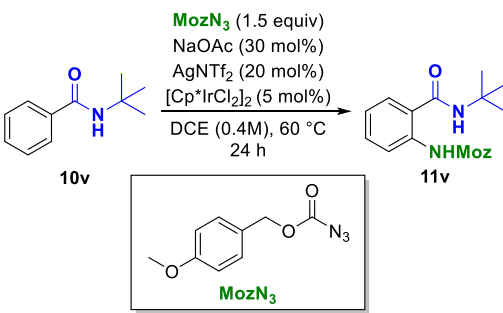
test the lower limits of miniaturization in order to even further decrease the material consumption associated with screening.

5.2 Results and Discussion

5.2.1 Optimization

As with our work on amination of benzoic acids,¹⁰³ the optimization of this methodology was conducted with the aim of HTE applications. The reaction conditions published in 2016 by the Chang group were used as the starting point.¹¹⁹ Deviating from the published procedure, we decided to use MozN₃ as the nitrogen source, as this reagent is commercially available, and the obtained Moz-protected amines should allow for tunable deprotection under a range of reaction conditions (Table 16, Entry 1). The omission of insoluble silver additives was once again made possible by the use of [Cp*Ir(H₂O)₃]₂SO₄ as catalyst, with the desired product obtained with improved conversion (Entry 2). Lowering the catalyst loading, increasing MozN₃ loading and decreasing the reaction temperature were all detrimental to the reaction outcome (Entries 3-5). Finally, albeit with slight decrease in conversion, we decided to proceed with higher dilution of the reaction mixture (0.2M vs 0.4M, Entry 6), as this would better facilitate the use of stock solutions for later applications.

Table 16. Initial optimization.

<div style="display: flex; align-items: center; justify-content: center;"> <div style="text-align: center;">  <div style="margin-left: 20px;"> <p>MozN₃ (1.5 equiv) NaOAc (30 mol%) AgNTf₂ (20 mol%) [Cp*IrCl₂]₂ (5 mol%) DCE (0.4M), 60 °C 24 h</p> </div> </div> <div style="margin-left: 20px;"> <p>[Ir]: [Cp*Ir(H₂O)₃]₂SO₄ [Cp*IrCl₂]₂ I II</p> </div> </div>		
Entry	Deviation	Conversion (%)
1 ¹¹⁹	None	42
2	Catalyst I (10 mol%), no AgNTf ₂	65
3	Catalyst I (5 mol%), no AgNTf ₂	31
4	Catalyst I (10 mol%), no AgNTf ₂ , MozN ₃ (2.5 equiv)	56
5	Catalyst I (10 mol%), no AgNTf ₂ , 23 °C	0
6	Catalyst I (10 mol%), no AgNTf ₂ , DCE (0.2M)	55

Entry 1 based on literature procedure.¹¹⁹ Conversions determined by LCMS (UV trace).

With subsequent optimizations we established the applicability of the reaction conditions to heterocyclic directing groups (miniaturization to 5 μ mol reaction scale), and found that a range of acetate additives with different counterions were all detrimental to the reaction outcome (not shown). After that, we turned our attention to solvent screening (Table 17). With a series of eight solvents tested against two substrates, we again consistently observed the detrimental effect of the NaOAc additive. With 2-(*m*-tolyl)pyridine (**11c**, Table 17), high conversions were consistently observed throughout the solvents tested. On the other hand, with *N*-(*tert*-butyl)benzamide (**11v**, Table 17) the conversions were significantly lower. Even with DCE as solvent, only 21% conversion was observed in this screening, while 55% was observed in the previous round under identical conditions (Table 16, Entry 6). We attribute this difference to the different method of reaction set-up. While in the previous round the reagents were weighed in manually, followed by addition of solvent, in this round the catalyst was added as a stock solution in water, followed by solvent swap. We speculate that the decrease in conversion was caused by residual moisture. Similar to scale-up from small scale batch reactions to large scale, scaling down and changing the reaction format to plates is often accompanied with unanticipated challenges, as demonstrated with this example. Four solvents were chosen from this solvent screening for further investigations.

Table 17. Solvent screening.

Product	11c		11v	
Solvent	No additive	NaOAc ^a	No additive	NaOAc ^a
NMP	100	0	0	0
IPA	100	7	12	0
2-MeTHF	100	0	12	0
EtOAc	100	0	16	0
Acetone	100	0	11	0
DCE	100	3	21	0
PhMe	86	0	19	0
CPME	100	0	21	0

Conversions determined by LCMS (UV trace). Highlighted solvents further investigated.

NMP was chosen for its high boiling point, which would be beneficial with further miniaturization, as solvent loss is a major limiting factor with small scale applications. EtOAc and CPME were chosen as these present a greener solvent alternative to the halogenated solvent DCE, which is widely used in the field. Finally DCE was chosen for its superior performance in the solvent screening and in C–H activations in general, as shown by reported literature.¹³ With the selected solvents and generally applicable screening conditions, we embarked on investigating the directing group applicability and solvent effects on the transformation. A directing group informer library was devised, where a series of 48 representative substrates containing a variety of directing groups commonly present in building blocks and pharmaceuticals were tested under screening conditions against four solvents (Figure 13). The informer library approach, initially propagated by Krska and coworkers (Merck),^{52,53} allows for evaluation of a reaction applicability on a range of complex substrates based on the output of successful and unsuccessful reactions.

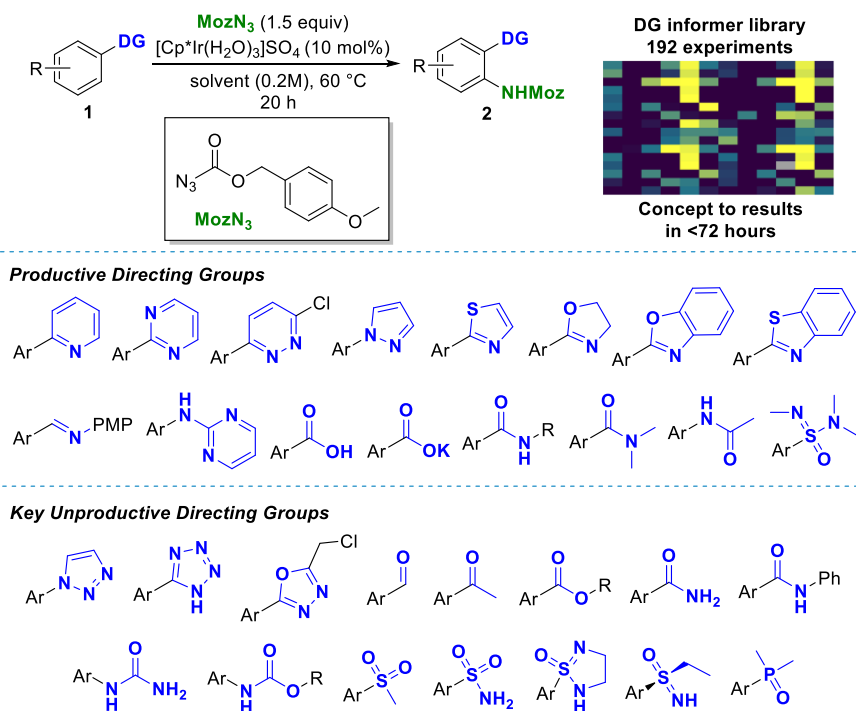


Figure 13. DG informer library. Four solvents and 48 substrates tested. Productive DGs and key classes of unproductive DGs depicted (Detailed structures and conversions in manuscript supporting information).

In our case, out of 48 DGs tested, 16 were productive for the desired C–H amination, with conversions ranging from 10 to >99%. These were encouraging results with the variations of DGs tested in mind. We anticipated that the conversions on the lower end could be further improved in a later stage by

single substrate optimization. The observations based on solvent variation were as follows: Highest conversions throughout the scope were observed with DCE. EtOAc and CPME were successful with a comparable substrate scope, however, not exceeding DCE in terms of conversion. NMP showed promising results with carboxylic acids and heterocycles, but was unproductive with amides. As anticipated earlier, single substrate optimization was shown to enable further improvement of the screening conditions, as shown by the example of 2-(*m*-tolyl)pyridine **10c** (Table 18 and 19).

Table 18. Single substrate optimization for solvent selection.

Solvent		NMP	DCE	EtOAc	CPME
Ir (mol%)	10	90.9	99.1	99.5	99.5
	8	92.7	99.2	>99.5	99.4
	6	88.1	99.1	64.4	98.6
	4	57.4	99.5	25.1	65.4
	2	13.1	83.2	11.1	21.8

Conversions determined by LCMS (UV trace).

In two rounds of optimization the catalyst and reagent loadings were reduced, while maintaining high conversions. In the first round, the investigation of catalyst loading and solvent selection revealed superior performance of DCE with lowest catalyst loading at 4 mol%, closely followed by CPME at 6 mol%, providing a greener alternative in terms of solvent selection (Table 18).

Table 19. Single substrate optimization for finetuning reagent loading.

Solvent		DCE			NMP		
Ir (mol%)		2	4	6	4	6	8
MozN ₃ (equiv)	1.0	77.9	84.7	83.5	53.1	88.0	89.0
	1.1	75.1	91.6	92.3	47.7	94.0	95.1
	1.3	80.1	>99.5	>99.5	46.6	88.4	94.1
	1.5	71.0	>99.5	>99.5	53.8	85.8	90.9
	2.0	57.2	98.0	>99.5	47.4	70.5	88.0
	3.0	53.4	86.6	>99.5	44.9	68.6	86.2

Conversions determined by LCMS (UV trace).

In the second round of optimization a trend of decreased conversion was observed with high MozN₃ loading (Table 19). The same trend of decreased conversion with increased MozN₃ loading was observed with NMP as solvent.

Single substrate optimization was also successfully utilized for tuning mono/di selective functionalization of 1-phenyl-1H-pyrazole. Useful monoselectivity was achieved by decreasing catalyst and MozN₃ loadings (Table 20). On the other hand, increased difunctionalization product content was obtained with higher loadings.

Table 20. Single substrate optimization for mono/di selectivity.

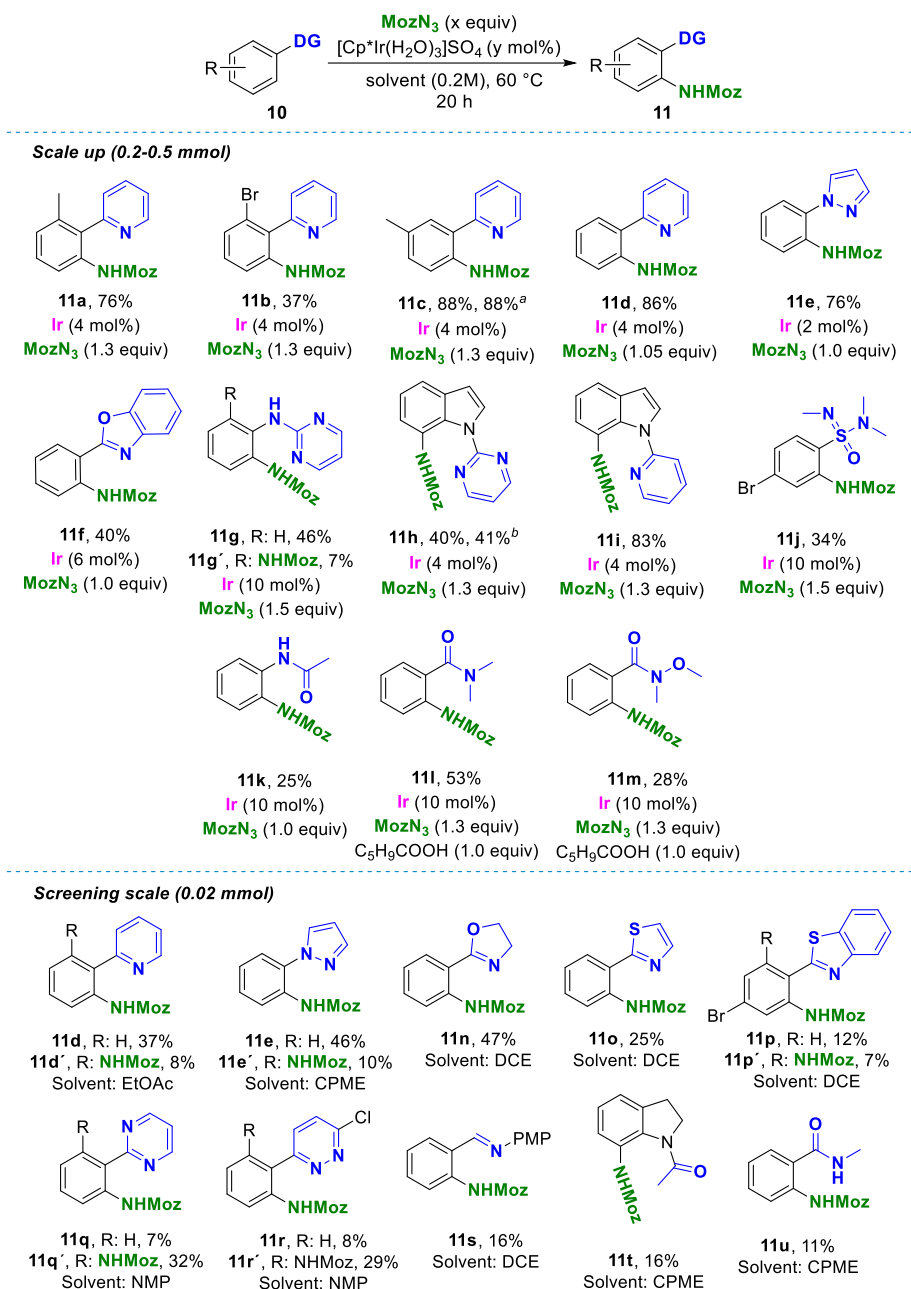
c1ccc(cc1)n2cc[nH]2 (10e)
 $\xrightarrow[\text{DCE (0.2M), 60 }^{\circ}\text{C, 20 h}]{\text{MozN}_3 \text{ (x equiv), [Cp*Ir(H}_2\text{O)}_3\text{]SO}_4 \text{ (y mol\%)}}$
c1ccc(cc1)n2cc[nH]2Nc3ccccc3 (11e) + c1ccc(cc1)n2cc[nH]2Nc3ccccc3Nc4ccccc4 (11e')

10e				11e		11e'	
Ir (mol%)		2		4		6	
		11e	11e'	11e	11e'	11e	11e'
MozN ₃ (equiv)	1.0	86.4	9.5	86.9	9.4	86.9	10.2
	1.1	85.9	10.4	86.8	7.7	85.6	13.0
	1.3	78.0	21.2	77.6	22.1	73.7	26.3
	1.5	81.1	17.5	53.9	45.8	49.6	50.1
	2.0	84.3	10.6	53.4	46.0	22.7	76.4

Conversions determined by LCMS (UV trace). Best results for mono/di selectivity highlighted in red.

5.2.2 Reaction Scope

With the screening results and a better understanding of reactivity trends we turned our attention to product isolation and reaction scale-up (Scheme 34). The substrate selection was based on the results from the directing group screening. First, substitution effects were investigated on the 2-phenylpyridine system. In terms of *ortho* substituents, the smaller methyl group was well tolerated (Scheme 34, **11a**), while significant decrease in yield was observed with the sterically demanding bromo substituent (**11b**). *Meta* substitution in **11c** was well tolerated. Application of CPME as a greener solvent alternative was successful, and matching yields were obtained with catalyst loading of 6 mol%. Sterically unbiased 2-phenylpyridine bearing two equivalent *ortho* C–H bonds was selectively monoaminated, providing compound **11d** in 86% yield.



Scheme 34. Building blocks scope. Isolated yields depicted. Top: Compounds obtained after single substrate optimizations and scale-up. Bottom: Compounds isolated directly from DG informer library screening plate. ^aCPME as solvent. ^bEtOAc as solvent.

Monofunctionalization with high selectivity was also achieved with the pyrazole (**11e**) and benzoxazole (**11f**) directing groups. We were also pleased to see that functionalization mediated by formation of 6-membered iridacycles

was possible in the **11g** – **11i** series, as with our carboxylate-directed work (Papers I to III) only functionalization through 5-membered iridacycles was accessible. With compound **10g** a mixture of mono and difunctionalization products was obtained under screening conditions. Indoles **11h** and **11i** were accessed with full selectivity for the 7-position *via* a 6-membered iridacycle. Successful utilization of a sulfonimidamide as directing group was confirmed upon scale up, providing compound **11j**. Sulfonimidamides present an emerging compound class within drug discovery,¹²⁴ and to the best of our knowledge, the example of **11j** is the first application of this moiety in directed C–H activations. Utilization of oxygen-centered directing group was also successfully demonstrated with the **11k** – **11m** series. Functionalization of acetanilide **10k** demonstrates the accessibility of 6-membered iridacycles to oxygen-centered DGs, albeit with relatively low yield. **11l** was obtained with improved yield by adding 1 equiv. of cyclopentane carboxylic acid. The yield improvement with amide DGs was first observed during the LSF scope investigation with Bezafibrate **12j** (Scheme 36). This is potentially a result of a change in reaction mechanism for the substrate class, resulting in higher TONs. This further extended the substrate scope to Weinreb amides, as demonstrated with compound **11m**. This DG was previously unproductive under screening conditions (Figure 13).

We also investigated the possibility to extend the utility of screening plates by small scale product isolation. At the 20 μ mol scale, products of a series of 10 building blocks were isolated and characterization by NMR spectroscopy. The potential utility of product isolation from small scale reaction plates extends beyond compound characterization. In drug discovery, as little as one milligram of material can be sufficient for essential studies.¹²⁵ However, a common drawback of such small scale reactions are decreased yields due to material loss in sample handling and purification, as observed with **11d** and **11e** when compared to scale-up entries. The heterocyclic DGs scope was further extended with dihydrooxazole **11n**, thiazole **11o**, benzothiazole **11p**, pyrimidine **11q** and pyridazine **11r**. The PMP-protected imine **11s** was isolated with low yield due to product hydrolysis during purification. Finally, products from oxygen-centered directing groups in *N*-acetyl indoline **10t** and *N*-methyl benzamide **10u** were successfully obtained.

5.2.3 Functional Group Tolerance Studies

As the next step, functional group tolerance of the method was investigated by studying the effects of 46 additives on the reaction outcome under screening conditions. The additives were chosen based on the earlier presented benzoic acid C–H amination study (Paper III). 2-(*o*-tolyl)pyridine was chosen as the model substrate, and 2 solvents were tested

Table 21. Functional group tolerance study

$ \begin{array}{c} \text{MozN}_3 \text{ (1.5 equiv)} \\ \text{[Cp*Ir(H}_2\text{O)}_3\text{]SO}_4 \text{ (10 mol\%)} \\ \text{NMP or DCE (0.2M), 60 }^\circ\text{C} \\ \text{20 h} \end{array} \rightarrow $						
	10a					11a
	1	2	3	4	5	6
A	None	H ₂ O (1 equiv)	H ₂ O (10 equiv)			
B						
C						
D						
E						
F						
G						
H						

Additive compatibility was quantified based on conversion to the desired product (LCMS, UV trace). Depicted color bars (green >50%, orange 25-50%, red <25%).

(Table 21, NMP top bar, DCE bottom bar). Out of 47 modified conditions tested, in 35 cases no effect on the reaction outcome was observed and full conversion retained. The following conclusions were made: (1) The reaction tolerates moisture, even at 10 equivalents of water the conversion remained unchanged. (2) The presence of DMSO has detrimental effect on conversion,

while all other commonly used polar solvents tested were well tolerated. (3) Most of the polar functional groups commonly present in building blocks and drug-like molecules tested were well tolerated. The list includes, primary, secondary and tertiary amides, alcohols, phenols, aldehydes, ketones, carboxylic acids, esters, aromatic and aliphatic halides, organoboron compounds, *N*-oxides, Weinreb amides, Sulfonamides, a substantial number of heterocycles and alkenes. (4) The presence of amines; primary, secondary and tertiary, poses a limitation. Anilines, alkynes and thioureas are also detrimental to the reaction outcome. While pyridine halts the reaction, sterically hindering the heterocyclic nitrogen (2,6-lutidine) restores reactivity.

At this point we turned our attention to the ultimate goal of this methodology in terms of applications, LSF. While the directing group screening and functional group tolerance studies provided us with a certain level of predictive power in terms of LSF applicability (unproductive DGs, problematic functional groups), the functionalization of complex drugs and natural products presents the added challenge of regioselectivity, functional group combination effects, steric and electronic effects on the directing group and C–H bonds and last but not least substrate solubility. Nonetheless, we decided to screen 48 complex drugs and natural products under screening conditions against two solvents, DCE and NMP. DCE was chosen for its superior performance for the transformation, NMP for its capacity to solubilize most drugs and other complex polar compounds. Out of 48 tested, 11 were considered successful (conversion >10%), with structures confirmed by NMR spectroscopy. Product formation of 4 compounds was observed by LCMS but was not confirmed due to failed purification caused by low conversion and/or product decomposition. With the 33 remaining compounds the following is proposed based on the directing group screening and functional group tolerance studies: 14 examples of substrates with unproductive directing groups, 9 examples of amine-containing substrates. The remaining 10 substrates were unsuccessful likely due to steric effects, combination effects of functional groups and/or presence of unproductive DGs not investigated in the DG informer library.

5.2.4 Reaction Scope: Late-stage Functionalization

Similar to the building blocks applications, single substrate optimization for LSF compounds was also possible. Atazanavir, an antiretroviral agent used for treatment of HIV/AIDS,¹²⁶ was selectively mono- and difunctionalized as a result of catalyst and reagent-controlled selectivity (Table 22). With decreased catalyst loading at 2 mol% and decreased MozN₃ loading, highly monoselective conditions were obtained. On the other hand, increasing both catalyst and MozN₃ loading led to selective difunctionalization. These results

translated smoothly into scale-up, and monosubstituted **12a** and disubstituted **12a'** were successfully obtained (Scheme 35).

Table 22. Single substrate optimization of Atazanavir for mono/di selectivity.

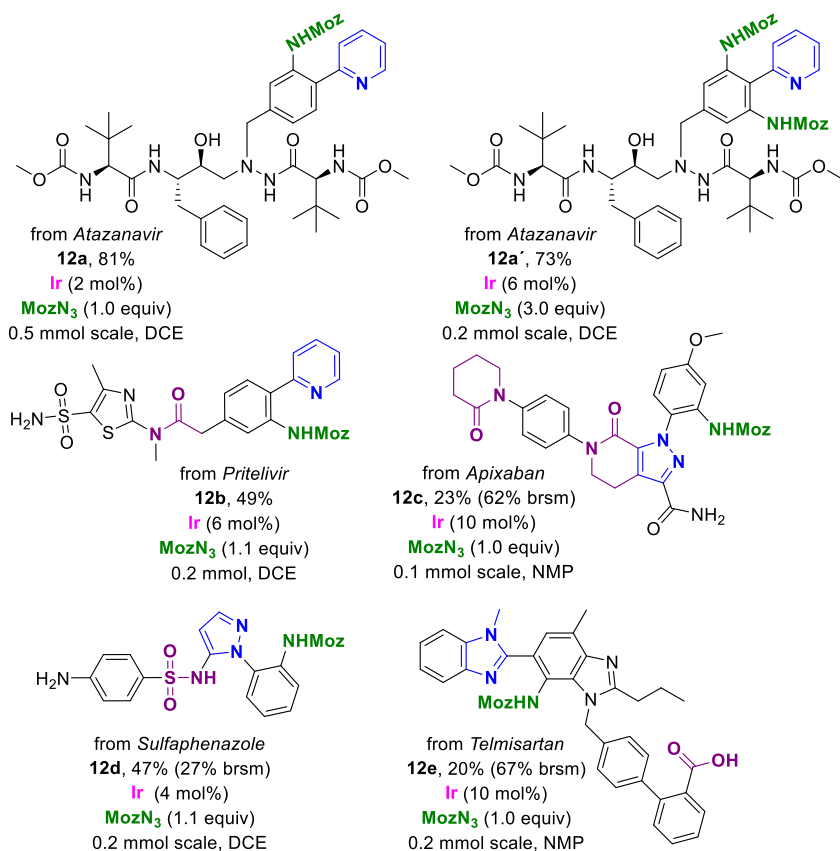
Atazanavir $\xrightarrow[\text{solvent (0.2M), 60 } ^\circ\text{C, 20 h}]{\text{MozN}_3 \text{ (x equiv)}, [\text{Cp}^*\text{Ir}(\text{H}_2\text{O})_3]\text{SO}_4 \text{ (y mol\%)}}$

12a R = H
12a' R = NHMoz

Ir (mol%)		2		4		6	
		12a	12a'	12a	12a'	12a	12a'
MozN ₃ (equiv)	1.0	86.5	3.3	90.2	3.7	92.0	4.0
	1.1	89.2	4.5	92.1	7.9	94.2	5.8
	1.3	83.3	16.7	80.0	20.0	80.9	19.1
	1.5	63.0	37.0	63.9	36.1	65.0	35.0
	2.0	43.5	56.5	14.3	85.7	13.0	87.0
	3.0	61.4	38.6	21.9	21.9	0.0	>99.5

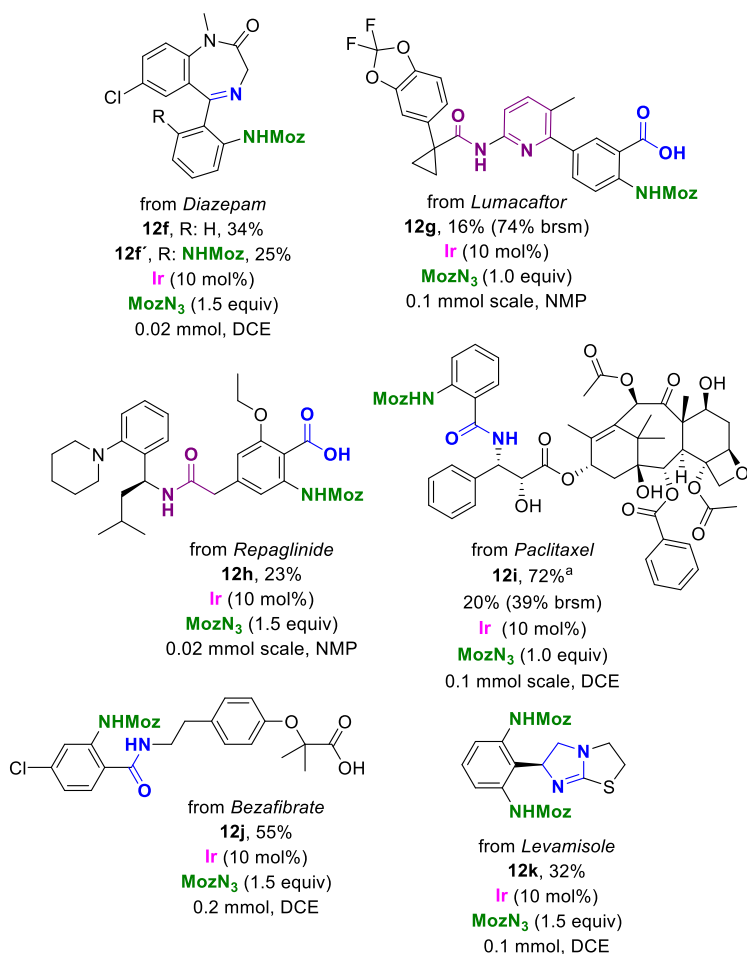
Conversions determined by LCMS (UV trace). Best results for mono/di selectivity highlighted in red.

The amide and carbamate functionalities, as well as the secondary alcohol were well tolerated under the reaction conditions. Pritelivir, an antiviral helicase-primase complex inhibitor used for treatment of herpes simplex virus,^{127,128} was successfully functionalized, yielding compound **12b** with complete regioselectivity. The presence of primary sulfonamide, thiazole and tertiary amide functionalities did not impede the reaction. The importance of solvent variation was demonstrated with the example of Apixaban, an anticoagulant used for stroke and blood clot prevention.¹²⁹ This compound was largely insoluble in DCE, however, by switching to NMP compound **12c** was isolated with 23% yield. 62% of unreacted starting material was also recovered, illustrating the generally observed clean reaction profile. The substituents on the modified pyrazole were tolerated, with the core serving as a productive directing group, showcasing complete regioselectivity over the anilide-directed functionalizations. Functionalization of the antibacterial agent Sulfaphenazole¹³⁰ resulted in the selective formation of compound **12d**. The substituted pyrazole core served as a productive directing group. Given the observations from functional group tolerance studies, the aniline was tolerated beyond expectations, presumably as an effect of altered electronic properties arising from the presence of the sulfonamide group. The result of the functionalization of Telmisartan,



Scheme 35. LSF scope, part 1. Isolated yields shown.

an angiotensin II receptor antagonist used for the treatment of hypertension,¹³¹ heart failure and diabetic kidney disease,¹³² was somewhat surprising in terms of regioselectivity. Initially we expected product formation directed by the carboxylate, however, complete selectivity for the benzimidazole-directed C–H activation product was observed. This result is consistent with our observation in the methylation work. The direct isolation of reaction products from the LSF screening plate on a small scale proved to be achievable, even to the extent where mono/di-functionalization mixtures were successfully separated. Thus monofunctionalized **12f** and difunctionalized **12f'** were obtained from the anxiolytic drug Diazepam (Scheme 36).¹³³ The utility of oxygen-centered directing groups was also demonstrated with LSF examples. Lumacaftor, a therapeutic agent used for the treatment of cystic fibrosis,¹⁰⁶ was functionalized with complete selectivity for the carboxylate-directed product formation over the pyridine and amide directed products, consistent with our



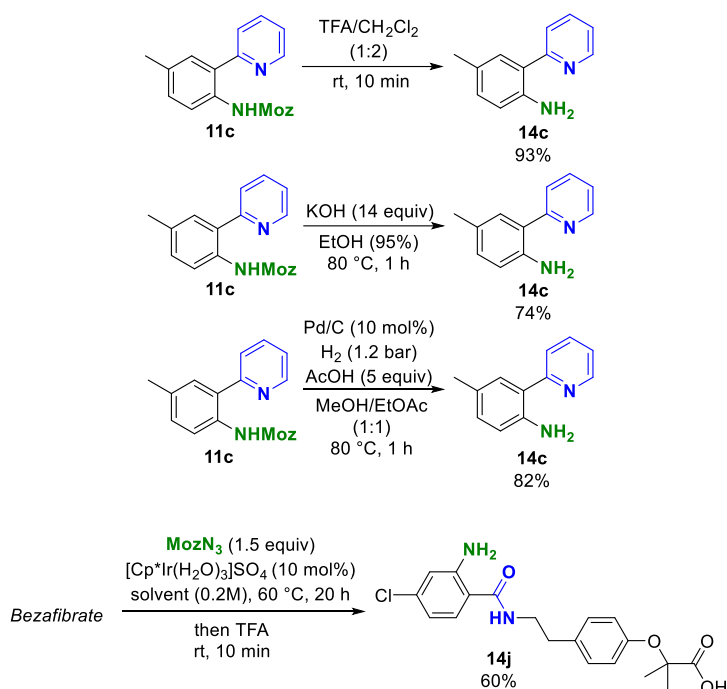
Scheme 36. LSF scope, part 2. Isolated yields shown. ^a C₅H₉COOH (1 equiv) additive used. Potential competing DGs highlighted in purple.

previous work on aminations of benzoic acids. Similarly the Repaglinide analogue **12h** was obtained. Repaglinide is used for blood sugar control in type 2 diabetes mellitus.^{78,79} A powerful example of the applicability of the presented amination method is the functionalization of the natural product Paclitaxel. Paclitaxel is used as a chemotherapeutic agent for the treatment of several types of cancer.¹³⁴ At first, the aminated analogue was obtained with a 20% yield, however, the yield was significantly improved in presence of cyclopentane carboxylic acid as additive (**12i**, 72%). To the best of our knowledge, this presents the highest yielding example of Paclitaxel LSF to date, and a rare example of directed C–H activations applied to this challenging substrate.⁵¹ Bezafibrate, used as a lipid-lowering agent for patients with hyperlipidaemia,¹³⁵ was successfully functionalized at the anticipated position, yielding compound **12j** in 55% yield. It was with this particular substrate

that we observed the positive effect of acid additives on conversions with amides as directing groups, further demonstrating the potential gains from in-former libraries and HTE in generating unanticipated results as a virtue of exploring a larger chemical space. Finally, an outlier in terms of selectivity was Levamisole, a drug used for the treatment of parasitic worm infections in veterinary medicine.¹³⁶ With this substrate we did not observe the formation of a monofunctionalization product by LCMS, only clean difunctionalization. This is likely caused by differences in the catalytic cycle, where we speculate that rather than ligand exchange, the catalyst-bound monofunctionalized product undergoes a second C–H activation. This substrate is also the only example with an sp^3 centered directing group for this reaction.

5.2.5 Deprotection Studies

The Moz protecting group was initially selected not only for the commercial availability of the corresponding azide, but also for the potential to access a number of distinct deprotection protocols. A suitable deprotection protocol tolerant of the functional groups of the substrate of interest could then be chosen to access the free amine. Moz deprotection was demonstrated under 3 distinct conditions (Scheme 37). With the model substrate **10c**, the highest yield was obtained with deprotection under acidic conditions. The protecting group was also successfully deprotected under basic conditions, albeit under these conditions the reaction was not as clean and the isolated yield was significantly lower. Finally, hydrogenolysis also afforded the desired product in 82% yield. While deprotection at room temperature was also possible, elevated temperatures were not detrimental to the reaction outcome and afforded the product in shorter time. Finally, applicability to complex molecules and a one-pot protocol for accessing free amine analogues was demonstrated with the example of Bezafibrate. The target compound **14j** was also obtained with improved yield compared to the Moz-protected analogue (60% vs 55%), as a result of better separation by preparative HPLC.



Scheme 37. Moz deprotection studies. Isolated yields shown.

5.2.6 Miniaturization Studies

As the final part of our studies we decided to further investigate reaction miniaturization, using NMP as a non-volatile solvent. Using the Mosquito[®] multichannel pipetting system from SPT Labtech we found that with as little as one microliter of total reaction volume conversion was observed throughout the selected substrates with reasonable reproducibility (Figure 14). This application shows great promise for future applications in miniaturization and HTE and presents an opportunity for decreasing material consumption, thus increasing the sustainability of reaction screening. As seen in Figure 14, deviations in conversions were observed for a number of substrates. For hit identification purposes on small scale this is not a major issue, since running reactions in multiples of (usually 2-4) is standard procedure. This is not too surprising, given that we operate at the lower volume range accessible by the liquid dispensing system, resulting in some inaccuracy. A further source of deviations was caused by our analytical technique, as once again we operate on the lower range of reaction scales for LCMS conversion assessment by UV trace.

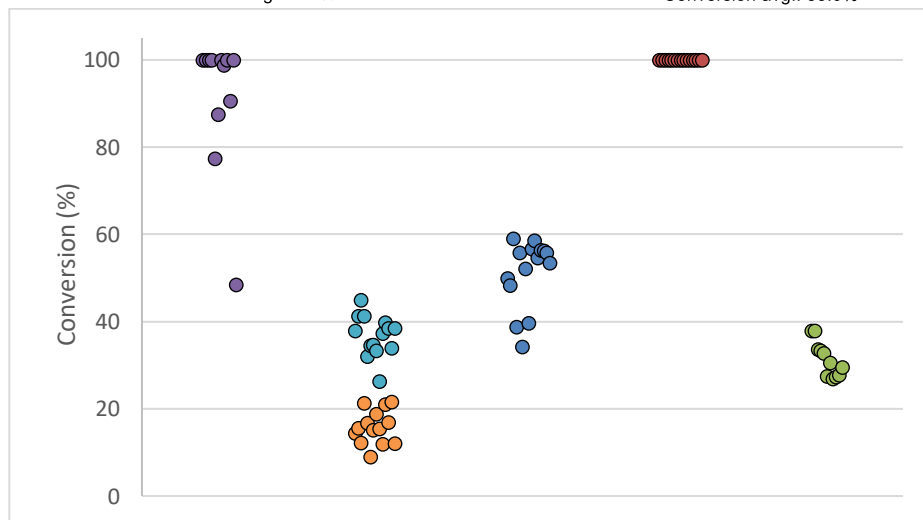
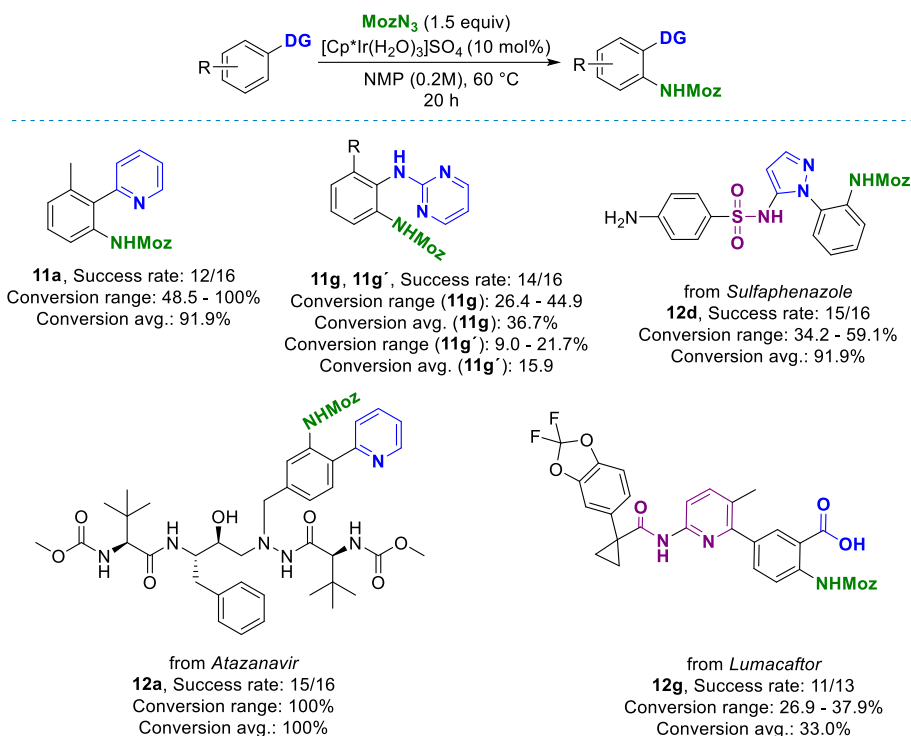


Figure 14. Reaction miniaturization study. 200 nmol scale, total volume 1.0 μL per reaction . Analyzed by LCMS (UV trace). No substrate or product detected with unsuccessful reactions. Purple (**11a**, 2-(*o*-tolyl)pyridine), Light blue (**11g**, 2-phenylpyrimidine-2-amine mono), orange (**11g'**, 2-phenylpyrimidine-2-amine di), Dark blue (**12d**, Sulfaphenazole), Red (**12a**, Atazanavir), Green (**12g**, Lumacaftor).

Further miniaturization is in principle possible, however, this would require a different analytical method. We were able further decrease the reaction scale

by using acoustic dispensing for reaction set-up.¹³⁷ We were able to detect product formations in reaction with as little as 5 nL total volume (1 nmol scale). However, we were not able to quantify conversions on this scale, only to qualitatively assess reaction success. An AMI-MS analytical method to mitigate this issue is currently in development.¹³⁸

5.2.7 Application Guidelines

To complement the developed methodology and summarize the limitations and opportunities for potential users the following guidelines are presented (Figure 15). (1) The first step in predicting the success of the reaction is in directing group selection. In total 21 productive DGs were described in the DG informer library and with the LSF scope. Non-productive directing groups from the DG informer library are also presented (Figure 13). (2) Tolerated functional groups assessment is aided by the results of the functional group tolerance study and the LSF informer library. The major limitations are presence of amines, alkynes, thioureas, and DMSO. The DMSO sensitivity is important to consider in drug discovery, as intermediates are often stored as DMSO solutions. (3) Steric effects should be examined to determine selectivity and/or productivity of a given substrate. The reaction proceeds on the less sterically hindered *ortho* position when two suitable sites are available. Sterically demanding *meta* substituents block 1,2,3-substitution. Substituents on the DG and in the *ortho* position of the substrate can negatively impact the reaction outcome by twisting the DG out of plane.¹³⁹

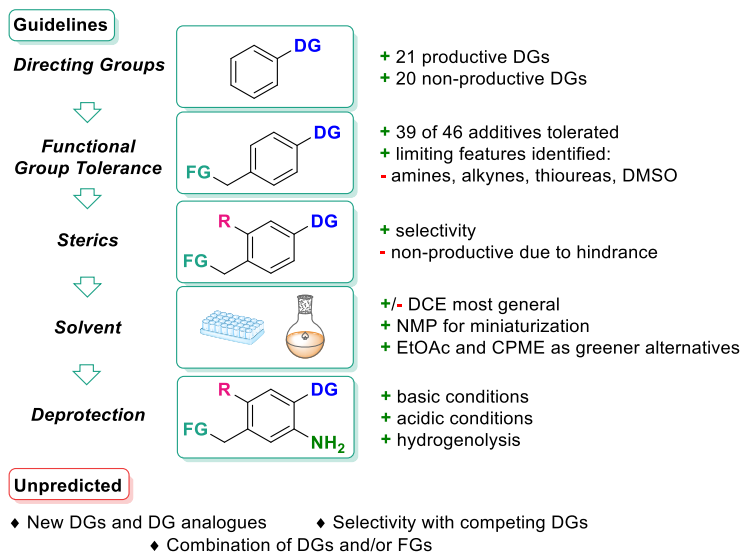


Figure 15. Application guidelines for the C–H amination methodology.

(4) Solvent choice is to be considered according to the desired application. Although DCE showed best overall performance, this can be substituted by EtOAc or CPME as greener alternatives. NMP is optimal for miniaturization at low μL volume range, as well as for applications with polar drug-like substrates with low solubility in DCE. (5) Suitable deprotection conditions are chosen based on the functional groups present in the substrate. The presented deprotection protocols should satisfy the requirements of the vast majority of applications. The applicability of the presented model is limited in terms of applicability to uninvestigated DGs and their analogues. Selectivity between DGs, while observed in all presented cases, was not investigated in depth. Finally, although the functional group tolerance studies provide the basic rules, combination effects of multiple groups are not predicted.

5.3 Conclusions

The presented C–H amination methodology was successfully applied for high-throughput investigations, allowing rapid assessment of reaction scope and limitations. The functionalization of 21 building blocks bearing 16 distinct directing groups is described, as well as late-stage applications on 11 diversely decorated pharmaceuticals. In terms of directing group applicability, the productivity of the reaction was demonstrated with 21 distinct directing groups. The three distinct deprotection protocols presented allow for Moz deprotection tailored to the substrate requirements. Continuing the HTE and miniaturization theme in this dissertation, the methodology presents the culmination of our HTE efforts and applicability. Tolerance to air and moisture allows for reaction set-up under atmospheric conditions, which allowed us to use automation and miniaturization equipment largely unexplored in synthetic chemistry. The use of soluble reagents, complemented with successful use of non-volatile solvents allowed us to perform reactions in sub-microliter volumes. To the best of our knowledge, these examples are the smallest scale C–H activations presented to date. This is of special importance in terms of material consumption, given the high value of hit and lead compounds in the drug discovery process, as well as in terms of use of precious metals used in catalysis. A far-reaching benefit of the presented work is the reporting of negative results, which, at least according to the author of this thesis, is highly valuable, and unfortunately largely underrepresented in published literature. The broader picture presented, together with the application guidelines are intended to aid the potential users with predicting the applicability of the method to their desired transformations, ultimately saving time and resources on unproductive transformations.

6. Concluding remarks

As a final note, it is important to put this dissertation in the appropriate context. The results presented here represent a small advancement in the field of organic chemistry, despite summarizing four years of work. However, it is crucial to keep in mind that the state-of-the-art in all scientific disciplines is, more often than not, a result of incremental work and small advancements made by the people involved. At its best, this system leads to progress and enables innovation beneficial for humanity, experiment by experiment, paper by paper.

The main contribution of the work presented in this dissertation is in exploring and expanding the applicability of catalytic C–H activations in pharmaceutical research. The challenges in functional group tolerance, selectivity, substrate scope, and predictability of reaction outcome that were encountered on this journey are representative of the hurdles that need to be overcome in order for C–H activations to become more appealing for the wider medicinal chemistry community. The iodination, methylation and amination methodologies demonstrate a range of opportunities unlocked by addressing these challenges.

- 1) Allowing access to previously unexplored advanced building blocks relevant to drug discovery.
- 2) Introduction of small substituents to structurally complex pharmaceuticals in a late stage, allowing rapid access to valuable analogues.
- 3) Introduction of linkers, allowing access to new modalities for challenging targets in drug discovery.
- 4) Tuning reactions to facilitate high-throughput experimentation, allowing the exploration of an increasingly large chemical space.
- 5) Reaction miniaturization and solvent recycling, addressing some of the sustainability challenges associated with organic synthesis.

The reward for good work is more work. An insatiable appetite for knowledge, a childlike curiosity, and a faith in progress motivates many of us to dedicate our lives to science. It is my hope that this modest contribution will be useful to fellow researchers. We shall continue our work in service of humanity, advancing the greater body of knowledge, and improving the quality of life for all. Thank you for reading this dissertation.

Appendix A: Author's Contributions

Paper I

Major contribution to the formulation of the research problem. Performed all experimental work and compound characterization. Wrote the article draft and supporting information.

Paper II

Formulation of the research problem. Performed all experimental work and compound characterization. M.A.H. interpreted the results of biological studies. Wrote the article and supporting information.

Paper III

Formulation of the research problem. Performed all experimental work and compound characterization, with the exception of purification of conjugates. Wrote the article and supporting information.

Paper IV

Formulation of the research problem. Performed all experimental work and compound characterization, except: P. K. performed small scale purification and accurate mass measurements, M. J. performed the nmol scale synthesis. Wrote the article and supporting information.

Appendix B: Reprint Permissions

The distribution and reproduction of the articles attached in this thesis is permitted under the Creative Commons CC BY license.

Original work:

Paper I.

Weis, E.; Johansson, M. J.; Martín-Matute, B. *Chem. Eur. J.* **2020**, *26*, 10185.
© 2020 The Authors. Published by Wiley-VCH Verlag GmbH & Co. KGaA

Paper II.

Weis, E.; Hayes, M. A.; Johansson, M. J.; Martín-Matute, B. *iScience* **2021**, *24*, 102467.
© 2021 The Authors. Published by Elsevier

Paper III.

Weis, E.; Johansson, M. J.; Martín-Matute, B. *Chem. Eur. J.* **2021**, *Accepted*,
<https://doi.org/10.1002/chem.202103510> (Preprint)
© 2021 The Authors. Published by Wiley-VCH Verlag GmbH & Co. KGaA

Paper IV.

Weis, E.; Johansson, M.; Korsgren, P.; Martín-Matute, B.; Johansson, M. J. *ChemRxiv* **2021**, Cambridge: Cambridge Open Engage; This content is a preprint and has not been peer-reviewed.
DOI: 10.26434/chemrxiv-2021-vp0kl

The cover feature associated with Paper I was included with permission from the John Wiley and Sons publishing house.

Original work:

Weis, E.; Johansson, M. J.; Martín-Matute, B. *Chem. Eur. J.* **2020**, *26*, 10155.
© 2020 The Authors. Published by Wiley-VCH Verlag GmbH & Co. KGaA

Acknowledgements

I would like to express my deepest gratitude and thanks to:

My supervisors, **Prof. Belén Martín-Matute** and **Dr. Magnus Johansson**, for giving me the opportunity to pursue Doctoral studies and working with you. Thank you for giving me freedom to pursue exciting chemistry under your guidance, for your support and scientific input over the years.

Dr. Stig Friis, friend and mentor, for his help and support in and outside of the lab, especially during the challenging early stages.

Assistant supervisor **Prof. Göran Widmalm** for his support.

Prof. Kálmán Szabó for taking the time and showing interest in this dissertation and for his comments and corrections.

Dr. Nicklas Selander for his role as opponent for the half-time report and for his input on the report text that became the basis for this dissertation.

Dr. Martin Hayes for his work on the biological studies in Paper II and all the discussions over the years.

Maria Johansson and **Dr. Pernilla Korsgren** for their on Paper IV, it was a pleasure working with you. Thank you for your hard work, for the scientific discussions, and for making my days brighter.

Dr. Johan Johansson, **Dr. Christopher Kourra**, **Dr. Laurent Knerr** and **Dr. Maria Ölwegård Halvarsson** for consultations related to new modalities chemistry in Paper III.

Dr. Mark Patchey for taking the time to proofread this dissertation and for his input and suggestions.

Dr. Robert Sheppard for his support as my line manager.

Dr. Malin Lemurell for her support throughout my years at AstraZeneca.

Current and past **members of the BMM group**.

Current and past **members of the iLab** at AstraZeneca Gothenburg, and to all the **colleagues at Medicinal Chemistry AstraZeneca R&D** in Gothenburg.

The Swedish Foundation for Strategic Research for funding *via* the industrial doctoral student program.

My parents, **Adriana** and **Robert**, for always believing in me and for their support over the years. Without you I would not have made it all the way here.

Julia, for your love, for sharing moments of great happiness and supporting me during my deepest lows over the past years. There shall be more time for us now.

References

- (1) Mitscherlich, E. *Annalen der Physik und Chemie* **1834**, *31*, 625.
- (2) Guillemard, L.; Kaplaneris, N.; Ackermann, L.; Johansson, M. J. *Nat. Rev. Chem.* **2021**, *5*, 522.
- (3) Börgel, J.; Ritter, T. *Chem* **2020**, *6*, 1877.
- (4) Cernak, T.; Dykstra, K. D.; Tyagarajan, S.; Vachal, P.; Krska, S. W. *Chem. Soc. Rev.* **2016**, *45*, 546.
- (5) McGrath, N. A.; Brichacek, M.; Njardarson, J. T. *J. Chem. Educ.* **2010**, *87*, 1348.
- (6) Angell, R.; Aston, N. M.; Bamborough, P.; Buckton, J. B.; Cockerill, S.; deBoeck, S. J.; Edwards, C. D.; Holmes, D. S.; Jones, K. L.; Laine, D. I.; Patel, S.; Smee, P. A.; Smith, K. J.; Somers, D. O.; Walker, A. L. *Bioorg. Med. Chem. Lett.* **2008**, *18*, 4428.
- (7) Aynedinova, D.; Callens, M. C.; Hicks, H. B.; Poh, C. Y. X.; Shennan, B. D. A.; Boyd, A. M.; Lim, Z. H.; Leitch, J. A.; Dixon, D. J. *Chem. Soc. Rev.* **2021**, *50*, 5517.
- (8) Wender, P. A. *Nat. Prod. Rep.* **2014**, *31*, 433.
- (9) Sezen, B.; Sames, D. *What is C-H Bond Activation?* in *Handbook of C-H Transformations*, G. Dyker (Ed.), Wiley, **2008**.
- (10) Roudesly, F.; Oble, J.; Poli, G. *J. Mol. Catal. A Chem.* **2017**, *426*, 275.
- (11) Evano, G.; Theunissen, C. *Angew. Chem. Int. Ed.* **2019**, *58*, 7202.
- (12) Mkhaliid, I. A. I.; Barnard, J. H.; Marder, T. B.; Murphy, J. M.; Hartwig, J. F. *Chem. Rev.* **2010**, *110*, 890.
- (13) Sambiagio, C.; Schönbauer, D.; Blicke, R.; Dao-Huy, T.; Pototschnig, G.; Schaaf, P.; Wiesinger, T.; Zia, M. F.; Wencel-Delord, J.; Besset, T.; Maes, B. U. W.; Schnürch, M. *Chem. Soc. Rev.* **2018**, *47*, 6603.
- (14) Stamenković, N.; Ulrih, N. P.; Cerkovnik, J. *Phys. Chem. Chem. Phys.* **2021**, *23*, 5051.
- (15) Snieckus, V. *Chem. Rev.* **1990**, *90*, 879.
- (16) Duncton, M. A. J. *MedChemComm* **2011**, *2*, 1135.
- (17) Groweiss, A. *Org. Process Res. Dev.* **2000**, *4*, 30.
- (18) Crivello, J. V. *J. Org. Chem.* **1981**, *46*, 3056.
- (19) Beak, P.; Snieckus, V. *Acc. Chem. Res.* **1982**, *15*, 306.
- (20) Gandeepan, P.; Müller, T.; Zell, D.; Cera, G.; Warratz, S.; Ackermann, L. *Chem. Rev.* **2019**, *119*, 2192.
- (21) Das, R.; Kapur, M. *Asian J. Org. Chem.* **2018**, *7*, 1524.
- (22) Zhang, Z.; Tanaka, K.; Yu, J.-Q. *Nature* **2017**, *543*, 538.

- (23) Bag, S.; Patra, T.; Modak, A.; Deb, A.; Maity, S.; Dutta, U.; Dey, A.; Kancherla, R.; Maji, A.; Hazra, A.; Bera, M.; Maiti, D. *J. Am. Chem. Soc.* **2015**, *137*, 11888.
- (24) Sharma, R.; Sharma, U. *Catal. Rev.-Sci. Eng.* **2018**, *60*, 497.
- (25) Kuninobu, Y.; Ida, H.; Nishi, M.; Kanai, M. *Nat. Chem.* **2015**, *7*, 712.
- (26) Hartwig, J. F.; Larsen, M. A. *ACS Cent. Sci.* **2016**, *2*, 281.
- (27) Wang, P.; Verma, P.; Xia, G.; Shi, J.; Qiao, J. X.; Tao, S.; Cheng, P. T. W.; Poss, M. A.; Farmer, M. E.; Yeung, K.-S.; Yu, J.-Q. *Nature* **2017**, *551*, 489.
- (28) Dick, A. R.; Hull, K. L.; Sanford, M. S. *J. Am. Chem. Soc.* **2004**, *126*, 2300.
- (29) Leow, D.; Li, G.; Mei, T.-S.; Yu, J.-Q. *Nature* **2012**, *486*, 518.
- (30) Liégault, B.; Lapointe, D.; Caron, L.; Vlassova, A.; Fagnou, K. *J. Org. Chem.* **2009**, *74*, 1826.
- (31) Ishiyama, T.; Takagi, J.; Ishida, K.; Miyaura, N.; Anastasi, N. R.; Hartwig, J. F. *J. Am. Chem. Soc.* **2002**, *124*, 390.
- (32) Gallego, D.; Baquero Edwin, A. In *Open Chem.* **2018**, *16*, 1001.
- (33) Periana, R. A.; Bergman, R. G. *Organometallics* **1984**, *3*, 508.
- (34) Webster, C. E.; Fan, Y.; Hall, M. B.; Kunz, D.; Hartwig, J. F. *J. Am. Chem. Soc.* **2003**, *125*, 858.
- (35) Lara, P.; Paneque, M.; Poveda, M. L.; Santos, L. L.; Valpuesta, J. E. V.; Carmona, E.; Moncho, S.; Ujaque, G.; Lledós, A.; Álvarez, E.; Mereiter, K. *Chem. Eur. J.* **2009**, *15*, 9034.
- (36) Gorelsky, S. I.; Lapointe, D.; Fagnou, K. *J. Am. Chem. Soc.* **2008**, *130*, 10848.
- (37) Raghuvanshi, K.; Zell, D.; Ackermann, L. *Org. Lett.* **2017**, *19*, 1278.
- (38) Gensch, T.; Hopkinson, M. N.; Glorius, F.; Wencel-Delord, J. *Chem. Soc. Rev.* **2016**, *45*, 2900.
- (39) Erbing, E.; Sanz-Marco, A.; Vázquez-Romero, A.; Malmberg, J.; Johansson, M. J.; Gómez-Bengo, E.; Martín-Matute, B. *ACS Catal.* **2018**, *8*, 920.
- (40) Sadler, S. A.; Tajuddin, H.; Mkhallid, I. A. I.; Batsanov, A. S.; Albesa-Jove, D.; Cheung, M. S.; Maxwell, A. C.; Shukla, L.; Roberts, B.; Blakemore, D. C.; Lin, Z.; Marder, T. B.; Steel, P. G. *Org. Biomol. Chem.* **2014**, *12*, 7318.
- (41) Özdemir, İ.; Demir, S.; Gürbüz, N.; Çetinkaya, B.; Toupet, L.; Bruneau, C.; Dixneuf, P. H. *Eur. J. Inorg. Chem.* **2009**, *2009*, 1942.
- (42) Chen, X.; Hao, X.-S.; Goodhue, C. E.; Yu, J.-Q. *J. Am. Chem. Soc.* **2006**, *128*, 6790.
- (43) Chessari, G.; Grainger, R.; Holvey, R. S.; Ludlow, R. F.; Mortenson, P. N.; Rees, D. C. *Chem. Sci.* **2021**.
- (44) Griffen, E.; Leach, A. G.; Robb, G. R.; Warner, D. J. *J. Med. Chem.* **2011**, *54*, 7739.

- (45) Valeur, E.; Guéret, S. M.; Adihou, H.; Gopalakrishnan, R.; Lemurell, M.; Waldmann, H.; Grossmann, T. N.; Plowright, A. T. *Angew. Chem. Int. Ed.* **2017**, *56*, 10294.
- (46) Shevlin, M. *ACS Med. Chem. Lett.* **2017**, *8*, 601.
- (47) Mennen, S. M.; Alhambra, C.; Allen, C. L.; Barberis, M.; Berritt, S.; Brandt, T. A.; Campbell, A. D.; Castañón, J.; Cherney, A. H.; Christensen, M.; Damon, D. B.; Eugenio de Diego, J.; García-Cerrada, S.; García-Losada, P.; Haro, R.; Janey, J.; Leitch, D. C.; Li, L.; Liu, F.; Lobben, P. C.; MacMillan, D. W. C.; Magano, J.; McInturff, E.; Monfette, S.; Post, R. J.; Schultz, D.; Sitter, B. J.; Stevens, J. M.; Strambeanu, I. I.; Twilton, J.; Wang, K.; Zajac, M. A. *Org. Process Res. Dev.* **2019**, *23*, 1213.
- (48) Krska, S. W.; DiRocco, D. A.; Dreher, S. D.; Shevlin, M. *Acc. Chem. Res.* **2017**, *50*, 2976.
- (49) Uehling, M. R.; King, R. P.; Krska, S. W.; Cernak, T.; Buchwald, S. L. *Science* **2019**, *363*, 405.
- (50) DiRocco, D. A.; Dykstra, K.; Krska, S.; Vachal, P.; Conway, D. V.; Tudge, M. *Angew. Chem. Int. Ed.* **2014**, *53*, 4802.
- (51) Friis, S. D.; Johansson, M. J.; Ackermann, L. *Nat. Chem.* **2020**, *12*, 511.
- (52) Kutchukian, P. S.; Dropinski, J. F.; Dykstra, K. D.; Li, B.; DiRocco, D. A.; Streckfuss, E. C.; Campeau, L.-C.; Cernak, T.; Vachal, P.; Davies, I. W.; Krska, S. W.; Dreher, S. D. *Chem. Sci.* **2016**, *7*, 2604.
- (53) Dreher, S. D.; Krska, S. W. *Acc. Chem. Res.* **2021**, *54*, 1586.
- (54) Gohier, F.; Mortier, J. J. *Org. Chem.* **2003**, *68*, 2030.
- (55) Nguyen, T.-H.; Chau, N. T. T.; Castanet, A.-S.; Nguyen, K. P. P.; Mortier, J. J. *Org. Chem.* **2007**, *72*, 3419.
- (56) Mei, T.-S.; Giri, R.; Maugel, N.; Yu, J.-Q. *Angew. Chem. Int. Ed.* **2008**, *47*, 5215.
- (57) Weis, E.; Johansson, M. J.; Martín-Matute, B. *Chem. Eur. J.* **2020**, *26*, 10185.
- (58) Barnett, J. R.; Andrews, L. J.; Keefer, R. M. *J. Am. Chem. Soc.* **1972**, *94*, 6129.
- (59) Cunningham, R. F.; Israili, Z. H.; Dayton, P. G. *Clin. Pharmacokin.* **1981**, *6*, 135.
- (60) Frasco, D. A.; Lilly, C. P.; Boyle, P. D.; Ison, E. A. *ACS Catal.* **2013**, *3*, 2421.
- (61) Simmons, E. M.; Hartwig, J. F. *Angew. Chem. Int. Ed.* **2012**, *51*, 3066.
- (62) Kim, H.; Shin, K.; Chang, S. *J. Am. Chem. Soc.* **2014**, *136*, 5904.
- (63) Barreiro, E. J.; Kümmerle, A. E.; Fraga, C. A. M. *Chem. Rev.* **2011**, *111*, 5215.
- (64) Sun, S.; Fu, J. *Bioorg. Med. Chem. Lett.* **2018**, *28*, 3283.
- (65) Schönherr, H.; Cernak, T. *Angew. Chem. Int. Ed.* **2013**, *52*, 12256.
- (66) Gomtsyan, A.; Bayburt, E. K.; Keddy, R.; Turner, S. C.; Jinkerson, T. K.; Didomenico, S.; Perner, R. J.; Koenig, J. R.; Drizin, I.; McDonald, H. A.; Surowy, C. S.; Honore, P.; Mikusa, J.; Marsh, K. C.; Wetter, J.

- M.; Faltynek, C. R.; Lee, C.-H. *Bioorg. Med. Chem. Lett.* **2007**, *17*, 3894.
- (67) Jones, C. D.; Andrews, D. M.; Barker, A. J.; Blades, K.; Byth, K. F.; Finlay, M. R. V.; Geh, C.; Green, C. P.; Johannsen, M.; Walker, M.; Weir, H. M. *Bioorg. Med. Chem. Lett.* **2008**, *18*, 6486.
- (68) Shamovsky, I.; de Graaf, C.; Alderin, L.; Bengtsson, M.; Bladh, H.; Börjesson, L.; Connolly, S.; Dyke, H. J.; van den Heuvel, M.; Johansson, H.; Josefsson, B.-G.; Kristoffersson, A.; Linnanen, T.; Lisius, A.; Männikkö, R.; Nordén, B.; Price, S.; Ripa, L.; Rognan, D.; Rosendahl, A.; Skrinjar, M.; Urbahns, K. *J. Med. Chem.* **2009**, *52*, 7706.
- (69) Zimmerman, D. M.; Leander, J. D.; Cantrell, B. E.; Reel, J. K.; Snoddy, J.; Mendelsohn, L. G.; Johnson, B. G.; Mitch, C. H. *J. Med. Chem.* **1993**, *36*, 2833.
- (70) Feng, K.; Quevedo, R. E.; Kohrt, J. T.; Oderinde, M. S.; Reilly, U.; White, M. C. *Nature* **2020**, *580*, 621.
- (71) Giri, R.; Mangel, N.; Li, J.-J.; Wang, D.-H.; Breazzano, S. P.; Saunders, L. B.; Yu, J.-Q. *J. Am. Chem. Soc.* **2007**, *129*, 3510.
- (72) Lv, W.; Wen, S.; Liu, J.; Cheng, G. *J. Org. Chem.* **2019**, *84*, 9786.
- (73) Shang, R.; Ilies, L.; Nakamura, E. *J. Am. Chem. Soc.* **2016**, *138*, 10132.
- (74) Rosen, B. R.; Simke, L. R.; Thuy-Boun, P. S.; Dixon, D. D.; Yu, J.-Q.; Baran, P. S. *Angew. Chem. Int. Ed.* **2013**, *52*, 7317.
- (75) Shin, K.; Park, Y.; Baik, M.-H.; Chang, S. *Nat. Chem.* **2018**, *10*, 218.
- (76) Kim, J.; Shin, K.; Jin, S.; Kim, D.; Chang, S. *J. Am. Chem. Soc.* **2019**, *141*, 4137.
- (77) Weis, E.; Hayes, M. A.; Johansson, M. J.; Martín-Matute, B. *iScience* **2021**, *24*, 102467.
- (78) Culy, C. R.; Jarvis, B. *Drugs* **2001**, *61*, 1625.
- (79) Grell, W.; Hurnaus, R.; Griss, G.; Sauter, R.; Rupprecht, E.; Mark, M.; Luger, P.; Nar, H.; Wittneben, H.; Müller, P. *J. Med. Chem.* **1998**, *41*, 5219.
- (80) Duvic, M.; Hymes, K.; Heald, P.; Breneman, D.; Martin, A. G.; Myskowski, P.; Crowley, C.; Yocum, R. C. *J. Clin. Oncol.* **2001**, *19*, 2456.
- (81) Gniadecki, R.; Assaf, C.; Bagot, M.; Dummer, R.; Duvic, M.; Knobler, R.; Ranki, A.; Schwandt, P.; Whittaker, S. *Br. J. Dermatol.* **2007**, *157*, 433.
- (82) Azuma, H.; Banno, K.; Yoshimura, T. *Br. J. Pharmacol.* **1976**, *58*, 483.
- (83) Darakhshan, S.; Pour, A. B. *Pharmacol. Res.* **2015**, *91*, 15.
- (84) Steverlynck, J.; Sitdikov, R.; Rueping, M. *Chem. Eur. J.* **2021**, *27*, 11751.
- (85) Stringer, R. A.; Williams, G.; Picard, F.; Sohal, B.; Kretz, O.; McKenna, J.; Krauser, J. A. *Drug Metab. Dispos.* **2014**, *42*, 954.
- (86) Parcella, K.; Eastman, K.; Yeung, K.-S.; Grant-Young, K. A.; Zhu, J.; Wang, T.; Zhang, Z.; Yin, Z.; Parker, D.; Mosure, K.; Fang, H.; Wang, Y.-K.; Lemm, J.; Zhuo, X.; Hanumegowda, U.; Liu, M.; Rigat, K.;

- Donoso, M.; Tuttle, M.; Zvyaga, T.; Haarhoff, Z.; Meanwell, N. A.; Soars, M. G.; Roberts, S. B.; Kadow, J. F. *ACS Med. Chem. Lett.* **2017**, *8*, 771.
- (87) Gant, T. G. *J. Med. Chem.* **2014**, *57*, 3595.
- (88) DeWitt, S. H.; Maryanoff, B. E. *Biochemistry* **2018**, *57*, 472.
- (89) Sun, Q.; Yoshikai, N. *Org. Chem. Front.* **2018**, *5*, 2214.
- (90) Han, X.; Yuan, Y.; Shi, Z. *J. Org. Chem.* **2019**, *84*, 12764.
- (91) Zhou, K.; Zhu, Y.; Fan, W.; Chen, Y.; Xu, X.; Zhang, J.; Zhao, Y. *ACS Catal.* **2019**, *9*, 6738.
- (92) Falb, E.; Ulanenko, K.; Tor, A.; Gottesfeld, R.; Weitman, M.; Afri, M.; Gottlieb, H.; Hassner, A. *Green Chem.* **2017**, *19*, 5046.
- (93) Säll, C.; Houston, J. B.; Galetin, A. *Drug Metab. Dispos.* **2012**, *40*, 1279.
- (94) Katoh, M.; Matsui, T.; Yokoi, T. *Drug Metab. Dispos.* **2007**, *35*, 583.
- (95) Zhang, Y.-Y.; Liu, Y.; Mehboob, S.; Song, J.-H.; Boci, T.; Johnson, M. E.; Ghosh, A. K.; Jeong, H. *Xenobiotica* **2014**, *44*, 404.
- (96) Welton, T. *Proc. R. Soc. A* **2015**, *471*, 20150502.
- (97) Huang, H.-M.; Bellotti, P.; Ma, J.; Dalton, T.; Glorius, F. *Nat. Rev. Chem.* **2021**, *5*, 301.
- (98) Brown, D. G.; Boström, J. *J. Med. Chem.* **2016**, *59*, 4443.
- (99) Rogge, T.; Kaplaneris, N.; Chatani, N.; Kim, J.; Chang, S.; Punji, B.; Schafer, L. L.; Musaev, D. G.; Wencel-Delord, J.; Roberts, C. A.; Sarpong, R.; Wilson, Z. E.; Brimble, M. A.; Johansson, M. J.; Ackermann, L. *Nat. Rev. Methods Primers* **2021**, *1*, 43.
- (100) Ng, K.-H.; Ng, F.-N.; Yu, W.-Y. *Chem. Commun.* **2012**, *48*, 11680.
- (101) Lee, D.; Chang, S. *Chem. Eur. J.* **2015**, *21*, 5364.
- (102) Kim, H.; Chang, S. *ACS Catal.* **2015**, *5*, 6665.
- (103) Weis, E.; Johansson, M. J.; Martín-Matute, B. *Chem. Eur. J.* **2021**, <https://doi.org/10.1002/chem.202103510>
- (104) Arcaniolo, D.; Conquy, S.; Tarcan, T. *Eur. Rev. Med. Pharmacol. Sci.* **2015**, *19*, 719.
- (105) G Keller, S.; Kamiya, M.; Urano, Y. *Molecules* **2020**, *25*, 5964.
- (106) Berger, J.; Li, M.; Berger, S.; Meilak, M.; Rientjes, J.; Currie, P. D. *J. Cell. Mol. Med.* **2020**, *24*, 6680.
- (107) Green, S. P.; Wheelhouse, K. M.; Payne, A. D.; Hallett, J. P.; Miller, P. W.; Bull, J. A. *Org. Process Res. Dev.* **2020**, *24*, 67.
- (108) Blanco, M.-J.; Gardinier, K. M. *ACS Med. Chem. Lett.* **2020**, *11*, 228.
- (109) Yang, W.; Gadgil, P.; Krishnamurthy, V. R.; Landis, M.; Mallick, P.; Patel, D.; Patel, P. J.; Reid, D. L.; Sanchez-Felix, M. *AAPS J.* **2020**, *22*, 21.
- (110) Dasa, S. S. K.; Suzuki, R.; Gutknecht, M.; Brinton, L. T.; Tian, Y.; Michaelsson, E.; Lindfors, L.; Klibanov, A. L.; French, B. A.; Kelly, K. A. *J. Control. Release* **2015**, *220*, 556.
- (111) Konstantinidou, M.; Li, J.; Zhang, B.; Wang, Z.; Shaabani, S.; Ter Brake, F.; Essa, K.; Dömling, A. *Expert Opin. Drug Discov.* **2019**, *14*, 1255.

- (112) Nalawansha, D. A.; Crews, C. M. *Cell Chem. Biol.* **2020**, *27*, 998.
- (113) Trippier, P. C. *ChemMedChem* **2013**, *8*, 190.
- (114) Afanasyev, O. I.; Kuchuk, E.; Usanov, D. L.; Chusov, D. *Chem. Rev.* **2019**, *119*, 11857.
- (115) Boström, J.; Brown, D. G.; Young, R. J.; Keserü, G. M. *Nat. Rev. Drug Discov.* **2018**, *17*, 709.
- (116) Shin, K.; Kim, H.; Chang, S. *Acc. Chem. Res.* **2015**, *48*, 1040.
- (117) Park, Y.; Park, K. T.; Kim, J. G.; Chang, S. *J. Am. Chem. Soc.* **2015**, *137*, 4534.
- (118) Kim, H.; Park, G.; Park, J.; Chang, S. *ACS Catal.* **2016**, *6*, 5922.
- (119) Park, Y.; Kim, Y.; Chang, S. *Chem. Rev.* **2017**, *117*, 9247.
- (120) Hong, S. Y.; Hwang, Y.; Lee, M.; Chang, S. *Acc. Chem. Res.* **2021**, *54*, 2683.
- (121) Patel, P.; Chang, S. *Org. Lett.* **2014**, *16*, 3328.
- (122) Hwang, Y.; Park, Y.; Chang, S. *Chem. Eur. J.* **2017**, *23*, 11147.
- (123) Schiesser, S.; Cox, R. J.; Czechtizky, W. *Future Med. Chem.* **2021**, *13*, 941.
- (124) Cernak, T.; Gesmundo, N. J.; Dykstra, K.; Yu, Y.; Wu, Z.; Shi, Z.-C.; Vachal, P.; Sperbeck, D.; He, S.; Murphy, B. A.; Sonatore, L.; Williams, S.; Madeira, M.; Verras, A.; Reiter, M.; Lee, C. H.; Cuff, J.; Sherer, E. C.; Kuethe, J.; Goble, S.; Perrotto, N.; Pinto, S.; Shen, D.-M.; Nargund, R.; Balkovec, J.; DeVita, R. J.; Dreher, S. D. *J. Med. Chem.* **2017**, *60*, 3594.
- (125) Wood, R. *Expert Rev. Anti-infect. Ther.* **2008**, *6*, 785.
- (126) Wozniak, M. A.; Frost, A. L.; Itzhaki, R. F. *Antiviral Res.* **2013**, *99*, 401.
- (127) Wald, A.; Timmler, B.; Magaret, A.; Warren, T.; Tying, S.; Johnston, C.; Fife, K.; Selke, S.; Huang, M.-L.; Stobernack, H.-P.; Zimmermann, H.; Corey, L.; Birkmann, A.; Ruebsamen-Schaeff, H. *JAMA* **2016**, *316*, 2495.
- (128) Budovich, A.; Zargarova, O.; Nogid, A. *Pharm. Ther.* **2013**, *38*, 206.
- (129) Foye, W. O. in *Kirk-Othmer Encyclopedia of Chemical Technology*, Wiley, **2004**.
- (130) Sharpe, M.; Jarvis, B.; Goa, K. L. *Drugs* **2001**, *61*, 1501.
- (131) Pavliukovych, N.; Pavliukovych, O.; Tryphonyuk, L.; Kozar, M. *Atherosclerosis* **2019**, *287*, e153.
- (132) Calcaterra, N. E.; Barrow, J. C. *ACS Chem. Neurosci.* **2014**, *5*, 253.
- (133) Kuk, K.; Taylor-Cousar, J. L. *Ther. Adv. Respir. Disc.* **2015**, *9*, 313.
- (134) Weaver, B. A. *Mol. Biol. Cell* **2014**, *25*, 2677.
- (135) Goldenberg, I.; Benderly, M.; Goldbourt, U. *Vasc. Health Risk Manag.* **2008**, *4*, 131.
- (136) Page, S. W. In *Small Animal Clinical Pharmacology (Second Edition)*; Maddison, J. E., Page, S. W., Church, D. B., Eds.; W.B. Saunders: Edinburgh, **2008**, p 198.
- (137) Wong, E. Y.; Diamond, S. L. *Anal. Chem.* **2009**, *81*, 509.

- (138) Sinclair, I.; Bachman, M.; Addison, D.; Rohman, M.; Murray, D. C.; Davies, G.; Mouchet, E.; Tonge, M. E.; Stearns, R. G.; Ghislain, L.; Datwani, S. S.; Majlof, L.; Hall, E.; Jones, G. R.; Hoyes, E.; Olechno, J.; Ellson, R. N.; Barran, P. E.; Pringle, S. D.; Morris, M. R.; Wingfield, J. *Anal. Chem.* **2019**, *91*, 3790.
- (139) Tóth, B. L.; Monory, A.; Egyed, O.; Domján, A.; Bényei, A.; Szathury, B.; Novák, Z.; Stirling, A. *Chem. Sci.* **2021**, *12*, 5152.